INAUGURAL-DISSERTATION

zur

Erlangung der Doktorwürde

der

Naturwissenschaftlich-Mathematischen Gesamtfakultät

der

Ruprecht-Karls-Universität

Heidelberg

vorgelegt von

Wendyam Armand GUIGUEMDE

aus Bordeaux (FRANKREICH)

Tag der mündlichen Prüfung: 25. November 2005

Thema

Functional characterization of a putative *Plasmodium falciparum* calcium/hydrogen antiporter *pfcha*

Gutachter: Prof. Dr. Michael Lanzer

Prof. Dr. Heiner Schirmer

Die vorliegende Arbeit wurde am Hygiene-Institut, Abteilung Parasitologie, Heidelberg in der Zeit von März 2001 bis September 2005 unter der Leitung von Prof. Dr. Michael Lanzer durchgeführt.

ACKNOWLEDGEMENTS

I am very thankful to Prof. Dr. Lanzer for having given me the chance to work in his laboratory, for his patience, his constant encouragements and support.

I am also thankful to Prof. Dr. Schirmer for his generosity, his kindness, his approachability and modesty despite the vast knowledge he has. Thank you Prof. Schirmer.

Special thanks to Dr. Cecilia Sanchez who had the hard job to teach a neophyte the molecular biology techniques and to Dr. Susanne Nessler for her help with the oocytes. A special mention to Elisabeth for her willingness to help in the lab.

A “polite” thank to Dr. Jeremy Mclean for his help to review the manuscript of my thesis and also for the nice scientific discussions.

To my colleagues and friends of my group “dangerous” thanks for the nice atmosphere in the lab: Judith (S), Elise (3), Kathrin (AM), Jude, Weidong, Yvonne, Hannes, Tim, Philipp, Theodora, Marina.

Thanks to the colleagues from Nouna with a special attention to Dr. Bocar Kouyaté, Dr. Boubacar Coulibaly and Yazoumé for their collaboration.

Lastly, I would like to thank my parents and brothers for their love and support.

ABBREVIATIONS

℃	Celsius
µCi	Microcuries
µg	Microgramm
µl	Microliter
µM	Micromolar
3D7	*Plasmodium falciparum* clone 3D7
A	Adenine
aa	Amino acid
Ab	Antibody
ADH	Aldehyde deshydrogenase
Amp	Ampicillin
APS	Ammonium persulphate
ATP	Adenosine triphosphate
b	Base
Bis-AA	N´, N´-Methylene -bisacrylamide
bp	Base pairs
BSA	Bovine serum albumin
CAX	Calcium exchanger
CDC	Center for disease control
cDNA	Complementary DNA
Cfu	Colonies forming unit
Ci	Curie
cm	Centimeter
CNRS	Centre National de la Recherche Scientifique
CQ	Chloroquine
CQR	Chloroquine resistance
CQS	Chloroquine sensitive
cRNA	Complementary RNA
D	Dalton
DEPC	Diethylpyrocarbonate
DIW	Deionized water
DMSO	Dimethylsulfoxide

DNA	Deoxyribonucleic acid
DNase	Desoxyribonuclease
dNTP	Deoxyribonucleoside triphosphate
dsDNA	Double stranded DNA
DTT	Dithiothreitol
E. coli	*Escherichia coli*
EDTA	Ethylene diaminotetraacetate
ER	Endoplasmic reticulum
EtOH	Ethanol
g	Gram or gravitational force
G	Guanine
g/l	gram per liter
GFP	Green Fluorescent Protein
GPI	Glycosylphosphatidylinisotol
GSH	Glutathion
h	Hour
HEPES	4-(2-hydroxyethyl)-1-piperazineethanesulfonic acid
ICAM	Intercellular adhesion molecule
IFA	Indirect immunofluorescence assay
IFN	Interferon
Ig	Immunoglobulin
K	Lysin
kb	Kilobase pair
kD	Kilodalton
KPi	Inorganic phosphate potassium salt
Krpm	Thousand rounds per minute
l	Liter
LB-Medium	Luria-Broth-Medium
LiAc	Lithium Acetate
m	Meter
M	Molar
mA	Milliampere
MACS	Magnetic activated cell sorter

MES	Morpholineethanesulfonic acid
mg	Milligram
min	Minute
ml	Milliliter
mM	Millimolar
mRNA	Messenger RNA
mV	Millivolt
MW	Molecular weight
n	Nano
NaN_3	Sodium azide
NEB	New England Biolabs
nt	Nucleotide
NTP	Nucleoside triphosphate
O/N	Over night
OD	Optical density
p	Pico
P. falciparum	*Plasmodium falciparum*
PAGE	Polyacrylamide gel electrophoresis
PBS	Phosphate buffered saline
PCR	Polymerase chain reaction
PEG	Polyethylene glycol
PFA	Paraformaldehyde
PfCRT	*P. falciparum* Chloroquine Resistance Transporter (Protein)
PfEMP-1	*Plasmodium falciparum* erythrocyte membrane protein 1
pfmdr-1	*P. falciparum* multidrug resistance gene 1
pH	*„potentia hydrogenii“*
POD	Peroxidase
PRBC	*P. falciparum* infected red blood cell
RBC	Red blood cell
RNA	Ribonucleic acid
RNase A	Ribonuclease A
RPM	Revolutions per Minute

RPMI	Rosewell Park Memorial Institute
RT	Room temperature
s	Second
S	Serine
S. cerevisiae	*Saccharomyces cerevisiae*
SDS	Sodium dodecylsulphate
ß-ME	ß Mercaptoethanol
T	Thymine
TAE	Tris/Acetate/EDTA
Taq	Thermus aquaticus
TE	Tris/EDTA
TEA	Triethanolamine
TEMED	Triethylmethylethyldiamine
TM	Transmembrane domain
Tris	Tris (hydroxymethyl)-aminomethane
U	Units
UV	Ultraviolet
V	Volt
Vol	Volume
X. laevis	*Xenopus laevis*
YNB	Yeast nitrogen base
YPD	Yeast peptone dextrose

TABLE OF CONTENTS

1. INTRODUCTION

1.1 Malaria

1.1.1 History of malaria

Malaria, derived from the latin *Malus aria* or the Italian *mala aria* both meaning bad air, was so named because the disease was thought to be caused by the breathing of bad air from the swamps. Its other name was swamp fever. Probably one of the oldest known diseases, malaria remains one of the most widespread illness with nearly 40% of the world population at risk (Snow *et al.*, 2005). These areas are limited to the tropical and subtropical regions, most common between the latitudes of 23.5° North and 23.5° South (Fig.1). Ea ch year 300 to 500 million people contract malaria with a death toll estimated at 1.5 to 2 million and more than 90 % of the infections happen in Africa (Snow *et al.*, 2005). The highest risk groups are children under 5 years old, pregnant women and none-immune travellers: an estimated 50 to 70 million Western travellers are exposed to malaria infection annually (Schlagenhauf, 2004). Beyond the clinical issues, malaria also poses an economic problem as the disability provoked influences negatively the productivity at work (Sachs and Malaney, 2002).

In 1880, Alphonse Laveran who won the Nobel Prize for his major contribution in the field of malaria discovered the parasite responsible for malaria. The causative agent of malaria is the unicellular eukaryotic parasite of the protozoa group from the genus *Plasmodium*, (phylum *Apicomplexa*, class *Sporozoa*, order *Coccidida*, genus *Haemosporidiae*, and family *Plasmodiidae*). The four species affecting humans are *Plasmodium falciparum, Plasmodium vivax, Plasmodium ovale* and *Plasmodium malariae*. These parasites give rise to different forms of malaria: Malaria tropica (*P. falciparum*), Malaria tertiana (*P .vivax, P. ovale*) and Malaria quartana (*P. malariae*). *P. falciparum* is the most serious form of malaria, with shorter prepatent periods (the period between infection and appearance of parasites in the blood) and higher parasitemia. The parasites of *P. falciparum* multiply very rapidly because *P. falciparum* invades red cells of all ages, whereas *P. vivax* and *P. ovale* prefer invading younger red cells, the reticulocytes, while *P. malariae* seeks mature red cells (Mons, 1990).

Sir Ronald Ross, another major contributor to the understanding of malaria transmission, observed that the parasites are spread by the female Anopheles mosquitoes (phylum *Arthropoda*, class *Insecta*, order *Diptera*, genus *Nematocera*, and family *Culicidae*). The mosquitos become infected upon feeding on a malaria-infected person. These infected mosquitos then go on to infect further hosts upon blood feeding. Of the approximately 380 known *Anopheles* species only 60 can function as a vector for *Plasmodium* spp. All *Plasmodium* parasites seem capable of adapting to any non-refractory Anopheline mosquito, given sufficient time and contact. Sporogony within the mosquito is governed by environmental temperature as Anopheline mosquitoes are poikilotherms. The mosquitoes live at optimal temperatures between 18℃ and 33℃ (Fang and McCutcha n, 2002).

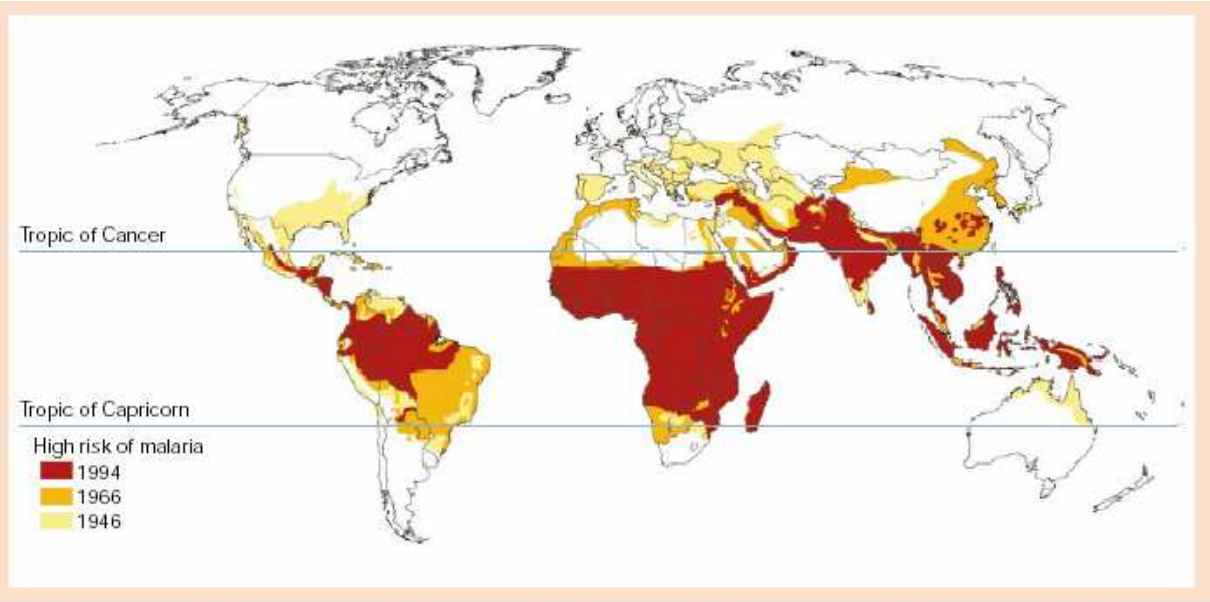

Fig 1.1: Distribution of malaria in the world from 1946 to 1994 (Sachs and Malaney, 2002)

1.1.2 The *Plasmodium* life cycle

Knowledge of the life cycle of Plasmodium is a key to understanding the clinical features, the treatment, and the research on malaria. *Plasmodium* is an obligate endoparasite and has a complex life cycle. The parasite has two major stages: the asexual stage, called schizogony, which takes place in the human host and the sexual stage, called sporogony, which takes place into the *Anopheles* mosquito. The life cycle is summarized in the Fig 2.

During its blood feeding between dusk and dawn, the female anopheles mosquito injects sporozoites from its saliva into the skin of the human host. Males subsist on nectar; therefore they do not have a blood meal. Those sporozoites, after approximately half an hour, reach the liver where they infect hepatocytes and therein proliferate to give thousands of merozoites for each single hepatocyte. This step, called the exoerythrocytic cycle, can last for 9-16 days. The parasites from *P.vivax* and *P.ovale* can remain dormant in the liver as hypnozoites, leading to recurrent infection or relapse. The merozoites rupture from the hepatocytes and are delivered to the blood stream where they invade erythrocytes. During this erythrocytic stage, the merozoites develop into ring trophozoites, mature trophozoites and then into schizonts which then release 8 to 32 merozoites to further infect other erythrocytes. After some cycles, some merozoites, after the invasion of erythrocytes, differentiate into gametocytes. The gametocytes are ingested by female Anopheles mosquito during a blood feeding.

The development of the parasite in the mosquito is known as the sporogonic cycle. Whilst in the stomach of the mosquito, the microgamete fertilizes the female macrogamete, generating a zygote. The zygote in turn becomes motile and elongated (ookinete) and invades the midgut wall of the mosquito, where it develops into an oocyst. Within the oocyst, many sporozoites are formed by mitotic division. The oocyte grows and ruptures, thereby releasing infective sporozoites. After the cyst ruptures, the sporozoites escape into the haemocoele and migrate to and penetrate into the salivary gland cells, where they remain for up to 59 days. Inoculation of these sporozoites into a new human host perpetuates the malaria life cycle. In *P. falciparum*, erythrocytic schizogony takes 48 h and the sporogony takes 10-12 days.

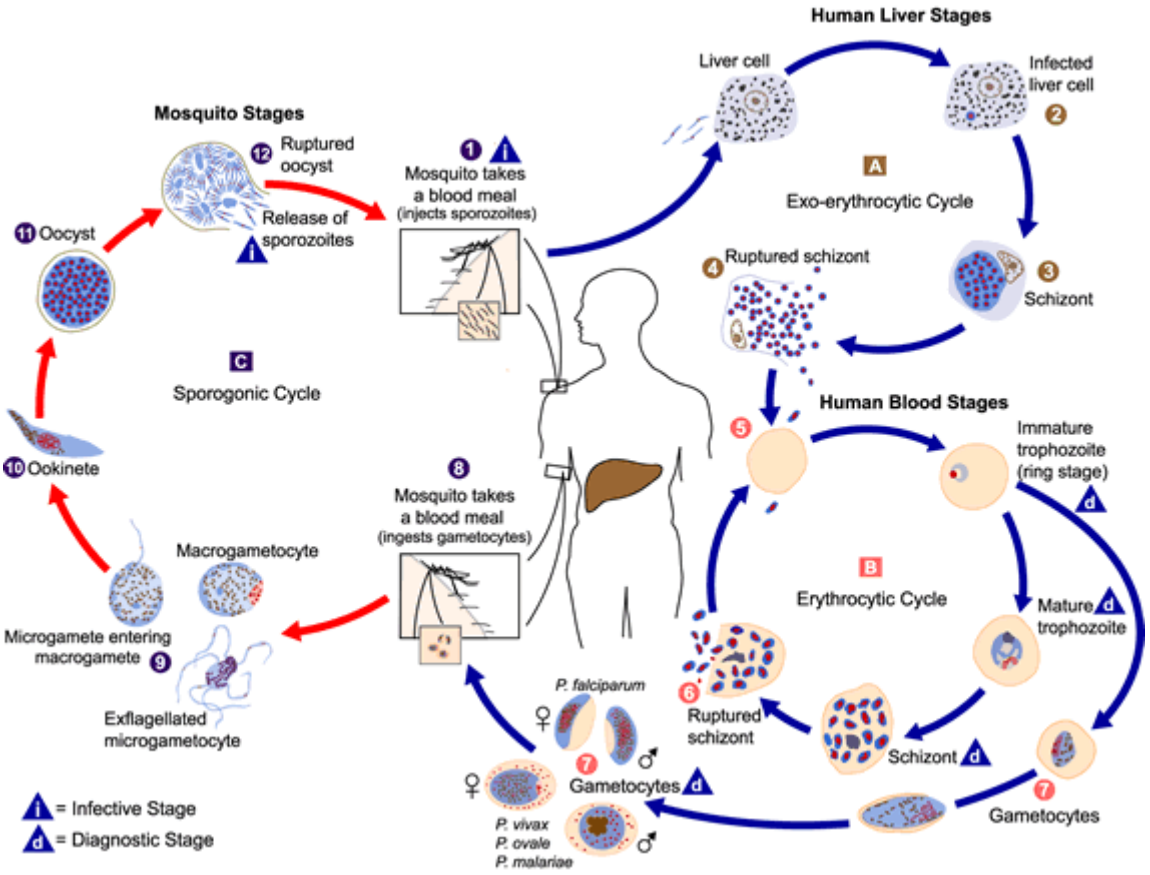

Fig 1.2: Life cycle of *Plasmodium falciparum*. The malaria parasite life cycle involves two hosts. During a blood feeding, a malaria-infected female *Anopheles* mosquito inoculates sporozoites into the human host[1]. Sporozoites infect liver cells [2]and mature into schizonts[3], which rupture and release merozoites[4]. (Of note, in *P. vivax* and *P. ovale* a dormant stage [hypnozoites] can persist in the liver and cause relapses by invading the bloodstream weeks, or even years later.) After this initial replication in the liver (exo-erythrocytic schizogony[A]), the parasites undergo asexual multiplication in the erythrocytes (erythrocytic schizogony[B]). Merozoites infect red blood cells[5]. The ring stage trophozoites mature into schizonts, which rupture releasing merozoites[6]. Some parasites differentiate into sexual erythrocytic stages (gametocytes)[7]. Blood stage parasites are responsible for the clinical manifestations of the disease. The gametocytes, male (microgametocytes) and female (macrogametocytes), are ingested by an *Anopheles* mosquito during a blood meal[8]. The parasites' multiplication in the mosquito is known as the sporogonic cycle[C]. While in the mosquito's stomach, the microgametes penetrate the macrogametes generating zygotes[9]. The zygotes in turn become motile and elongated (ookinetes)[10] which invade the midgut wall of the mosquito where they develop into oocysts[11]. The oocysts grow, rupture, and release sporozoites[12], which make their way to the mosquito's salivary glands. Inoculation of the sporozoites into a new human host perpetuates the malaria life cycle[1] (National Center for Infectious Diseases, Division of Parasitic Diseases)

1.1.3 Clinical features and pathogenicity

1.1.3.1 Clinical symptoms

Fever is the most characteristic symptom of malaria. Other common symptoms include chills, headache, myalgias, nausea, and vomiting. Diarrhea, abdominal pain, and coughing are occasionally observed. As the disease progresses, some patients may develop the classic malaria paroxysm with bouts of illness alternating with symptom-free periods. The malaria paroxysm comprises three successive stages. The first is a 15-to-60 min cold stage characterized by shivering and a feeling of cold. Next comes the 2-to-6 h hot stage, in which there is fever, sometimes reaching 41℃, flushed, dry skin, and often headache, nausea, and vomiting. Finally, there is the 2-to-4 h sweating stage during which the fever drops rapidly and the patient sweats. In all types of malaria the periodic febrile response is caused by rupture of erythrocytic mature schizonts. In *P. vivax* and *P. ovale* malaria, a brood of schizonts matures every 48 hr, so the periodicity of fever is tertian (“tertian malaria”), whereas in *P. malariae* disease, fever occurs every 72 h (“quartan malaria”). The fever in falciparum malaria may occur every 48 hr, but is usually irregular, showing no distinct periodicity. These classic fever patterns are usually not seen early in the course of malaria, and therefore the absence of periodic, synchronized fevers does not rule out a diagnosis of malaria. (Baron, 1996).

If the diagnosis of malaria is missed or delayed, especially in *P. falciparum* infections, potentially fatal complicated malaria may develop in the so called severe malaria. The major forms syndromes of severe malaria are cerebral malaria, caused by obstruction of small vessels of the brain by sequestered parasites, and severe anemia caused by the destruction of the erythrocytes. In cerebral malaria the clinical features are: impaired consciousness, convulsions and long-term neurological deficit. In severe anemia is the impaired consciousness frequent, other symptoms include respiratory distress and shock.

Other complications in both forms include: hyperparasitemia (more than 3 to 5 percent of the erythrocytes parasitized), severe hypoglycemia, lactic acidosis, prolonged hyperthermia, pulmonary, cardiac, hepatic, or renal dysfunction, seizures, spontaneous bleeding, or high-output diarrhoea or vomiting, gram-negative sepsis, aspiration pneumonia and splenic rupture. These manifestations are associated with poor prognosis. Persons at increased risk of severe disease from malaria include

older persons, children, pregnant women, non-immune persons and those with underlying chronic illness.

1.1.3.2 The pathogenic basis of malaria

The symptoms of malaria begin with the invasion of the erythrocytes by the merozoites and the rupture of host cells and the release of parasite products into the blood stream. The fever is caused by the release of malaria toxins and antigens, and the release of pro-inflammatory cytokines such as TNF alpha and Interleukin (Kwiatkowski *et al.*, 1989). Those pro-inflammatory cytokines are also involved in cerebral malaria (Sanni *et al.*, 2004;Troye-Blomberg *et al.*, 1999).

Anemia is caused by the destruction of erythrocytes during schizogony. The asexual replication leads to tremendous amplification with parasite burdens that may reach 10^{12} parasites per patient (Arav-Boger and Shapiro, 2005). Anemia is also caused by the absorption of antigen on non-parasitized erythrocytes with complement-mediated lysis, suppression of hematopoiesis by cytokines (McDevitt *et al.*, 2004), and the therapy-associated hemolysis induced by medications in G6PD deficiency.

Hypoglycemia is common in malaria; as malaria parasitized erythrocytes utilize glucose 75 times faster than uninfected cells but there is no direct correlation between hypoglycemia and parasitaemia (Elased and Playfair, 1996). In addition, treatment with quinine and quinidine stimulate insulin secretion, reducing blood glucose (Davis *et al.*, 2002).

Cerebral malaria is caused as previously mentioned by obstruction of small vessels of the brain by sequestered parasites (Smith *et al.*, 2000).. Parasites sequester themselves also in the placenta, the lung, the liver, the kidney and subcutaneous tissues (Gamain *et al.*, 2001). The surface changes of the infected erythrocytes allowing this sequestration are parasite encoded adhesions that are the contact point with the host cells (Luse and Miller, 1971; Smith *et al.*, 2001). A single protein PfEMP1, expressed at the surface of the infected erythrocyte mediates adherence to many endothelial receptors (Baruch *et al.*, 1997). PfEMP1 is the product of the *var* gene family that is involved in antigenic variation thus playing a major role in the pathogenesis of malaria (Newbold *et al.*, 1997). The extracellular region of PfEMP1 possesses multiple adhesion domains which allow binding to a broad range of endothelial cell receptors (Smith *et al.*, 2000), inlcuding CSA, ICAM1,

and CD36 for the placenta, the brain and the vascular endothelium (Baruch *et al.*, 1997).

1.1.4 Chemotherapy

1.1.4.1 Mode of action of antimalarial drugs

1.1.4.1.1 Quinolines

Discovered just before World War II in 1934, chloroquine (CQ) has been for decades a cheap, efficient, safe, fully synthetic antimalarial drug. The emergence of the chloroquine resistance (CQR) in the early 1960s and its spread worldwide has seriously compromised its use nowadays for treatment against malaria (Farooq and Mahajan, 2004).

Chloroquine is thought to exert its antimalarial effect by binding to toxic haem, thereby preventing the detoxification of haem. Haem is released during proteolysis of haemoglobin and detoxified by crystallisation in the parasites acidic food vacuole (Sullivan *et al.*, 1996). Other heme detoxification pathways that had been considered include peroxidative degradation (Loria *et al.*, 1999; Zhang *et al.*, 1999), and glutathione-dependent degradation (Zhang *et al.*, 1999; Ginsburg *et al.*, 1998). The heme-chloroquine complex strongly promotes the peroxidative cleavage of phospholipid membrane (Sugioka, 1991). This mode of action is thought to be similar for other quinolines (Zhang *et al.*, 1999).

1.1.4.1.2 Folic Acid Antagonists

The most widely used antimalarial drugs of this type include pyrimethamine, proguanil, sulfadoxine and dapsone. They have the best defined molecular targets, namely the enzymes dihydrofolate reductase (DHFR) and dihydropteroate synthase (DHPS) respectively inhibited by pyrimethamine, proguanil and sulfadoxine, dapsone, which function in the folate metabolic. The products of this pathway, reduced folate cofactors, are essential for DNA synthesis and the metabolism of certain amino acids (Hyde, 2005).

1.1.4.1.3 Hydroxynaphthoquinones

Atovaquone inhibits respiration and collapses the mitochondrial membrane potential in live intact malaria parasites by inhibiting the cytochrome bc1 complex (Srivastava *et al.*, 1997; Srivastava *et al.*, 1999).

1.1.4.1.4 Artemisinins

Artemisinins are extracted from sweet wormwood (Artemisia annua) and are the most potent antimalarials available, rapidly killing all asexual stages of *Plasmodium falciparum*. Artemisinins remain the last hope for the containment of malaria. Artemisinins are sesquiterpene lactones, which possibly act by targeting the SERCA of the parasite (Eckstein-Ludwig *et al.*, 2003). The affordability in terms of cost of the drug is still its limitation but the recent discovery that the peroxide bridge is the key of its mode of action and the synthesis of a peroxide antimalarial is promising (Vennerstrom *et al.*, 2004).

1.1.4.2 Mechanism of resistance

1.1.4.2.1 Chloroquine

Over the past years many different theories regarding chloroquine resistance have been proposed. Presently three main theories are still debated:

1) *The pH*. CQ, by virtue of its weak base properties, concentrates in the acidic compartment(s) of the intraerythrocytic parasite. Drug accumulation is essential for it to exert its pharmacological activity (Bray *et al.*, 1998). Drug resistance has been thought to result from insufficient acidification of drug-accumulating organelle(s). The difference in pH between the CQ sensitive and CQ resistant strains, allowing differential accumulation of CQ could explain the resistance (Ginsburg and Stein, 1991). Nevertheless studies on the vacuolar pH of CQR and CQ sensitive are very controversial (Krogstad *et al.*, 1992; Dzekunov *et al.*, 2000)

2) *The binding affinity of CQ to heme*. CQ resistant strains of *P. falciparum* have evolved a mechanism to reduce the saturable uptake and this saturable accumulation of chloroquine is due to intracellular binding to ferriprotoporphyrin IX (Bray *et al.*, 1999).

3) *The efflux of CQ*. Chloroquine-resistant *P. falciparum* accumulate significantly less chloroquine than susceptible parasites, and this is thought to be the basis of their

resistance. The resistant parasite has now been found to release chloroquine 40 to 50 times more rapidly than the susceptible parasite, although their initial rates of chloroquine accumulation are the same (Krogstad *et al.*, 1987). Verapamil and two other calcium channel blockers, as well as vinblastine and daunomycin, each slowed the release and increased the accumulation of chloroquine by resistant (but not susceptible) *P.falciparum*. These results suggest that a higher rate of chloroquine efflux explains the lower chloroquine accumulation, and thus the resistance observed in resistant *P. falciparum* (Krogstad *et al.*, 1987). Recently, compelling biochemical evidences further strongly support the theory of a CQ efflux mechanism (Sanchez *et al.*, 2004) linked to the *pfcrt* gene product, PfCRT, a food vacuoler membrane protein that has several conserved amino cid substitutions in CQR parasites (Naude *et al.*, 2005; Fidock *et al.*, 2000).

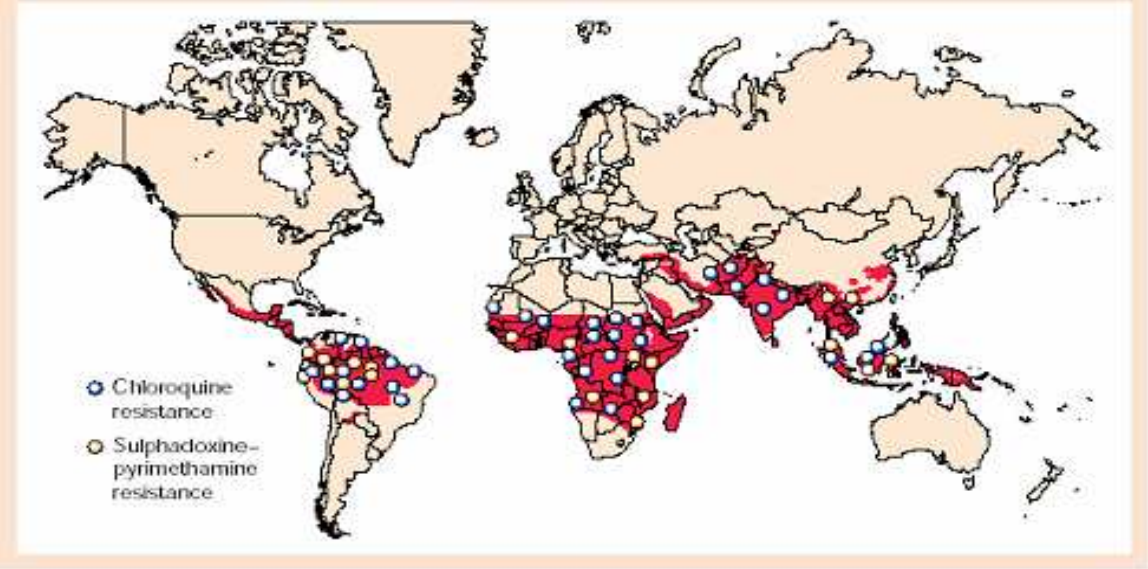

Fig. 1.3: Global status of resistance to chloroquine and sulfadoxine/pyrimethamine, the two most widely used antimalarial drugs (Ridley, 2002).

1.1.4.2.2 Other antimalarials

Apart from CQ where the mechanism of resistance is still unclear, most of the other antimalarials have known mechanisms of resistance which arise from defined genetic mutation(s) of the drug target. Mutations in *P. falciparum* cytochrome b that are associated with atovaquone resistance are located at the Y268 residue (Korsinczky *et al.*, 2000, Peters *et al.*, 2002). A point mutation N108 in dihydrofolate

reductase-thymidylate synthase confers resistance to pyrimethamine (Peterson *et al.*, 1988) while mutations in the dihydroopterotate synthase determines sulfadoxine resistance (Wang *et al.*, 1997;Triglia *et al.*, 1998). The N1042D mutation on the PfMDR1 was shown to significantly contribute to quinine resistance and the triple mutations S1034C/N1042D/D1246Y found to enhance parasite susceptibility to mefloquine, halofantrine and artemisinin (Sidhu *et al.*, 2005).

1.2 The calcium homeostasis

1.2.1 General overview

Ca^{2+} is a highly versatile intracellular signal that operates over a wide temporal range to regulate many different cellular processes (Lodish H, 2000). An extensive Ca^{2+}-signalling toolkit exists to assemble signalling systems with very different spatial and temporal dynamics. Rapid highly localized Ca^{2+} spikes regulate fast responses, while slower responses are controlled by repetitive global Ca^{2+} transients or intracellular Ca^{2+} waves. Ca^{2+} also has a direct role in controlling the expression patterns of its signalling systems that are constantly being remodelled in both health and disease (Berridge *et al.*, 2003).

The calcium concentrations outside the cells are 10 000 times higher than free intracellular Ca^{2+}, $(Ca^{2+})_i$, the physiologically active form of calcium (Rasmussen and Rasmussen, 1990). The level of $(Ca^{2+})_i$ is regulated and maintained as low as ~100 nM through the concerted action of a number of binding proteins and ion exchange mechanisms. Soluble proteins, such as calmodulin, contribute to the buffering of cell Ca^{2+}, but membrane-intrinsic transporting proteins are more important. Ca^{2+} signal transduction is based on increases in free cytosolic Ca^{2+} concentration. This increase in Ca^{2+} can originate from the extracellular space or be released from intracellular stores. Extracellular Ca^{2+} enters the cell through various types of plasma-membrane Ca^{2+} channels, and leaves the cell via pumps and Na^{+}/Ca^{2+} exchangers (Kasai and Muto, 1990; Balasubramanyam *et al.*, 1993). The endoplasmic reticulum (ER) is a major site for sequestered Ca^{2+} ions. Ca^{2+} is accumulated into intracellular stores by means of Ca^{2+} pumps and released by inositol 1,4,5-trisphosphate (IP_3) via IP_3 receptors and by cyclic adenosine diphosphate ribose (cADPr) via ryanodine receptors (Clapham, 1995, Clapham, 1995, Putney, 1999). A connection has been

demonstrated between the filling status of the intracellular calcium stores and the plasma membrane calcium channel activity (Putney, 1990).

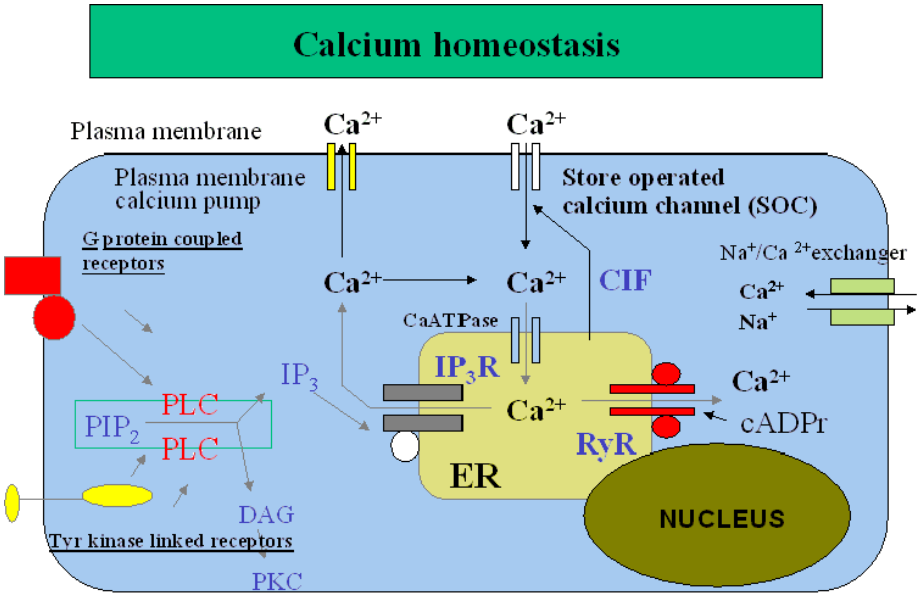

Fig. 1.4: The mechanism of Ca^{2+} transport in a eucaryotic cell. (Korkiamäki, 2002). Extracellular Ca^{2+} enters the cell through plasma membrane Ca2+ channels and leaves the cell using Ca^{2+} pumps and Na^{+} / Ca^{2+} exchangers. Endoplasmic reticulum (ER) is a major site for sequestered Ca^{2+} ions. Ca^{2+} is accumulates in intracellular stores by means of Ca^{2+} pumps and released by inositol 1,4,5-triphosphate (IP+) via IP_3 receptors (IP_3R) and by cycli adenosine diphosphate ribose (cADPr) via ryonodine receptors (RyR). Store-opened calcium channels (SOCs) open in responde to depletion of the (ER) Ca^{2+} stores. Calcium influx factor (CIF) has postulated to mediate the signal from IP_3R to the plasma membrane store-operated calcium channels (SOCs).

1.2.2 In *P. falciparum*

The calcium ion Ca^{2+} is also a major signaling molecule in a diverse range of human parasitic protozoa, such as *Trypanosoma spp*, *Leishmania spp*, *Plasmodium spp*, *Toxoplasma gondii*, *Giardia lamblia* and *Trichomonas vaginalis* (Vercesi *et al.*, 1997;Arrizabalaga *et al.*, 2004). Ca^{2+} is critical for the invasion of these intracellular parasites, and its cytosolic concentration is regulated by the concerted operation of several transporters present in the plasma membrane, endoplasmic reticulum, mitochondria and acidocalcisomes. Recent findings have shed the light on the function of these transporters, the roles that they play in cellular metabolism and their potential use for targeting them for in therapies (Moreno and Docampo, 2003).

The first evidence that calcium is essential for continuous growth of *P. falciparum in vitro* was observed in the 80s (Divo *et al.*, 1985). Later Calcium channel blockers were found to suppress parasite growth in vitro (Matsumoto *et al.*, 1987) and artemisinin, a potent antimalarial, inhibits the SERCA of *P. falciparum* (Mercereau-Puijalon and Fandeur, 2003; Eckstein-Ludwig *et al*, 2003). Moreover calmodulin, a calcium-dependent modulator protein, was shown to be indispensable for growth of erythrocytic stages of the human malaria parasite, *P.falciparum*. When the potent calmodulin antagonists W7, trifluoperazine (TFP) or R24571, were added to cultures of *P. falciparum* they inhibited invasion of erythrocytes by merozoites, and maturation of schizonts (Scheibel *et al.*, 1987).

Calcium is involved in various processes in the parasite including gametogenesis, invasion of hepatocytes and erythrocytes, cytoadherence and metabolic processes. The induction mechanism of gamete formation (gametogenesis) in a rodent malaria parasite is influenced by Ca^{2+} levels. Ca^{2+} release inhibition using acid 8-(diethylamino) octyl ester (TMB-8, a Ca^{2+} release inhibitor) blocked formation of male gametes by inhibiting DNA synthesis (Kawamoto *et al.*, 1993). Recent genetic evidence has revealed isoform-specific functions for calcium-dependent protein kinases CDPK and Ca^{2+} that are essential for *P. berghei* gametogenesis (Billker *et al.*, 2004). Invasion of hepatocytes and erythrocytes is also a Ca^{2+}dependent process. It has been proposed that the *P. falciparum* circumsporozoite protein (CS) central region plays a role in the invasion of hepatocytes, as a specific Ca^{2+} macroligand, a critical functions during attachment,

invasion, and development of the malaria parasite in the hepatic cell (Verdini *et al.*, 1991). Circumsporozoite protein (CS), the primary protein antigen found on the surface of sporozoites, binds to the basolateral domain, the heparin sulphate proteoglycans, of hepatocytes (Miller *et al.*, 2002).

Ca^{2+} was also shown to be indispensable for the invasion of erythrocytes by merozoites (Wasserman *et al.*, 1982). Indeed inclusion of ethyleneglycolbis (beta-amino-ethylether) N,N'-tetra-acetic acid (EGTA) caused blocking of the asexual cell cycle of the parasite in two sites, the first blockage occurring between 20 and 26 h after invasion of the erythrocyte (Wasserman *et al.*, 1982). This leads to morphologically abnormal parasites arrested in the mature trophozoite stage of the cycle. The second site of inhibition was probably one of the steps in the process of invasion of the erythrocyte by the merozoite (Wasserman *et al.*, 1982). When 1 mM EGTA was added 24--30 h after the culture was synchronized and the cell cycle of the parasite continued without any interference in the normal maturation until the development of schizonts and release of merozoites into the medium. However, reinvasion of fresh erythrocytes by these merozoites was impeded. The inhibition of reinvasion caused by EGTA was overcome by the addition of an excess of Ca^{2+} (Wasserman *et al.*, 1982). In another study Wassermann et al. (Wasserman *et al.*, 1990) showed that the Ca^{2+} concentration increased about 10 times in recently infected erythrocytes and conclude that a calcium influx into erythrocytes might precede or accompany merozoite invasion, which may trigger a series of molecular events, including phosphorylation and dephosphorylation of cystoskeletal proteins.

Serine proteases play crucial roles in erythrocyte invasion by merozoites of the malaria parasite (Blackman *et al.*, 1993). The *Plasmodium falciparum* subtilisin-like protease-1 (PfSUB-1) is synthesized during maturation of the intraerythrocytic parasite and accumulates in a set of merozoite secretory organelles, suggesting that it may play a role in host cell invasion or post-invasion events. It requires high levels of calcium for optimum activity and possesses at least 3 potential calcium binding sites (Withers-Martinez *et al.*, 2002). PfSUB2, another calcium-dependent serine protease could be responsible for the late MSP1 maturation step (Barale *et al.*, 1999).

The phenomenon of cytoadherence is also a Ca^{2+}-related process. In vitro studies have shown that pH and also high concentrations of Ca^{2+} enhance binding of

infected erythrocytes to amelanotic melanoma cells, the "target" cells in an in vitro cytoadherence assay (Smith *et al.*, 1992).

Moreover, Ca^{2+} levels are further important in various metabolic processes. Bloodstage malaria parasites require proteolytic activity for key processes as hemoglobin degradation and merozoite escape from red blood cells (RBCs). *P. chabaudi* and *P. falciparum* have a cytoplasmic dependent cysteine-protease activity elicited by Ca^{2+} (Farias *et al.*, 2005). Ca^{2+} plays a role in the signalling pathway of *Plasmodium* with the cAMP as second messengers in melatonin-dependent regulation of *P. falciparum* cell cycle (Beraldo *et al.*, 2005). Calcium dependent protein kinases are
found in various subcellular locations, suggesting an involvement in multiple signal transduction pathways (Moskes *et al.*, 2004).

Normal mammalian erythrocytes lack intracellular Ca^{2+} stores and maintain a low cytosolic Ca^{2+} concentration of between 20 and 30 nM (Lew *et al.*, 1982) through the action of a plasma membrane Ca^{2+} pump (a P-type ATPase) (Carafoli, 1987) which extrudes Ca^{2+} into the blood plasma where the Ca^{2+} concentration is 1-2 mM (Kirk, 2001). The high Ca^{2+} concentration in the infected erythrocyte is preferentially located inside an area, corresponding to the position and size of the parasite. In contrast, the Ca^{2+} concentration outside this area is not higher than that in normal red blood cells. This higher Ca^{2+} content becomes significant at the end of the ring stage. The concentration measured in 36 h schizonts reaches two times that measured in uninfected erythrocytes, and it peaks to four times control values in late schizonts (Adovelande *et al.*, 1993). The cytosolic Ca^{2+} concentration rises from 40 nM in the early trophozoite stage to 110-125 nM in the late schizonts (Garcia *et al.*, 1996).

A serie of recent studies on a range of different plasmodial species has provided evidence for the presence of a number of discrete intracellular Ca^{2+} pools within the intracellular parasite. One, presumed to be localized to the parasite's endoplasmic reticulum, is reportedly discharged by inhibitors of the endoplasmic reticulum Ca^{2+} pump (e.g., thapsigargin, 2,5-di-(*tert*-butyl)-1,4-hydroquinone, vanadate). Another pool, which is reportedly discharged by the alkalinizing agent NH_4Cl, by the H1 ionophores nigericin and monensin (which operate as K^+/H^+ and Na^+/H^+exchangers, respectively), by V-type ATPase inhibitors, and by the H1-PPase inhibitor aminomethylenediphosphonate has been attributed to an acidic

compartment within the parasite. This compartment is postulated to be comprised of a population of acidocalcisomes acidic Ca^{2+} storage organelles which are found in trypanosomatids and other apicomplexans and which are acidified by the combined action of a V-type H^+-ATPase and a H^+-PPase (Kirk, 2001). Another study has implicated the parasite's acidic food vacuole in Ca^{2+} storage (Biagini *et al.*, 2003). However, a recent study questioned conclusions by reporting comparable Ca^{2+} values of 300 and 400 mM for the parasite cytoplasm and food vacuole (Rohrbach *et al*, 2005). *P.falciparum* merozoites possess electron-dense organelles rich in phosphorus and calcium which are similar to the acidocalcisomes of other apicomplexans, but of more irregular form. Malaria parasites possess large amounts of short and long-chain polyphosphate (polyP), which are associated with acidocalcisomes in other organisms.

Mitochondria of malaria parasites are able to reversibly accumulate part of the Ca^{2+} released in the cytoplasm by pharmacological and physiological agents and suggesting that this organelle participates in the maintenance of Ca^{2+} homeostasis of Plasmodia (Gazarini and Garcia, 2004).

It is still unclear what pathway Ca^{2+} uses to pass from the blood plasma to the parasite, either via the RBC plasma membrane or by a more direct pathway such as a duct or the tubulovesicular membrane network (Lauer *et al.*, 1997).

So far, few genes in *Plasmodium spp* have been identified and studied that are involved in the Ca^{2+} sensing or in Ca^{2+} homeostasis. This includes the CDPKs or the calcium dependent protein kinases (Li *et al.*, 2000, Christodoulou *et al.*, 2004, Moskes *et al.*, 2004), the P-type Ca^{2+}-ATPases (Krishna *et al.*, 2001; Eckstein-Ludwig *et al.*, 2003; Trottein *et al.*, 1995), and the Ca^{2+} binding protein (Polson and Blackman, 2005). In addition the parasite has a putative Ca^{2+} /H^+.

A Ca^{2+}/proton exchanger activity was first discovered in bacteria (Tsuchiya and Rosen, 1976). In *E. coli*, Ca^{2+}/proton exchanger activity extrudes Ca^{2+} from the cell when coupled to a pH gradient across the membrane (Zimniak and Barnes, 1980). In yeast, a Ca^{2+}/proton exchanger ScVCX1 localized to the vacuole membrane was found to confer tolerance to high external concentrations of Ca^{2+} (Cunningham and Fink, 1994; Cunningham and Fink, 1996). To date Ca^{2+}/proton exchangers have been characterized in plant, yeast, and microbial species (Pittman and Hirschi, 2001) and in some animal tissues (Villa *et al.*, 1998;Cordeiro *et al.*, 2000,

Goncalves *et al.*, 2000). Ca^{2+}/proton exchangers have in general 10–14 transmembrane (TM)-spanning domains with about 400 amino acid residues (Waditee *et al.*, 2004). A Ca^{2+}/proton exchanger in cyanobacteria may be localized to the plasma membrane (Waditee *et al.*, 2004). Information on the molecular properties of Ca^{2+}/proton exchangers has emerged from studies on plant Ca^{2+}/proton exchangers, especially from Arabidopsis spp (Cheng *et al.*, 2003). Four *Arabidopsis* Ca^{2+}/proton exchangers (AtCAX1–4) were identified by their ability to sequester Ca^{2+} into yeast vacuoles in *Saccharomyces cerevisiae* mutants deleted of the vacuolar Ca^{2+}-ATPase and the Ca^{2+}/H+ antiporter (ScVCX1). It was shown that AtCAX1, AtCAX3, and AtCAX4 specifically transport Ca^{2+}, whereas AtCAX2 transports Ca^{2+}, Mn^{2+}, and Cd^{2+}. Those vacuolar type AtCAXs share an N-terminal autoinhibition domain and a conserved 9-amino-acid motif required for Ca^{2+} transport (Ca^{2+} domain) (Cheng and Hirschi, 2003).

So far, evidence for a Ca^{2+}/proton exchanger in Plasmodium across the parasite plasma membrane are based mainly on the possible coupling of Ca^{2+} transport in intraerythrocytic parasites to a proton-motive force across the Plasmodia plasma membrane. The evidence for the cotransport is based on the observations that H^{+}-ATPase inhibitor dicyclohexylcarbodiimide (DCCD) and the protonophore carbonyl-cyanide-m-chlorophenylhydrazone (CCCP) inhibited $^{45}Ca^{2+}$ influx and stimulated efflux from infected cell (Tanabe *et al.*, 1982; Tanabe *et al.*, 1983; Kramer and Ginsburg, 1991).

1.3 Aim of the study

The mortality and morbidity of malaria are increasing, in part because parasites acquired drug resistance mechanisms (Snow *et al.*, 2001). Given the limited antimalarial arsenal, the widespread of resistance and the unavailability of a vaccine, the short term strategy can only rely on the development of new compounds. One approach toward the development of new compounds is the identification of new target in the parasite. The parasite´s transporters are now seriously considered to be potential drug targets. Some have already been validated as drug target (Joet and Krishna, 2004).

The calcium metabolism has been proven to be vital for eukaryotic cells and even a slight variation in Ca^{2+} levels can be fatal. In *P. falciparum*, previous studies have highlighted the crucial role of calcium in major processes of the parasite life such as invasion, exflagellation, or important metabolic reactions. Targeting the sarco-endoplasmic reticulum Ca^{2+}-ATPase of *P.falciparum* by artemisinin, and its derivatives has proven to be an antimalarial option. Moreover, CQ resistance is reversible by verapamil, a Ca^{2+} channel blocker. However, the calcium metabolism is poorly understood and few genes involved in this metabolism are known.

With the completion the of genome sequence of *P. falciparum*, a putative Ca^{2+} proton exchanger has been identified. It is a single copy gene with few homologies to human proteins. In order to further understand the calcium homeostasis and to evaluate this exchanger as a drug target, the aim of this study was to functionally characterize the putative transporter using two heterologuous system: yeast and the *Xenopus* oocyte system.

2. MATERIAL AND METHODS

2.1 Material

2.1.1 Laboratory equipment

Analytic Scale L310 and 1872	Sartorius, Göttingen
Autoclave	Tuttnauer Systec 2540, Wettenberg
Camera (Gel photos)	Kodak, DC120 Zoom Digital Camera
Centrifuge J2-MC	Beckmann, Krefeld
Centrifuge Megafuge 2.0R	Heraeus Instruments, Hanau
Centrifuge RC5BPlus	Sorvall, Langenselbold
Confocal laser scanning microscope LSM 510	Zeiss, Jena
Computer-Software:	
Axo Tape 2.0	Axon Instr., USA
Adobe Photoshop®5.0	Adobe Systems Inc, USA
Sigma Plot 9.0	Jandel Scientifics, USA
EndNote 8.0.0	ISI Research Soft, CA, USA
MS Word 98	Microsoft Corporation, CA, USA
Internet Explorer	Netscape Communications Corp., USA
Developer Hyperprocessor	Amersham Pharmacia Biotech, Freiburg
Electrophoresis apparatus Mini Sub-Cell GT	Biorad, Munich
Electrophoresis apparatus Model 96	Biorad, Munich
Electroporator (Parasites) Gene pulser II	Biorad, Munich
Electroporation (for *E. coli* transformation)	Equibio, Easyject prima
Film exposition cassettes	Sigma, Taufkirchen
Fluorescent microscope	Zeiss, Axiovert 100M, Jena
Freezer	Liebherr, Biberach
Freezer –80℃, UF85-300S	Heraeus GmbH, Hanau
Fridges	Liebherr, Biberach
Gas burner gasprofi 1 micro	WLD - TEC

Gel dryer model 583	Biorad, Munich
Gel stainer	Pharmacia
GS Gene Linker UV Chamber	Biorad, Munich
Heating Block Laboratory devices	INC, Digi-Block JR, USA
Hybridisation tubes	Techne, Cambridge, UK
Hood	The Baker Company
Hybridisation oven HB-1D	Techne, Cambridge, UK
Ice machine AF 30	Scotsman, Mailand, Italy
Incubationer (Bacterial)	Heraeus, Function line
Incubationer (cell culture)	Heraeus, Cell Star Incubator, cytoperm 2
Incubator shaker innova 4000	New Brunswick Scientific Co.Inc
Incubator shaker innova 4300	New Brunswick Scientific Co.Inc.
Inverse Microscope Olympus IMT-2	Olympus, Hamburg
Inverse Microscope Axiovert 25	Zeiss, Jena
Light microscope Leica DMIL	Leica Microsystems, Wetzlar
Light microscope Axiolab	Zeiss, Jena
Liquid nitrogen tank BT40	Air Liquide, Ludwigshafen
Liquid scintillation counter, TRI-CARB 2100	Packard, Billerica, USA
MACS	Miltenyi Biotee
Magnetic stirrer MR 3001	Heidolph, Schwabach
Nanoject automatic injector	Drummond, Broomall, USA
PCR-Machine T96 gradient Thermocycler	Biometra, Göttingen
pH-Meter	WTW, pH 537
Pipetman Gilson P20, P200, P1000	Abimed, Langenfeld
Pipetman Pipetus-akku	Hirschmann Labortechnik, Eberstadt
Pipette: Multipette® plus	Eppendorf, Hamburg
Powder free examination gloves	Hartmann
Power supply Power Pac 300	Biorad, Munich
Power supply EPS 601	Amersham Pharmacia Biotech, Freiburg
Printer hp Laserjet 1300	Hewlett Packard, Heidelberg
Protein blotting apparatus	Biorad, Munich

Mini Trans Blot Protein electrophoresis equipment *Mini-Protean® 3*	Biorad, Munich
Puller P-87	Sutter Instruments, USA
Pump P-50	Amersham Pharmacia Biotech, Freiburg
Quartz cuvettes	Hellma, Müllheim
Rotors	
SS-34, GS-3, GSA, SM24	DuPont Instruments, Bad Homburg
JA 14, JA 20	Beckman
SW 41Ti	Beckman
Scintillation counter LS6000IC	Beckman
Semi-dry transfer cell	Biorad, Trans-blot SD
Stereomicroscope Stemi 2000	Zeiss, Jena
Spectrophotometer UVIKON 923	Kontron Instrument
Table-top Centrifuge (Biofuge pico)	Heraeus, Hanau
Timer	Roth, Karlsruhe
Ultracentrifuge RCM11206X	Sorvall, Langenselbold
Ultracentrifuge L60	Beckman
UV-Handlamp Typ N-6 L	Benda Laborgeräte and Ultraviolettstrahler
Vortex	Heidolph, REAXtop, Vortex Genie 2
Vortex-Genie 2	Scientific Industries, Roth, Karlsruhe
Water Bath Julabo 7A	Julabo, Seelbach

2.1.2 Disposables

Aluminium Foil	Roth, Karlsruhe
Cell culture plates 6, 24, 96 wells	Nunc, Wiesbaden und Greiner bio-one, Frickenhausen
Cover slips	Roth, Karlsruhe
Cryopreservation tubes	Nalgene
Electroporation cuvette (5 mm)	Bio Rad, Gene Pulser (for transfection) Easyject, EQUIBIO prima (for bacteria)
Eppendorf tube	Sarstadt
Film	Kodak, BioMax or X-OMAT
Glass wool	VWR International

Glass capillaries Drummond # 3-0000203-G/X	Helmut Saur, Reutlingen
Gloves	Unigloves GmbH, Troisdorf
Immersion oil	Zeiss, Jena
Immuno-Blot™ PVDF Membrane	Biorad, Munich
MACS-columns CS	Miltenyi Biotec, Bergisch Gladbach
Membrane for DNA blotting	Machery-Nagel
Microcentrifuge tubes (0.5 ml, 1,5 ml)	Sarstedt, Nürnbrecht
Microscope slides	Marienfeld, Lauda-Königshof
Mineral oil molecular biology tested	Sigma
Nylon membrane (positively charged)	BoehRinger Mannheim
Nitrocellulose membrane	Sartorius
Parafilm American International	CanTM, Chicago, USA
PCR-tubes	Greiner bio-one, Frickenhausen
Pasteur pipettes	Roth, Karlsruhe
Petri dishes	Greiner bio-one, Frickenhausen
Pipette Tipps	Greiner, Nürtingen /Steinbrenner, Heidelberg
Plastic cuvette	Sarstedt, Nürnbrecht
Plastic pipettes (1, 2, 5, 10 und 25 ml)	Corning incorporation, Bodenheim
Plastic falcons (15/50 ml)	Greiner bio-one, Frickenausen
Plastic wrap saran	Roth, Karlsruhe
Scintillation vial	Beckman
Scintillation cocktail	Lumafase
Sterile filters (0.2 µm, 0,4 µm)	Schleicher & Schuell, Einbeck
Sterile filter units (500, 1000 ml)	Corning incorporation, Bodenheim
Thermowell tubes (for PCR)	Corning Incorporation
WhatmanTM 3MM paper	Whatman Paper Company

2.1.3 Chemicals

All chemicals not listed were bought from the companies Roth, Merck, Sigma, Serva, J.T. Baker and AppliChem via the Chemical store of the University of Heidelberg, Germany.

Acrylamide/Bisacryl 30 %	Serva, Heidelberg
Agar	Fluka
Agarose (for electrophoresis)	Invitrogen
Agarose	Gibco BRL, Karlsruhe
Ammonium acetate	Ferak
Ammonium carbonate	Ferak
Ammonium persulphate	Biorad, Munich
Ampicillin (Na salts)	Applichem
Ampicillin	Sigma, Taufkirchen
Aprotinin	Sigma, Taufkirchen
Artemisinin	Sigma, Taufkirchen
Bacto-Agar	Difco Laboratories, Augsburg
Bacto-Peptone	Difco Laboratories, Augsburg
ß-Mercaptoethanol	Merck, Darmstadt
Bradford reagent	Biorad
Bromophenol Blue (Na salts)	Serva
BSA	AppliChem
Calcium chloride	Merck, Darmstadt
$^{45}CaCl_2$	Perkin Elmer, Boston, USA
Chloroform	Merck, Darmstadt
Chloroquine	Sigma, Taufkirchen
Coomassie Brilliant Blue R 250	Serva
Coomassie Brillant Blue G 250	Biorad
DAPI	Sigma, Taufkirchen
Diethylpyrocarbonate (DEPC)	Sigma, Taufkirchen
DMSO	Merck, Darmstadt
dNTP-Kit	Peqlab, Erlangen
DTT	Sigma, Taufkirchen
EDTA	Roth, Karlsruhe
Ethidium bromide	Sigma,Taufkirchen
Formaldehyde	Merck, Darmstadt
Gentamycin	Gibco BRL, Karlsruhe
Giemsa	Sigma, Taufkirchen
D(+)-Glucose	Merck, Darmstadt

Glycerol (Glycerin)	Gerbu, Gaiberg
Glycine	AppliChem
HEPES (free acid)	Roth, Karlsruhe
Hydrochloric acid	Baker
Hypoxanthine	CCPro
Isopropanol	Baker
Lanthanum chloride	Sigma, Taufkirchen
Leucine	Serva, Heidelberg
Leupeptin	Sigma, Taufkirchen
Lysine	Serva, Heidelberg
Magnesium chloride	J. T. Baker
Magnesium sulphate	Sigma, Taufkirchen
MOPS	Sigma, Taufkirchen
Paraformaldehyde	Serva, Heidelberg
PBS	Biochem
PMSF	Sigma, Taufkirchen
Potassium acetate	AppliChem
Potassium carbonate	Ferak
Potassium chloride	Roth, Karlsruhe
Pre-stained protein marker	Peqlab, Erlangen
Quinine	Sigma, Taufkirchen
RPMI 1640-Medium	GibcoBRL, Karlsruhe
SDS	AppliChem
Sephadex G-50	Amersham
Skim milk power	Fluka
Sodium chloride	Merck, Darmstadt
Sodium hydrogen phosphate	Sigma, Taufkirchen
Sodium hydroxide	Merck, Darmstadt
Sucrose	Serva, Heidelberg
TEMED	Sigma, Taufkirchen
Tris-Base	Roth, Karlsruhe
Triton X-100	Sigma, Taufkirchen
Trypton/peptone	Roth, Karlsruhe
Tryptophane	Serva, Heidelberg

Tween20	Merck, Darmstadt
Uracil	Sigma, Taufkirchen
Verapamil	Sigma, Taufkirchen
Xylene cyanol FF	Sigma, Taufkirchen
Yeast extract	Difco Laboratories, Augsburg, Germany

2.1.4 Antibodies

Anti-GFP	Roche Diagnostics, Mannheim
Anti vacuolar alkaline phosphatase	Molecular probes
Anti-HA	Dianova, Hamburg
Anti-mouse POD	Jackson ImmunoResearch Laboratories
Anti-Rabbit POD	BöhRinger, Mannheim

2.1.5 Enzymes

Calf intestinal phosphatase	Roche Diagnostics, Mannheim
Collagenase A (Typ II; 2 mg/ml)	Roche Diagnostics, Mannheim
DNA-Polymerase Pfu	Promega, Mannheim
DNase I	Stratagene, Heidelberg
Klenow polymerase	New England BioLabs, Schwalbach
E. coli DNA polymerase I	USB
Proteinase K	Roche Diagnostics, Mannheim
Protein kinase	New England BioLabs, Schwalbach
Restriction enzymes	New England BioLabs, Schwalbach
	Amersham Pharmacia, Freiburg
RNase A	Roche Diagnostics, Mannheim
Shrimp alkaline phosphatase	Promega, Mannheim
Taq DNA-Polymerase	Biotaq RED Bioline, Luckenwalde
T4-DNA-Ligase	New England BioLabs, Schwalbach
Zymolase 20T	ICN

2.1.6 Nucleic acids

Synthetic oligonucleotides as well as primers have been synthesized by the firm Invitrogen in Karlsruhe (Germany). The sequencing of DNA was made by Geneart.

2.1.6.1 Oligonucleotides

pSP64T forward	AGAATACAAGCTTGCTTGTTC
pSP64T reverse	GTAAGTTGGGTATTATGTAGC
Ca 5´ BglII	GCGCCGAGATCTAAAATGGTTATGGGTAGAG
Ca 3´BglII	AGAGATCTCATTAGGAGG
Ca 3´BglIIstop	AGAGATCTTTACATTAGGAGG
Ca 5´ Hind III	ACCAAGCTTAAAAATGG
Ca 3´ BamHI	GCGGGGATCCGGAGGTATCGAACC
Ca3´BamHIstop	GCGGGGATCCTTAGGAGGTATCGAACC
Ca600 5´	CCAACTTGTTGTTGGTTTG
Ca 950 3´	AATTCGGAATGAATGGAAACC
Ca3´BglIIHA	AATTAAAGATCTTTAAGCATAATCTGGAACATCATATGGATAGGAGGT ATAGAACCAGAAAAC
Vcx-5´ Hind III	GCTCAAGCTTACAATGGATTGCAACTACC
Vcx-3´ BamHI	CGCGGATCCTAAACTATTTCCAATAG
Vcx-3´ BamHIstop	CGCGGATCCTCATAAACTATTTCCAATAG
VcxPstI-3´	AATATACTGGAGATCATACACAGCTG
CaPstI-5´	ATGCCTGCAGAACATGTTGAACTC
5 UTR 5´	GGGTCTGCTTCAGTAAGCC
3 UTR 3´	TCTAGAGTCGACCTGCAGG
ADHpro	CTGCACAATATTTCAAGC
ADHter	GCAAGGTAGACAAGC
GFP-100	ACCGTAAGTAGCATCACC

2.1.6.2 Plasmids

pSP64T (S. Krishna, London)
pVT100-U (J. Stolz, Regensburg)
pVT GFP (J. Stolz, Regensburg)
pGEM-T (Promega, Mannheim)

2.1.6.3 Electrophorese markers

RNA-marker	New England Biolabs, Schwalbach
1 kb DNA-marker	New England Biolabs, Schwalbach
Roti® Mark Prestained	Roth, Karlsruhe
Prestained Marker, broad range	GibcoBRL, Karlsruhe

2.2 Methods

2.2.1 Parasitology

2.2.1.1 In vitro culture *of Plasmodium falciparum*

3D7 strain parasites were cultured by an adaptation of the method of Trager and Jensen (Trager and Jensen, 1976). The erythrocytic forms of *P. falciparum* were cultured in Petri dishes of 10 cm or 25 cm diameter. In a 10 cm diameter dish were mixed 14 ml of the parasite medium, 0.5 ml of fresh A^+ erythrocytes concentrate and some drops from a previous parasite culture. Respectively were mixed 30 ml of medium and 1.5 ml of fresh erythrocytes as well as some drops of infected erythrocytes for the 25 cm diameter Petri dish, so that the hematocrit was approximately 5%. The parasitaemia was checked and the medium changed every two or three days. In case the parasitaemia was higher than 5-10%, the culture was diluted in a new plate to avoid a death of parasites due to high levels of degraded products in the medium. The parasite cultures were incubated in an atmosphere of 3 % CO_2, 5 % O_2, 92 % N_2, and 95% humidity.

Preparation of the human serum and erythrocytes

Human group A^+ erythrocytes concentrate and A^+ human serum was obtained from the blood bank of the German Red Cross, Heidelberg. The human serum was prepared by the following. It was aliquoted into 50 ml falcon tubes. In each falcon tube was added 800 µl of sterile 1 M $CaCl_2$, incubated at 37℃ for 30 min and overnight at 4℃. The next day the tubes were centrifuged (4000 rpm, 30 min) to pellet the fibrin and incubated at 56℃ for 30 min to inactivate the serum. Thereafter the serum was kept at -20℃. The erythrocytes concentrate was aliquoted into 50 ml falcon tubes. 10 ml RPMI medium was added and the tubes were centrifuged (2300 rpm, 4 min) and then kept for two to three weeks in the fridge.

2.2.1.2. Staining of *P.falciparum* with Giemsa

To enable determination of parasitaemia, and parasite stage, thin smears of the culture were made as follows: 50 µl of culture was spread evenly onto the surface of a clean microscope slide, air dried, fixed in 100% methanol for 30 s, and air dried. Fixed cells were stained for 5-10 min in a solution of 10% Giemsa, washed with water and allowed to dry. Slides were examined microscopically on a light microscope using a 100X objective to view cells under oil immersion.

2.2.1.3 Determining parasitaemia

The parasitaemia is the percentage of *P. falciparum* infected erythrocytes. A single layer of stained cells was used. The number of both parasites and erythrocytes in ten consecutive fields were counted. The parasitaemia was then calculated according to the following formula:

(Number of parasites/Number of erythrocytes) X 100 = parasitaemia in %

2.2.1.4 Freezing parasites

Only the parasites from the ring stage can be recovered after freezing. The parasitaemia should be higher as 5%, to guarantee that the parasites will come up quickly after thawing. Infected erythrocytes were pelleted at 1900 rpm for 2 min. The supernatant was then removed, and the sediment re-suspended in 1 volume of sterile freezing solution (28% Glycerol, 3% Sorbitol, and 0.65% NaCl). The suspension was gently mixed, filled into a cryotube and snap frozen in an ethanol/dry ice slurry for 15

min. The tube was then transferred to –80^{o}C for not less than one day, before being stored at –196^{o}C in liquid nitrogen.

2.2.1.5 Thawing parasites

The cryotube was removed from the liquid nitrogen tank and thawed in a 37^{o}C water bath for 2 min before being transferred to a 50 ml centrifuge tube. Per 1 ml of blood was then added 200 µl of 12% NaCl at a rate of 2 drops per second, with constant mixing. After a 5 min incubation period at RT, a further 5 ml of 1.6% NaCl was then added as before. After further 5 min incubation, 5 ml of 0.9% NaCl/0.2% Glucose was then added. The suspension was then centrifuged as before, the supernatant removed, the parasite pellet washed in 25 ml of complete parasite medium, resuspended in 12 ml of complete parasite medium and transferred to a Petri dish. 0.5 ml of fresh blood was then added, and the dish transferred to the parasite incubator. The dish was allowed to incubate for 48 h before being treated as normal. All solutions were pre-warmed to 37^{o}C before starting the thawing procedure.

2.2.1.6 Parasites synchronisation with sorbitol

This sorbitol treatment causes osmotic lysis of late stage trophozoites (Lambros and Vanderberg, 1979). This selective lysis by osmotic shock is possible due to the presence of an induced transport pathway in the red cell membrane that is permeable to sorbitol, and absent in ring stage parasites. Culture media was removed from the culture dish, and the blood resuspended in 9 volumes of sterile, pre-warmed 5% D-sorbitol solution and transferred to a centrifuge tube. After a 5 min incubation at room temperature the suspension was then centrifuged (1900 rpm, 2 min, RT), the resulting pellet being resuspended in complete culture medium and returned to the culture dish (Lambros and Vanderberg, 1979). In order to achieve either highly or totally synchronised parasite cultures, this procedure was then repeated after respectively 48 or 4-6 h.

2.2.1.7 Enrichment of mature stage parasites by magnetic separation

Malaria parasites metabolise the haemoglobin of the erythrocyte, producing non-soluble oxidised haem products, which are then crystallized to give haemozoin (Pagola *et al.*, 2000). Due to magnetic properties of haemozoin pigment, it is possible to separate trophozoites and schizonts from non-infected and young stage parasites

(Uhlemann, 2000). Using this method, it is possible to reach a parasitaemia of 95-99%. A magnetic column (MACS Separation Columns CS) was secured in the magnet holder, following the manufacturers (Vario MACS, Miltenyi Biotec) instructions. The column was equilibrated with MACS buffer. A parasite culture was then slowly allowed to filter through the column, to allow late stage parasites to bind. The column was then washed with approximately 5-6 column volumes of MACS buffer, or until the flow-through was clear and contained no further erythrocytes. The column was then removed from the magnet and the parasites eluted with 15 ml of MACS buffer. The eluted parasites were then pelleted by centrifugation (1900 rpm, 2 min, RT) and resuspended in the required buffer.

2.2.1.8 PCR based mycoplasma testing

While bacterial and fungal infections of cultures are relatively easy to detect, to prevent and to treat, contamination with mycoplasmas represents a much bigger problem leading to diminished cell growth and eventually to the loss of cultures. Mycoplasmas are small free-living, self-replicating organisms between 0.2-2 µm in diameter, thus can pass through the sterile filter.

To test cell cultures for mycoplasma contamination, the following protocol was carried out at regular intervals:

100 µl of medium from parasite cultures were removed heated at 95^{o}C for 5 min and then centrifuged at full speed in a microcentrifuge for 5 s. A PCR reaction was then set up as follows: 2 µl of each prepared sample are then used for the PCR reaction, a positive control being used for every set of reactions. The PCR was performed according to the manufacturer's instructions. After cycling, 5 µl of the reaction mixture was analysed on a 1.5% agarose gel. A 500 bp band corresponds to a positive mycoplasma contamination.

2.2.2 Cell biology

2.2.2.1 Immunofluorescence assay

The immune fluorescent assay (IFA) is a method to analyse both expression and localisation of specific protein within fixed or pre-treated cells. After cells have been fixed, they are subject to treatment with specific antibodies. In the indirect IFA, a secondary antibody coupled to a fluorophore is then used to bind the primary

antibody. When excited at the correct wavelength, the fluorophore emit visible light, allowing visualisation of the fluorescent immune complexes, and thus target protein location. The protocol used was as follows: A small aliquot of infected erythrocytes (50 µl) was washed X2 in PBS to remove serum and media. The infected erythrocytes were then resuspended to 50% haematocrit in PBS. 5 µl of this suspension was then placed onto a clean microscope slide, and smeared as usual. The film was allowed to dry, and was then fixed for 5 min in acetone/10% methanol at -80^{o}C. After fixing, the slides were allowed to dry, and then wells were drawn directly onto the slide, using a liquid blocker pen. The prepared slides were blocked overnight with 5% skim milk/PBS in a humidity chamber at 4^{o}C. The next morning, the 1^{o} antibody was added, diluted in 5% skim milk/PBS and allowed to bind for 2-4 h. The slides were washed X3 in PBS/0.01% Tween for 5 min, and then for 5 min in PBS. The second antibody was added as above, and after the necessary incubation time, the slide was washed as before, allowed to dry and a cover slip added including anti-fade mounting medium. The slides were viewed on a Carl Zeiss LSM510 confocal laser scanning microscope.

2.2.2.2 Confocal microscopy

Whilst the idea for confocal microscopy has been around for over forty years, the first commercially available microscope was introduced in 1987. As opposed to conventional microscopy, in which the whole object field is illuminated, confocal microscopy illuminates only a small portion of the sample at one time, using a focussed laser beam which moves rapidly across the sample. This light is focussed through a lens, passes a dichromatic mirror, across several moveable mirrors, through the objective and is focused onto the sample. In this way fluorochromes can be excited which then emit longer wave light which is then collected by the objective, passes back through the dichromatic mirror and is then separated by filters. Normally when an object is imaged in a fluorescence microscope, the signal produced is from the full thickness of the specimen which does not allow most of it to be in focus to the observer. The confocal microscope eliminates this out-of-focus information from above and below the plane of focus of the object by means of a confocal "pinhole" situated in front of the image plane which acts as a spatial filter and allows only the in-focus portion of the light to be imaged. The scattered light from neighbouring and out-of focus areas is thus reduced. Thus, only one point is being viewed at a time.

The resulting signal is collected by a photomultiplier-detector (PMT). To build a full picture, the sample is rapidly scanned, and the resulting points are then reconstructed by the computer to give the finished picture.

2.2.2.3 Sub cellular fractionation of yeast organelles

The protocol for the subcellular fractionation of yeast organelles was done as the following: Cells were grown in 2 L of growth medium at 30℃ to the logarithmic phase (2.5 OD_{600} U/ml). Then all steps were performed at 4℃.

Cells were harvested by centrifugation at 3000 rpm for 8 min. The supernatant was discarded and the pellet washed in an equal volume of a 20 mM NaN_3 chilled solution. The volume of the pellet was estimated by resuspending it in a small known volume of the NaN_3 solution and the cells were harvested as before. The cells were converted to spheroplasts by incubation in 1:1 volume with freshly 20 mg added of zymolase, the cell wall lytic enzyme, in a buffer with the following composition: 1.4 M sorbitol, 50 mM KPi, 10 mM NaN_3, 40 mM ß-ME freshly added. The cells were incubated at 30℃ in 50 ml falcon tube by gently shakin g. The extent of spheroplast formation was determined spectrophotometrically. Every 5 min a 100 µl aliquot was removed and diluted in 900 µl of water and the OD_{600} value determined. As spheroplasts lyse in water due to lack of a cell wall, the reduction in the OD_{600} value is directly proportional to the amount of spheroplasts formed. The spheroplasts suspension was then centrifuged at 2500 rpm for 10 min. The spheroplasts were broken by suspending in a solution of 12% sucrose, 10 mM TEA, 1 mM PMSF, 1 mM EDTA. Spheroplasts further breakage was carried out by several up and down pipettings through a 22G needle. The lysate was centrifuged at 2500 rpm for 10 min. The supernatant was further centrifuged at 10 krpm for 10 min. The pellet was resuspended in a 1 mM $MgCl_2$ solution. The resuspended pellet was placed on top of a preformed 25%-55% discontinuous sucrose gradient in Beckman SW41 centrifuge tube. The sucrose solution contained 1 mM $MgCl_2$, 1 mM PMSF. The gradient was centrifuged at 4℃ for 90 min, at 25 krpm in a L8-80 Beckman centrifuge. Ten 3 ml fractions were collected from the top of the gradient. The samples were diluted with 2 vol. of cold water. After centrifugation at 50 krpm, the pellets were resuspended in the loading buffer for proteins.

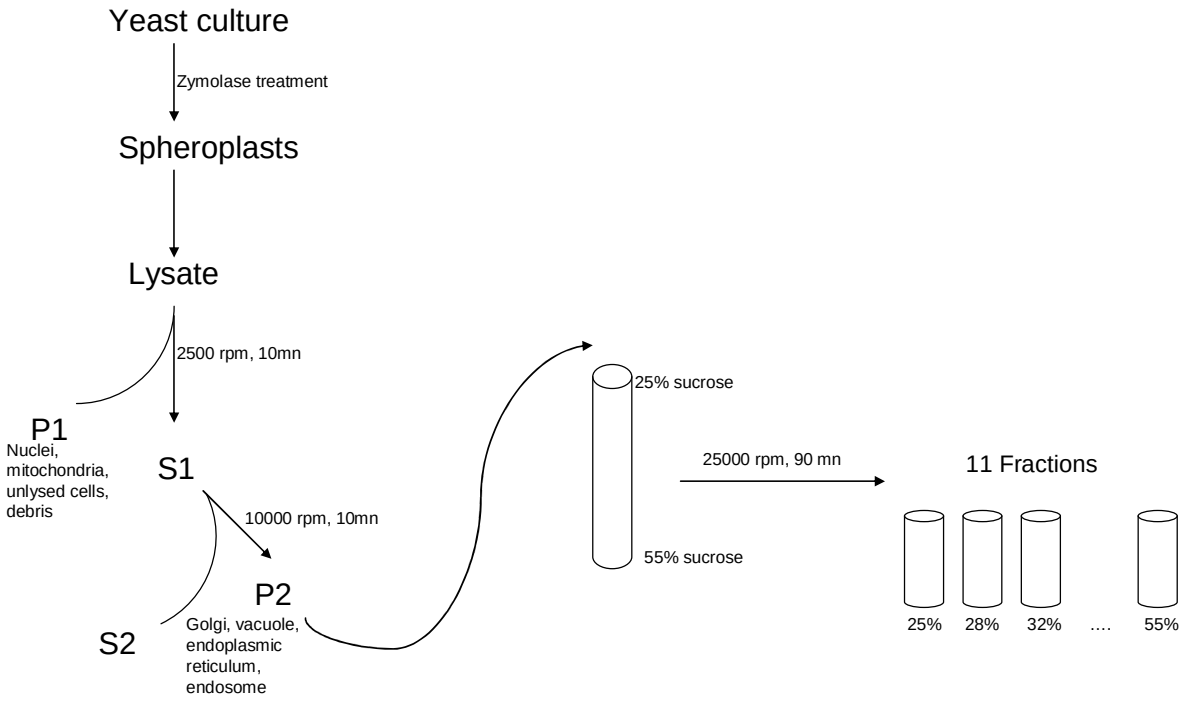

Fig. 2.1: Subcellular fractionation of yeast organelles

2.2.3 Molecular biology

2.2.3.1 DNA synthesis

Because of the high AT composition of the Plasmodium genome, the putative calcium hydrogen antiporter (*pfcha*) has been redesigned and synthesized by the firm Geneart (Regensburg) to allow an efficient transcription of mRNA in oocytes. The yeast codon usage system was used to design the new sequence of DNA to be sequenced while keeping the same amino acid sequence as the original putative protein sequence.

2.2.3.2 Culture and transformation of bacteria

2.2.3.2.1 Bacterial strains

PMC103 (Doherty *et al.*, 1993): *mcrA* Δ*mcrBC-hsd*RMS-*mrr*102 *rec*D *sbc*C.

One Shot® TOP10 Chemically Competent *E. coli* (Invitrogen): F- *mcr*A .(*mrr-hsd*RMS-*mcr*BC) Φ80*lac*Z.M15.*lac*X74 *rec*A1 *deo*R *ara*D139.*(araleu*)7697 *gal*U *gal*K *rps*L (Str$_R$) *end*A1 *nup*G.

2.2.3.2.2 Preparation of competent *E. coli*

a) Production of chemically competent *E. coli*

Chemically competent *E. coli* Top 10 cells for standard cloning reactions were prepared by a modification of the of the method of Inoue (Inoue *et al.*, 1990). Briefly, Top 10 cells were streaked out onto an LB agar plate containing 30 µg/ml of streptomycin, and single colonies were allowed to grow overnight. 1 colony was then picked and inoculated into 5 ml of LB medium with streptomycin overnight. The next morning, 2 ml from the preculture were inoculated into 50 ml of LB medium with streptomycin. The cells were allowed to grow at 37°C with shaking (250rpm) until an OD_{600} of 0.6 had been reached. The cells were harvested in a 50 ml falcon by centrifugation at 4000 rpm for 10 min at 4°C. The pellet was washed in ice cold 0.1 M $CaCl_2$, centrifuged once more as above and the pellet was resuspended in 2 ml of ice cold 0.1 M $CaCl_2$. 200 µl of glycerol was added, mixed, and the cells were aliquoted to 50 µl in microcentrifuge tubes and frozen in a dry ice/ethanol bath for 15 min. Cells were transferred to –80°C for storage. The competence of the cells was checked by transformation. The cells were competent when the transformation efficiency was at least 10^6 cfu per µg of plasmid.

b) Production of electro-competent *E. coli*

Ultra-competent PMC103 *E. coli* were prepared as follows: A single colony was picked from a freshly prepared LB agar plate and inoculated into 10 ml of Super Broth. This culture was shaken (250 rpm) overnight at 37°C. The following morning, this culture was diluted 1:100 in a further 600 ml of Super Broth and allowed to shake further for 3.5 h at 37°C. Cells were harvested at 7000 rpm for 10 min at 4°C. The resulting pellet was washed a total of three times in 600 ml of ice cold Millipore water

with centrifugation as above. One further wash was carried out with 600 ml of ice cold 10% glycerol and the cells were then re-suspended in 1.2 ml of 10% glycerol before being snap frozen in 100 µl aliquots in an EtOH/dry ice slurry. Cells were transferred to –80^{o}C for storage

2.2.3.2.3 Transformation of competent *E. coli*

a) Transformation of chemically competent *E. coli*

An aliquot of cells was removed from –80^{o}C and allowed to thaw on ice. The cells were incubated on ice for 10 min with repeated gentle mixing (Cosloy and Oishi, 1973). The DNA was added, gently mixed and the mixture was incubated on ice for a further 30 min. Cells were then heat shocked in a 42^{o}C water bath for 30 seconds, and immediately returned to ice for 2 min before addition of pre-warmed at 37℃ 150 µl of SOC medium. The tube was then transferred to a 37^{o}C shaker for 1hr to allow recovery. Transformation reactions were then spread onto LB agar plates containing the appropriate selective antibiotic and transferred to a 37^{o}C incubator overnight.

b) Transformation of electro-competent *E. coli*

The cells were allowed to thaw on ice and then divided into 50 µl aliquots. The DNA was added and the mixture was then transferred to a pre-chilled 0.2 cm gap cuvette. Electroporation took place at 2.5 kV. in a gene pulser II (Biorad). The cuvette was then returned to ice and a disposable Pasteur pipette was used to add 1 ml of pre-warmed SOC media, and transfer the transformation mix to a 15 ml tube. From this point on the protocol progresses as that for chemically competent cells.

2.2.3.2.4 Production of glycerol stocks

The required colony was inoculated into super broth containing the required selective agent, and incubated overnight. The culture was then mixed 1:1 with a sterile solution of 20% glycerol, aliquoted into cryotubes and stored at –80^{o}C for up to two years.

2.2.3.3 Culture and transformation of yeast

2.2.3.3.1 Yeast strain

S. cerevisiae strain K667 (*MAT*a *ade2-1 can1-100 his3-11*, *15 leu2-3*, and *112 trp1-1 ura3-1 cnb1*::*LEU2 pmc1*::*TRP1 vcx1*Δ)

2.2.3.3.2 Transformation of yeast

The protocol followed the small scale yeast transformation protocol from Invitrogen. 10 ml of YPD medium was inoculated with one colony and shaked overnight at 30℃. The next morning the culture was diluted to an OD_{600} of 0.4 in 50 ml of YPD medium and grew for an additional 4 h. The cells were then pelleted at 2500 rpm for 10 min and resuspended in 40 ml of 1X TE. The cells were pelleted one more time as before and resuspended in 2 ml of 1X LiAc/0.5X TE and incubated at room temperature for 10 min. For each transformation, 1 µg of plasmid DNA, 100 µg denatured sheared salmon sperm DNA and 100 µl of the yeast culture were mixed together. 700 µl of 1X LiAc/40% PEG-3350/1X TE was added, well mixed and incubated at 30℃ for 30 min. Then was added 88 µl of DMSO and the cells were heat shocked for 7 min at 42℃. The cells were pelleted, washed in 1X TE and re-pelleted and resuspended in 50-100 µl 1X TE and plated on a selective plate. The plate was incubated for at least 3 days at 30℃.

2.2.3.3.3 Production of glycerol stocks

The selected yeast colony was inoculated into YPD medium and incubated overnight. The culture was then mixed 1:1 with a sterile solution of 20% glycerol, aliquoted into cryotubes and stored at –80^{o}C for up to two years.

2.2.3.4 Isolation and purification of DNA

2.2.3.4.1 Isolation of plasmid DNA from *E. coli*

a) Minipreparations for restriction digest

To obtain plasmid DNA for restriction endonuclease digestion, a miniprep method following the protocol from Sambrook (Sambrook, 1989) was used. Briefly a single colony was grown overnight in 10 ml of LB medium containing the appropriate

by incubating in a shaker. The next morning the culture transferred to a 14 ml tube was pelleted by centrifugation (4000 rpm, 10 min, 4℃). The pellet was resuspended in 500 µl of solution A, lysed on ice with 1 ml of solution B for 3.5 min. 750 µl of chilled solution C was added to precipitate the proteins and the genomic DNA. The mix was centrifuged (10 krpm, 10 min, 4℃). 2 ml of the supernatant was taken and added to 5 ml of ethanol, vortexed and centrifuged as above. The pellet was resuspended was in 0.5 ml of solution D and 1 ml of ethanol was added, then vortex and centrifuged again as before. The pellets was dried and after resuspended with 200 µl of TE and transferred to a microcentrifuge. The suspension was centrifuged (13 krpm, 5 min) and the supernatant containing the plasmid DNA was transferred to a new microcentrifuge. 1 µl of 10 mg/ml RNAse A. was added.

b) Minipreparation for sequencing

To ensure that sequencing reactions achieved good results, and maximum read length, a commercial mini-preparation kit was used to obtain highly pure plasmid DNA (High Pure Miniprep, Roche, Mannheim). Following the manufacturers' recommendations yielded 10 µg of high quality plasmid DNA

c) Midiprep and Maxiprep

To obtain higher amounts of DNA, the Qiagen Plasmid Maxi Kit was used. The plasmid purification protocols are based on a modified alkaline lysis procedure, followed by binding of plasmid DNA to QIAGEN Anion-Exchange Resin under appropriate low salt- and pH conditions. Plasmid DNA is eluted in a high-salt buffer and then concentrated and desalted by isopropanol precipitation. The DNA yield was respectively for the midiprep and the maxiprep 100 µg and 500 µg.

2.2.3.4.2 Determination of DNA concentration and purity

Determination of DNA concentration was carried out using a UV-spectrophotometer to measure absorption of DNA solutions at OD_{260} and OD_{280}. The OD_{260} was used to calculate the dsDNA concentration using the following formula: (OD_{260} x dilution factor x 50)/1000= DNA concentration (µg/ml). As the absorption wavelengths of protein overlaps that of DNA and can therefore cause the DNA concentration to be overestimated is necessary to measure OD_{280}, allowing a measure of DNA purity to be calculated using the following formula:

OD_{260}/OD_{280} = relative purity of DNA. A figure of between 1.8-1.9 is a sign of extremely pure DNA. At a ratio 260/280 of 1, only 50% of the OD_{260} reading is actually DNA, the rest being protein (Sambrook, 1989).

2.2.3.4.3 Precipitation of DNA (Ream, 1999)

To precipitate DNA, 2 vol of 100% ethanol at -20^{o}C and 0.1 vol of 3M NaOAC (pH 5.2) were added to the DNA solution in a microcentrifuge tube. After mixing the tube was kept at -20℃ for at least 30 min and then was spun at full speed in a microcentrifuge for 15 min at 4^{o}C. The supernatant was removed, and the DNA pellet washed with 70% ethanol, centrifuged as before. The supernatant was removed and the pellet allowed to dry, and resuspended in a suitable buffer.

2.2.3.4.4 DNA analysis by agarose gel electrophoresis (Darbre, 1999)

Agarose gel electrophoresis was used to estimate double stranded DNA concentration, to size fractionate fragments for restriction enzyme mapping , to isolate specific DNA fragments for cloning and to visualise the result of PCR amplification. Typically, 0.8-1.5% agarose gels (w/v in 1xTAE buffer, containing 0.5 µg/ml ethidium bromide) were cast and submerged in 1xTAE buffer. DNA samples were mixed with 6xDNA loading buffer (5:1), loaded into the wells and separated at a constant voltage of between 5-10 V/cm. DNA was visualised by UV (312 nm) transillumination and sized by comparison with 1kb+ DNA marker. When necessary, DNA bands were visualised using a hand held long wave UV lamp to avoid damage to the DNA, excised from agarose gels using a clean cover slip and purified using the Qiagen gel extraction kit, following the manufacturers´ protocol.

2.2.3.4.5 Purification of DNA

DNA was purified (for example after enzymatic manipulations, PCR products) either according to the method of Sambrook, or using a modified protocol from the Qiagen PCR purification kit.

a) <u>Phenol/chloroform extraction</u>

The solution volume was adjusted to 500 µl with water. An equal volume of TE-saturated phenol/chloroform/isoamyl alcohol (25:24:1) was added and mixed by vortexing. The phases were separated by centrifugation in a microcentrifuge for 10

min at full speed. The upper aqueous layer was then removed to a fresh tube. Depending upon the purity of the initial DNA, this step may have been repeated. To remove carried over phenol; one volume of chloroform was added and mixed by vortexing. The sample was then centrifuged again as above and the aqueous layer containing purified DNA removed to a fresh tube.

b) Purification using a Qiaquick column

The principle of Qiaquick system is based on the selective binding properties of a uniquely-designed silica-gel membrane. DNA adsorbs to the silica membrane in the presence of high salt while the contaminants pass through the column. The pure DNA is then eluted with Tris-buffer or water. For DNA samples in solution 5 volumes of buffer PB (Qiagen) were added to the sample. The sample was then loaded onto Qiaquick column and spun at maximum speed in a microcentrifuge for 1 min. The Flow through was discarded and the column was washed with 750 µl of buffer PE. The column was dried by centrifugation as above and the sample eluted into a fresh tube with 30-50 µl of EB (Qiagen). The same kit was used for the purification of DNA from agarose gels but with some modifications. The cut agarose gel was solubilised by adding the buffer QG and incubating for 10 min at 50℃. The sample was loaded onto the Qiaquick column and the protocol was followed as describe above for the DNA sample in solution.

2.2.3.5 Enzymatic manipulation of DNA

2.2.3.5.1 Restriction endonuclease digestion of DNA

Plasmid DNA for restriction analysis was digested for 1-2 h at the manufacturers recommended temperature, and in the recommended 1X reaction buffer. Typically, 1 µg of plasmid DNA was digested with 1 unit (U) of enzyme in an end volume of 20 µl. Double digests were carried out either in a buffer compatible with both enzymes, or in a sequential manner. Preparative restriction digests (for cloning) were carried out for 4 h as above, to ensure complete digestion of original plasmid DNA. The total volume of these reactions was also increased to 50 µl to ensure complete cleavage.

2.2.3.5.2 Enzymatic DNA amplification by polymerase chain reaction (PCR)

DNA was amplified by PCR. For analytical PCR reactions, the Taq DNA-Polymerase (MBI Fermentas and Bioline) were used. DNA fragments for cloning purposes were amplified using proofreading polymerases: The Phusion® polymerase (Finnzymes) and the mixture of Pfu (Promega, Mannheim) and Taq polymerase.
The PCR was done according to the manufacturers´ protocols.

2.2.3.5.3 DNA ligation

T4 DNA ligase catalyses the formation of a phosphodiester bond between juxtaposed 5´phosphate and 3´hydroxyl termini in duplex DNA or RNA. This enzyme will join blunt end and cohesive end as well. Ligation reactions were carried out in a 20 µl volume at 16^{o}C overnight or 1h at room temperature. Fragments for ligation were run on an agarose minigel to allow a rough estimation of relative concentration. A typical reaction contained at least 100 ng of DNA at a plasmid:insert molar ratio of 1:3. Before transformation of electrocompetent *E. coli* cells, the ligation reaction was ethanol precipitated to remove salts and re-suspended in 10 µl of water. 5 µl was then used to transform *E. coli*.

2.2.3.5.4 Dephosphorylation of sticky ends

To avoid re-ligation, de-phosphorylation of plasmid DNA sticky ends was carried out using shrimp alkaline phosphatase (SAP) or the calf intestinal phosphatase (CIP). Alkaline phosphatase catalyses the removal of 5´ phosphate group from DNA, RNA. Since alkaline phosphatase treated fragments lack 5´phosphoryl termini group required by ligases, they cannot self-ligate. De-phosphorylation of sticky ends was done according to the manufacturers´ protocols.

2.2.3.5.5 “Fill in” or blunt end reaction with Klenow fragment

Prior to ligation of none-cohesive DNA fragments, 5´ overhangs were filled in and 3´ overhangs were removed to form blunt ends by the polymerase Klenow. The reaction was done as the following: 10 µl DNA, 2.5 µl 10x Klenow buffer, 1 µl each dNTP, 2 µl Klenow (5U/µl), dH_2O to 25 µl. Reaction was allowed to proceed for 1 h at 30^{o}C, and then phenol/chloroform extracted and concentrated by EtOH precipitation. If needed, products were digested with the appropriate restriction enzymes, purified and ligated (total amount) to target vector.

2.2.3.6 Methods on RNA

2.2.3.6.1 Isolation of RNA from *Plasmodium falciparum*

RNA was isolated from parasites using a modification of the method of Kyes *et al* (Kyes *et al.*, 2000). It is important during RNA isolation to ensure that possible contamination with RNAses is reduced to a minimum. For this reason, it is desirable to use disposable, RNAse free plastic labware, and to try to limit the amount of time that the RNA is in contact with the atmosphere, as many RNAses are found freely floating in the air. All reactions were be carried out on ice, unless stated otherwise. Gloves were changed at regular intervals. 12 ml of culture at >5% parasitaemia, containing mainly trophozoite and schizont parasites stages was pelleted by centrifugation (1900 rpm, 2 min, 4^{o}C). The pellet was resuspended in PBS containing 0.01% saponin. The tube was placed on ice for 10 min to ensure complete lysis, before being subjected to a second centrifugation step (1900 rpm, 10 min, 4^{o}C). The parasite pellet was resuspended in 5 ml of Trizol (Gibco). 1 ml of chloroform was added and the contents of the tube were mixed well by vortexing. The sample was centrifuged at (10000 g 10 min, 4^{o}C). The upper aqueous phase was removed to a fresh tube and the RNA precipitated by addition of 0.8 vol of isopropanol. The tube was left at –20^{o}C for at least 1 h before centrifugation at 10000 g for 1 h to pellet the precipitated RNA. The resulting pellet was allowed to dry under sterile conditions, and resuspended in 200 µl of DEPC treated sterile DIW, containing 1 µl of RNAse OUT RNAse inhibitor.

2.2.3.6.2 cRNA synthesis

The cRNA for injection in oocytes was made using the kit from Ambion mMESSAGE mMACHINE, a kit for the in vitro synthesis of large amount of capped RNA. Capped RNA mimics most eukaryotic mRNAs found in vivo, because it has a 7-methyl guanosine cap structure at the 5´ end during polymerisation, which strongly increases RNA stability.

The cRNA was made following the manufacturer's protocol. Briefly, the template used for the reaction was prepared as following: 10 µg of the plasmid containing the SP6 promoter was linearized with an enzyme cutting downstream the cDNA after the poly A (+) site. The restriction digest was purified with the QIAGEN

PCR purification kit and ethanol precipitated as mentioned in **2.2.3.4.5** and resuspended to a final concentration of 1 µg/µl.

1 µg of the linearized template was added to the transcription reaction mixture to a final volume of 20 µl and incubated for 2 h. At the end of the incubation, the DNA was degraded by DNase I treatment for 15 min. The RNA was recovered by the lithium chloride precipitation: The reaction was stopped and RNA precipitated by adding 30 µl of nuclease free water and of the LiCl solution, chilled for 30 min at -20℃ pelleted by centrifugation at maximum speed at 4 ℃. The pellet was washed with 70% ethanol and repelleted. The pellet was resuspended in nuclease free water to a concentration of 1 µg/µl and stored at -80℃.

The transcription products were analysed by a 0.7% agarose gel electrophoresis containing ethidium bromide under denaturing conditions with formaldehyde. The samples diluted 1 to 1 with the 2X loading buffer were heated for 3-5 min at 85℃ and then loaded on the gel. After r unning the gel, the products were visualized on the gel using a UV transilluminator. *Pfcha* coding sequence was subcloned into the BglII site of the pSP64T oocyte expression vector that encompasses the 5´ and 3´ untranslated regions of the *X. laevis* ß-globin gene (Falcone and Andrews, 1991). The pSP64Tcha plasmid was linearized with BamHI, and capped cRNA was synthesized by the mMessage mMachineTM (Ambion, Inc., Austin, TX). Oocytes were microinjected with 25–50 ng of cRNA.

2.2.3.7 Protein analysis and detection

2.2.3.7.1 Determination of protein concentration (Bradford method)

Upon binding protein, the absorption spectrum of Coomassie brilliant blue G-250 shifts from 465 nm to 595 nm. The increase in absorption by 595 nm is a measure of the protein concentration of the solution (Bradford, 1976). Using calibration curves of known protein concentration, it was possible to calculate the protein concentration of *P. falciparum* and *E. coli* extracts prior to SDS-PAGE.

2.2.3.7.2 Preparation of *P.falciparum* protein extracts

Sequential extraction of parasite material was carried out as follows: 1.5 ml of PRBC at parasitaemia of >5% were pelleted by centrifugation (1900 rpm, 2 min RT). The resulting pellet was resuspended in 10 ml of sterile DIW to osmotically lyse

erythrocytes and the lysate then centrifuged as above. The parasite pellet was washed x3 in PBS to remove residual haemoglobin. The parasite pellet was resuspended in 250 µl of buffer A (See appendix) transferred to a microcentrifuge, and incubated on ice for one hour, with periodic vortexing. The tube was centrifuged for 10 min (13000 rpm, 4^{o}C), and the supernatant, containing the Triton-X-100 soluble fraction removed to a separate tube and mixed with 250 µl of 2X SDS loading buffer. The remaining pellet was then resuspended in 125 µl PBS, before addition of 125 µl 2X SDS loading buffer. Both fractions were then boiled in a heat block for 4 min. Insoluble material in the SDS soluble fraction was removed by centrifugation (13000 rpm, 10 min, 4^{o}C). Both fractions were frozen at –80℃ until needed .

2.2.3.7.3 Preparation of membrane proteins extracts from *Xenopus*

To get membrane proteins for western blot, 20 oocytes were injected with cRNA and incubated for 3 days at 18℃ for expression of the PfCHA protein. The oocytes were then placed in a microcentrifuge tube. From this step, everything was done on ice to avoid any protease activity. 400 µl (20 µl per oocyte) of the homogenizing buffer were added to the oocytes and they were broken using a special homogenizer. The mixture was spun for 10 min at 4℃ at 3 krpm in a microcentrifuge. Three phases were obtained: the upper phase contained yolk proteins, the lower phase the debris, and the middle phase the membrane proteins which were carefully pipetted and transferred to another tube and centrifuged for 1 h at 4℃ at 50 krpm. The supernatant was mixed with the pellet from the first centrifugation and the pellet containing the membrane proteins was resuspended in 20 µl (1 µl/oocyte) of homogenizing solution.

2.2.3.7.4 SDS-Polyacrylamide gel electrophoresis

Polyacrylamide-Gel electrophoresis (PAGE) was used to separate proteins from bacterial and parasite cell lysates, for use in either Coomassie staining, or protein blotting experiments. Prepared protein samples were stored at –20^{o}C until needed. Uniform gel concentrations were prepared in a Protean II or Mini Protean vertical electrophoresis apparatus (Biorad). Glass plates were cleaned in methanol, rinsed in water and dried prior to assembly of the casting apparatus. A separating gel, typically 10% was cast and overlaid with water to achieve a flat interface; polymerisation was allowed to take place. The water was then removed by aspiration

and stacking gel cast above the separating gel, containing an appropriately sized comb. After polymerisation, the gel holder was removed from the casting holder and transferred to the electrophoresis tank. The tank was filled with 1x SDS running buffer. The comb was then removed, and the wells were "rinsed" using a syringe, to ensure that no unpolymerised acrylamide remained in the bottom of the wells. Samples and a suitable pre-stained molecular weight marker were loaded. Electrophoresis was carried out at constant current (15 mA per gel) until the samples exited the stacking gel, at which point the current was increased to 30 mA per gel. Electrophoresis was stopped when the bromophenol blue front reached the end of the gel. Plates were dismantled and the gels either stained with Coomassie blue to visualise proteins, or processed further for western blotting.

2.2.3.7.5 Western analysis

Western blotting was performed in a Mini Protean chamber (Biorad). The sponge was wetted with 1x transfer buffer and placed on the black side of the blot sandwich apparatus. Two pieces of 3MM paper were cut to size, and wetted with 1x transfer buffer and placed on top of the sponges. The resolved gel was then carefully placed on top of the 3MM paper. A suitably sized piece of PVDF membrane was activated in 100% methanol and equilibrated for 10 min in 1x transfer buffer before being carefully placed on top of the gel, ensuring that no air bubbles were present between gel and membrane. Two further pieces of 3MM paper and the final sponge were wetted in 1x transfer buffer, and placed on top of the assembled stack. The sandwich apparatus was closed and transferred to the blotting chamber, ensuring that the black side of the sandwich apparatus corresponded to the black side of the sandwich holder. The transfer tank was filled with 1x transfer buffer; a small stirrer bar was placed in the bottom of the tank. The entire apparatus was then placed in a plastic bath full of crushed ice and moved to a stirrer in a cold-room. Transfer took place at 100 V constant for 1 h. After transfer, the membrane was removed from the blotting apparatus, and blocked in PBS/milk powder for at least one hour. The membrane was then incubated for between 1-2 h at RT with primary antibody, diluted to a suitable concentration in PBS/5% skim milk powder. The membrane was then washed for 3x20 min in PBS/tween-20 at RT. Incubation with secondary antibody was carried out as for the primary, for 30 min-1 h at RT. The membrane was then washed for 3x20 min in PBS/0.1% Tween-20 at RT. Detection was performed using

the ECL detection system as recommended by the manufacturer. The exposure of autoradiographic films was performed in a dark room using a film cassette to insure a tight fit between membrane and film. Usually, 1 s up to 30 min exposure was performed.

For horseradish peroxidase based secondary antibodies, the membrane was immersed for several seconds in developing solution, allowed to drip dry, placed between a folded piece of transparency film attached to a suitably sized sheet of 3MM paper and placed in the film cassette. After exposure for a suitable period of time, the film was developed.

2.2.4 Functional assays

2.2.4.1 Oocytes expression

The female frogs were obtained from CNRS, Montpellier, France, or from Xenopus Express, Vernassal, France. Stage V-VI oocytes were harvested from *X. laevis* and defolliculated with collagenase (Sigma). For oocyte extraction, the frog was first anaesthetized by 15 min incubation in an ice-cold solution containing 2 mM Ethyl-n-aminobenzoat-methansulfonate. The frog was then brought on ice and a small incision was made to remove the oocytes. After isolation of the frog's oocytes, the incision was closed immediately and the frog was washed with water and returned to the tank. The oocytes were separated with fine forceps. The follicular cell layer was removed from the oocytes by 45 min incubation in a calcium free solution (OR2 solution) containing 2 mg/ml collagenase. After incubation, oocytes were washed first with OR2 solution and then with OR2 solutions containing increasing concentrations of calcium and finally with the SOS solution in which the oocytes are kept. Oocytes were allowed to recover from the collagenase treatment for at least 2 h before injection of RNA. Oocytes were injected at the latest the day after the collagenase treatment. The oocytes from stages V-VI were selected for cRNA injection. Pipettes used for cRNA injection were pulled using a standard pipette puller. Pipettes with an opening of ~15-20 µm in diameter were polished to obtain a needle-like shape which reduces oocytes damage during injection. Microinjection of cRNA (~50 nl per oocyte) was performed using an automatic injector.

2.2.4.2 $^{45}Ca^{2+}$ uptake experiments

Standard uptake solutions was made of Ringer solution containing 10 µCi/ml of $^{45}Ca^{2+}$, buffered with 5 mM Hepes, tricine or MES, respectively for the pHs 7.5, 8.5 and 6.5. In each batch of experiment, ten oocytes from both negative control (water injected oocytes) and cRNA injected oocytes were separately placed for different periods of time into 500 µl of the same solution supplemented with 10 µCi/ml $^{45}Ca^{2+}$. Uptake was performed at room temperature. For uptake experiments in presence of inhibitors, oocytes were preincubated for 15 min in a solution containing the inhibitor and then incubated in radioactive solution containing the inhibitor for 1 h. At the end of the incubation period oocytes were thoroughly washed three times with large volumes of the ice-cold Ringer solution with the corresponding pH in order to remove the extracellular radioactivity. Each individual oocyte was subsequently placed into a separate scintillation vial, dissolved for 30 min with 200 ml of 5% SDS, before addition of 2.5 ml of scintillation fluid, and the solution was counted for radioactivity in a Beckman LS2100 scintillation counter.

2.2.4.3 Extracellular pH measurements

A qualitative assay of external medium acidification was designed to estimate H^+ secretion by the oocytes. The assay followed a protocol from Jaissier *et al*. (Jaisser *et al.*, 1993). 3 days after injection of cRNA, the oocytes were transferred in a weakly buffered solution (96 mM NaCl, 2 mM KCl, 1 mM $CaCl_2$, 1mM $MgCl_2$, 500 µM MOPS adjusted to pH 8.1 with NaOH), containing the pH indicator Red phenol (200 mg/l). Oocytes were placed individually in a small drop of the same solution under oil. The volume of the droplet was then reduced to 0.5 to 1.0 µl by gently removing the solution with a thin glass pipette. After 1h incubation at room temperature, a picture was taken.

2.2.4.4 Membrane potential and internal pH measurements

The membrane potential and the internal pH were simultaneously measured with double barrelled microelectrodes. They were constructed as described previously (Anagnostopoulos and Planelles 1987, Cougnon *et al.* 1996). The pH sensitive channel was backfilled with the H^+-Ionophore 95291 from Fluka and the

shaft filled with 67 mM NaCl, 40 mM KH_2PO_4 und 23 mM NaOH. The Na^+ selective electrode was backfilled with Fluka 71196 and the shaft filled with 100 mM NaCl.

2.2.4.5 Growth assays

The PfCHA gene was expressed in *S. cerevisiae* defect in calcium tolerance strain. One single yeast transformed colony was picked and inoculated in 10 ml of selective medium. The incubation was done at 30℃ in a shaker (300 rpm) for 2 days to reach the stationary phase. 10 µl of this preculture were then inoculated into 10 ml of fresh selective medium and further incubated under the same conditions. In case different plasmid constructs were grown in parallel under the same conditions to be compared, the starting optical densities were checked and adjusted to be identical. At various time points, aliquots of the cultures were removed and growth was determined by measuring the optical density at 600 nm. Alternatively, in other experiments, the preculture was diluted to an OD_{600} of 0.4 and further grown to an OD_{600} of 1.0. Serial dilutions were made and 10 µl from each dilution was spotted onto selective agar plates and the plates were incubated at 30℃ at least for 3 days.

2.3 Appendix: Solutions, Buffers, media and miscellaneous

2.3.1 Solutions

Homogenizing solution for oocytes

Sucrose	0.3 M
Sodium phosphate pH 7.4	10 mM
Aprotinin	40 µg/ml
Leupeptin	20 µg/ml
PMSF	1 mM

Ampicillin (sodium salt)

Stock concentration	100 mg/ml
Working concentration	100 µg/ml

Streptomycin

Stock concentration	50 mg/ml
Working concentration	30 µg/ml

Solutions for yeast transformation

10X LiAc

Lithium Acetate pH 7.5	1 M

Adjust the pH to 7.5 with dilute glacial acetic acid and bring up the volume to 100 ml. Sterilize with a filter and store at room temperature.

1X LiAc/0.5X TE

Lithium Acetate pH 7.5	100 mM
Tris-HCl pH 7.5	5 mM
EDTA	0.5 mM

Sterilize with a filter and store at room temperature.

50% PEG-3350

For 100 ml, dissolve 50 g of PEG-3350 in 90 ml of deionised water. You may have to heat the solution to fully dissolve the PEG. Bring up the volume to 100 ml with deionised water. Autoclave and store at room temperature.

1X LiAc/40% PEG-3350/1X TE

Lithium Acetate pH 7.5	100 mM
PEG-3350	40%
Tris-HCl pH 7.5	10 mM
EDTA	1 mM

Prepare solution immediately prior to use. For 100 ml, mix together 10 ml of 10X LiAC, 10 ml of 10X TE, and 80 ml of 50% PEG-3350. Sterilize with a filter.

Solutions for oocytes experiments

OR-2 solution

NaCl	100 mM
KCl	2 mM
$MgCl_2$	1 mM
Hepes	5 mM

pH 7.6 with NaOH. Add 800 µl of 50 mg/ml gentamycin in 400 ml of solution.

SOS solution

NaCl	100 mM
KCl	2 mM
$CaCl_2$	1.8 mM
$MgCl_2$	1 mM
Hepes	5 mM

pH 7.6 with NaOH. Add 800 µl of 50 mg/ml gentamycin and 500 µl of 220 mg/ml pyruvate in 400 ml of solution.

Ringer solution

NaCl	96 mM
KCl	2 mM
$CaCl_2$	1 mM
$MgCl_2$	1 mM
Hepes	5 mM

pH 7.5 with NaOH. Use 5 mM MES or tricine to pH Ringer solution at pH 6.5 or 8.5.

2.3.2 Buffers

50X Tris-acetate-EDTA (TAE)

Tris base	242 g
Glacial acetic acid	57.1 ml
0.5 M EDTA pH 8.0	100 ml

5X Tris-borate-EDTA (TBE)

Tris base	54 g
Boric acid	27.5 g
0.5 M EDTA pH 8.0	20 ml

Buffers and gels for electrophoresis of RNA

20x MOPS-Buffer

MOPS	0.4 M
Natriumacetate	40 mM
EDTA pH 8.0	5 mM
H_2O dest.	ad 500 ml

RNA gel

MOPS-Buffer	1x
LE Agarose	0.7%
Formaldehyde	2.2 M

Buffers and gels for SDS-PAGE

Stacking gel

H_2O	3.4 ml
Acrylamide (29:1)	830 µl
1 M Tris-HCl pH 6.8	630 µl
10% APS	50 µl
TEMED	5 µl

Separating gel 12%

H_2O	3.3 ml
Acrylamide (29:1)	4.0 ml
1,5 M Tris-HCl pH 8.8	2,5 ml
10 % SDS	100 µl
10% APS	100 µl
TEMED	6 µl

Running buffer 1x

Glycin	250 mM
Tris/HCl, pH 6.8	25 mM
SDS	0.1%

2 x SDS protein sample buffer

Tris-HCl pH 6.8	100 mM
Mercaptoethanol	2%
SDS	4%
Bromophenol blue	2%
Glycerol	20%

Transfer buffer 1x	
Tris-base	48 mM
Glycin	39 mM
SDS	13 mM

TBS 1x	
Tris-HCl pH 7.5	50 mM
NaCl	0.15 M

TBST 1x	
TBS	1x
Tween 20	0.1%

2.3.2 Media

The parasite medium

RPMI 1640 with 25 mM HEPES, L-Glutamin, NaHCO3

10% human serum (A^+)

Hypoxanthin	10 mM
Gentamycin	4 µg/ml

Media for bacteria

LB medium

Tryptone	1%
Yeast extract	0.5%
NaCl	0.5%

Super Broth

Tryptone	3.5%
Yeast extract	2%
NaCl	0.5%
NaOH	5 mM

LB agar plates

LB medium	
Agar	1%

For agar plates, after autoclaving of the LB agar, it was let cooled down to 50℃, antibiotic was added and the agar was poured on Petri dishes.

SOC medium

Bacto-Trypton	2 %
Yeast extract	0.5 %
NaCl	10 mM
KCl	5 mM
$MgCl_2$	10 mM
$MgSO_4$ pH 6.8-7.0	10 mM

Before addition of magnesium salts, media were sterilised by autoclavation. Mg^{2+} salts were prepared separately, sterile filtered and added to the autoclaved medium.

Media for yeast

YPD

Yeast extract	1%
Peptone	2%
Glucose	2%

YPD selective medium Ca^{2+}

Yeast extract	1%
Peptone	2%
Glucose	2%
Ca^{2+}	200 mM

pH 5.5 with NaOH

YPD selective medium Mn^{2+}

Yeast extract	1%
Peptone	2%
Glucose	2%
Mn^{2+}	10 mM

YNB medium

Yeast nitrogen base	0.67%
Casamino acids	0.5%
Glucose	2%
Tryptophan	0.01%

Solutions of glucose, tryptophan and Ca^{2+} were separetely filter sterilized and added to the medium after autoclavation.

YPD agar: YPD, 2% agar
YPD selective medium Ca^{2+} agar: YPD selective medium Ca^{2+}, 2% agar
YNB agar: YNB, 2% agar

2.3.4 Miscellaneous

MACS buffer

PBS	1x
BSA%	0.5%
EDTA	2 mM

RNA Transcription reaction:

Nuclease free H_2O	ad 20 µl
10x reaction buffer	2 µl
2x NTP	10 µl
Template	1 µg
Enzyme	2 µl

6X gel loading buffer (10 ml)

Glycerol	6 ml
EDTA 0.5M	1.2 ml
Bromophenol blue	9 mg
Xylene cyanol	9 mg
DIW	2.8 ml

1 kb+ marker (600 µl)

1kb+ DNA ladder (Gibco)	50 µl
6X loading buffer	100 µl
1XTAE buffer	450µl

3. RESULTS

The calcium/hydrogen antiporters are known to be involved in various metabolic and physiological pathways in eukaryotic cells (Saris and Carafoli, 2005). In *Plasmodium* previous studies have postulated the existence of a calcium/hydrogen antiporter involved in important mechanisms in the parasite (Tanabe *et al.*, 1982; Tanabe *et al.*, 1983; Kramer and Ginsburg, 1991). The completion of the genome sequence of *P. falciparum* in 2002 has provided the information about a putative calcium hydrogen antiporter. To confirm and study the role of this putative gene in calcium homeostasis in *P. falciparum*, it was cloned and expressed in yeast and *Xenopus laevis* oocytes for characterization.

Because of the high A/T content of the Plasmodium genome, which has already been shown to be problematic for expression in heterologuous system (Baca and Hol, 2000), the sequence was redesigned and synthesized on the basis of the yeast codon usage. The gene was subsequently cloned in the oocyte expression vector pSP64T and the yeast expression vectors pVT100 and pVT100-GFP2.

3.1 Sequence features

Pfcha is a gene encoding a polypeptide of 441 amino acids, exhibiting 46% sequence identity (60% similarity) to the yeast vacuolar Ca^{2+}/H^{+} antiporter VCX1. It was also found to be 40% identical (53% similar) to the mung bean vacuolar Ca^{2+}/H^{+} antiporter VCAX1 and 37% identical (52% similar) to the Arabidopsis thaliana vacuolar Ca^{2+}/H^{+} antiporter.

Like others transporters from the calcium exchanger gene family, PfCHA contains a central hydrophilic motif that is rich in acidic amino acids, and which bisects the polypeptide into two groups of five and six transmembrane domains (Fig. 3.1). Computer-assisted hydropathy analyses of PfCHA generated a profile with an equivalent spacing and alternation of hydrophilic with hydrophobic domains, consistent with intrinsic membrane proteins that span the membrane 11 times (Fig. 3.2). It contains an N-terminus hydrophilic region that is similar to the CAX1 autoinhibitory domain. It contains also several phosphorylation sites and an acidic rich motif not found in the CAX-like gene family.

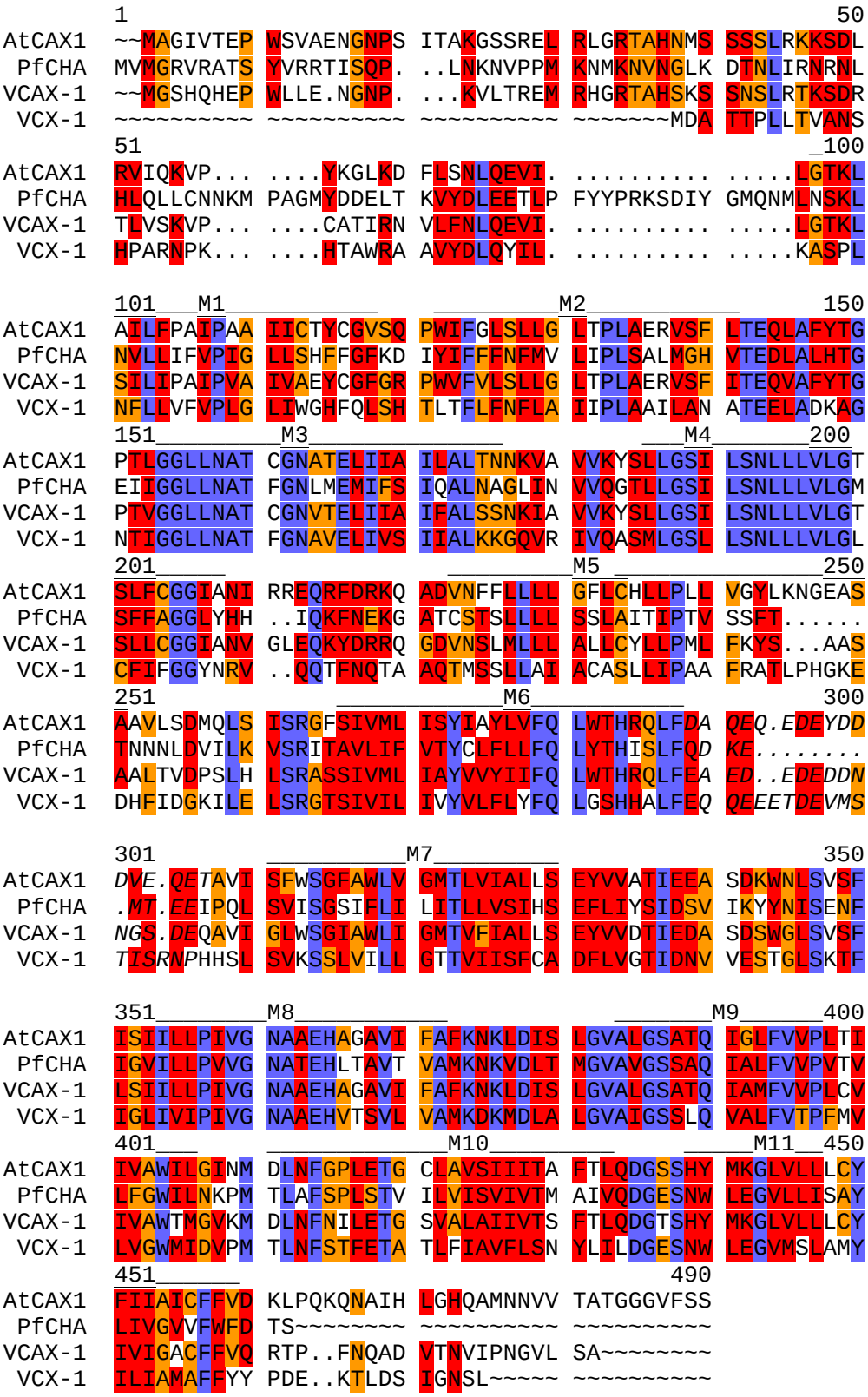

Fig. 3.1: Alignment of deduced amino acid sequences of polypeptides encoded by *A. thaliana* CAX1, the putative PfCHA, the mung bean VCAX1 and the *S. cerevisiae* VCX1. Sequences were aligned using CLUSTAL. Gaps were introduced to maximize the alignments and are denoted by hyphens. The 11 putative transmembrane domains (M1-M11) predicted for all transporters and the in acidic residues in the central hydrophilic are shown in italics.

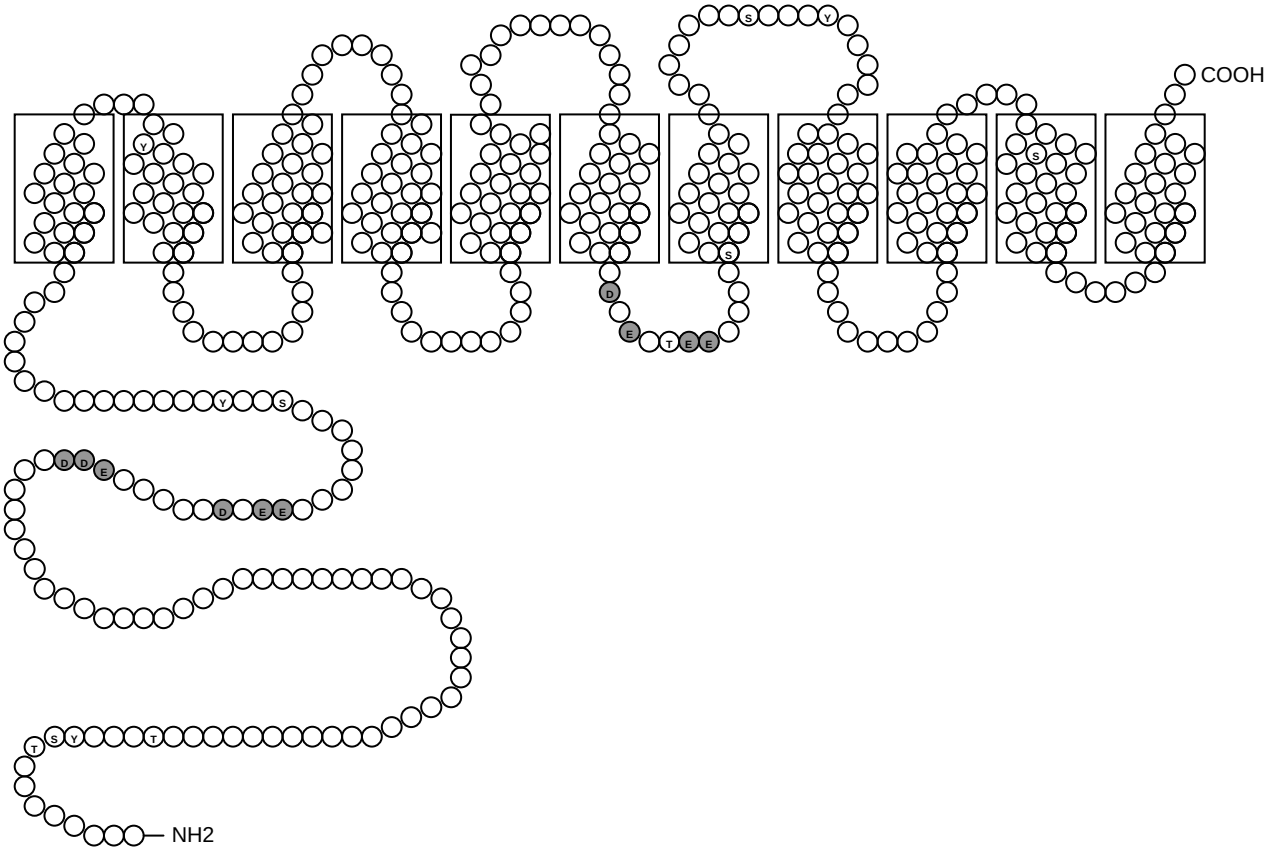

Fig. 3.2: Hydropathy plot of PfCHA. Phosphorylation sites (letters in open circle) were determined using the Netphos programme. Transmembrane domains are indicated in the boxes. Acidic amino acid motifs (grey coloured circles) are shown.

3.2 Functional complementation of *pfcha* in yeast

Several Ca^{2+}/H^{+} exchangers have been characterized in yeast (Hirschi *et al.*, 1996, Pozos *et al.*, 1996). To evaluate the Ca^{2+}-transport activity of PfCHA, it was introduced into *S. cerevisiae* K667 deleted for vacuolar Ca^{2+}/H^{+} antiporter (VCX1), the vacuolar Ca^{2+}-ATPase (PMC1) and the manganese resistance protein (CNB1). This strain is unable to grow on high Ca^{2+} media. In the present experiment, PfCHA was inserted between the aldehyde dehydrogenase promoter (ADH) and terminator of the pVT100U vector. pVT100U has uracil as a selectable marker. For the GFP-tagged variant of PfCHA, it was inserted in a pVTGFP vector. This vector has the same features as pVT100U and a GFP-tag at the 3´end upstream of the ADH terminator. GFP was at the C-terminus of PfCHA (Fig. 3.3).

As PfCHA may not contain the signal sequences to direct it to the yeast vacuole, a chimera construct was made by fusing the N-terminal part and the first transmembrane domain of vcx-1 to the *pfcha* gene minus its first transmembrane domain (Fig. 3.3). As a control we investigated VCX1, the yeast vacuolar Ca^{2+}/H^{+} antiporter.

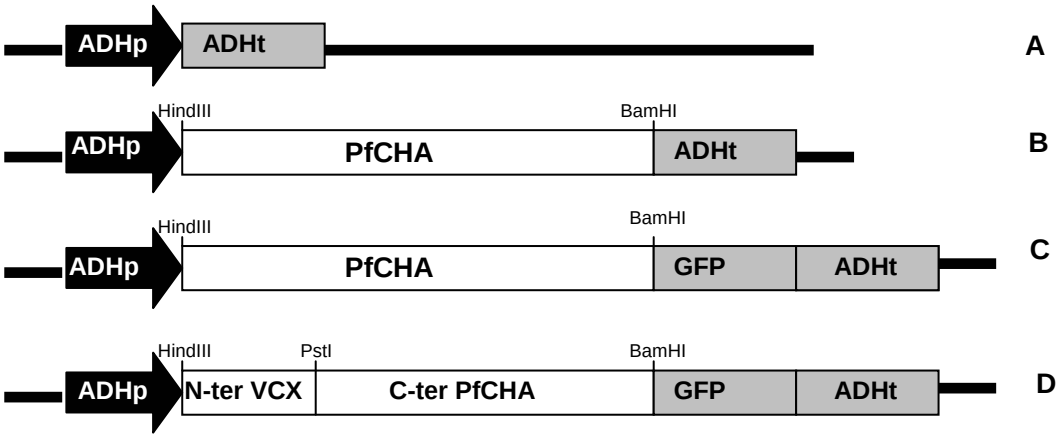

Fig. 3.3: Constructs for expression in yeast. Vector alone (A). The PCR amplified HindIII/BamHI fragment of *pfcha* was cloned between ADH promoter (ADHp) and terminator (B), between ADHp and GFP (C), as well as the fragments HindIII/PstI of vcx1 and PstI/BamHI of *pfcha* (D)

We first investigated the subcellular localisation of PfCHA in transformed yeast cells. In order to determine the subcellular localisation of the expressed proteins from our different constructs, several of experiments were performed. Initially, a fluorescence microscopy localization of GFP-tagged PfCHA, VCX1 and VCXPfCHA was performed. Yeast containing plasmids with the tagged-proteins were grown in selective media untill the logarithmic phase and observed under the confocal microscope using a 488nm laser. Confocal imagings of GFP fluorescence emitted from the transformed cells suggested a vacuolar localization of PfCHA (Fig. 3.4a). Although it is difficult to distinguish the ER from the vacuole in those pictures, the localisation of the green fluorescence in the positive control, VCX-1GFP and PfCHAGFP are similar. The chimera protein VCXPfCHA has also similar localization (data not shown). Given the previous evidence of the VCX-1 localisation to the vacuole and the similar fluorescence pattern, the data favour a localisation of PfCHA to the vacuole in yeast.

To further confirm this evidence, a biochemical subcellular localisation experiment was performed. The yeast expressing PfCHAGFP were grown to the stationary phase and lysed. The organelles were separated by sequential centrifugations and a sucrose gradient centrifugation. Proteins from different fractions of the sucrose gradient were separated on SDS-PAGE gels, and then transferred to nitrocellulose membranes. The membranes were probed with an anti-GFP antibody and an anti-vacuolar phosphatase antibody. The GFP antibody recognized a 80 kD protein which is consistent with the sum of sGFP (28 kD) and PfCHA (48 kD). The result of the Western analysis showed that the GFP-tagged protein containing fractions correlated with vacuolar phosphatase (Fig. 3.4b). This data further supports the evidence that PfCHA is localised to the vacuole in yeast.

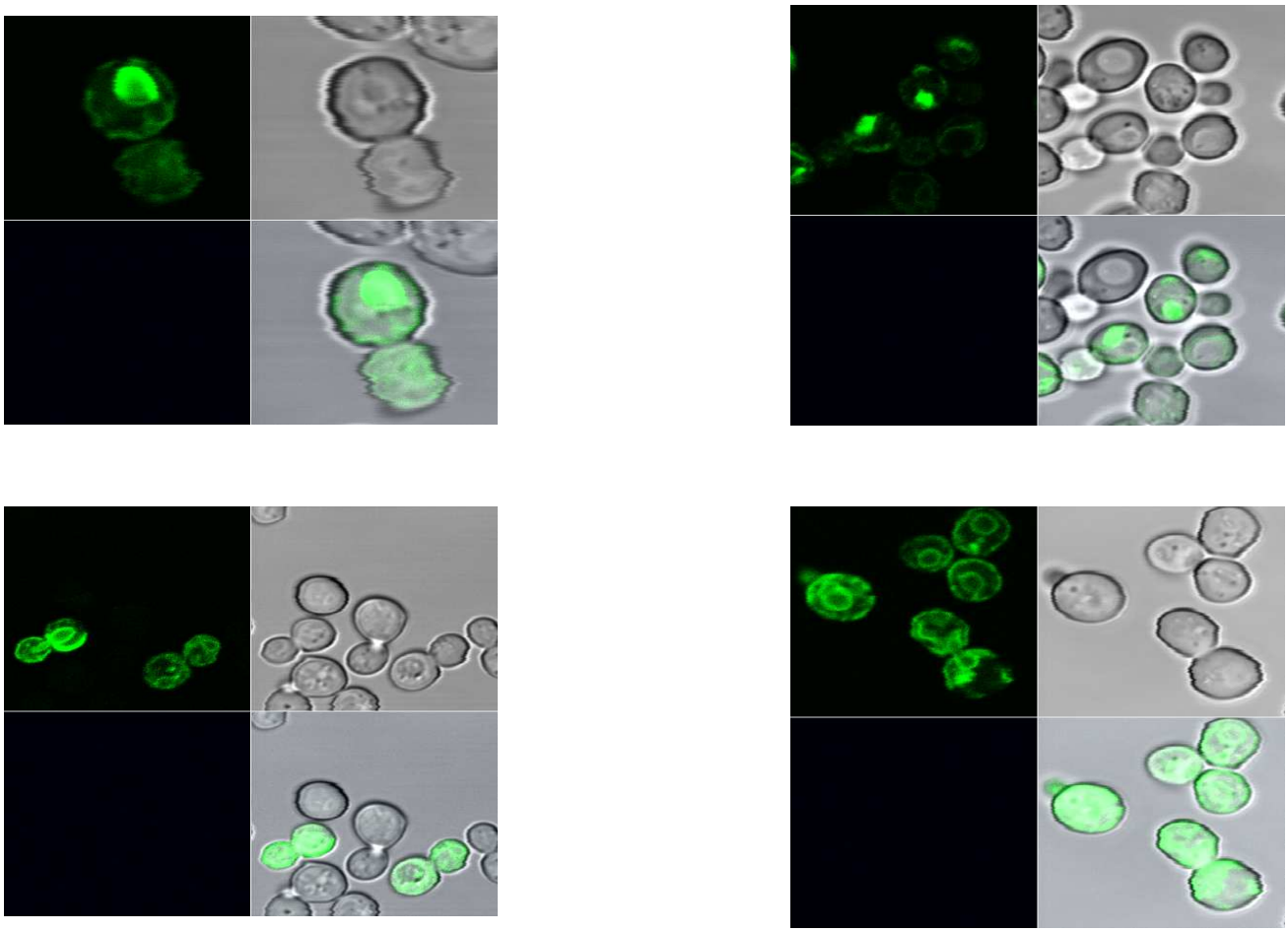

Positive control (Vcx-1) PfCHA

Fig. 3.4a: Subcellular localisation of GFP-tagged proteins by confocal microscopy. Cells were visualized by fluorescence microscopy during the logarithmic growth. Rows represent different digital zooms from the same magnification. In each panel: top left, GFP fluorescence; top right, differential interference contrast (DIC); bottom right, merge.

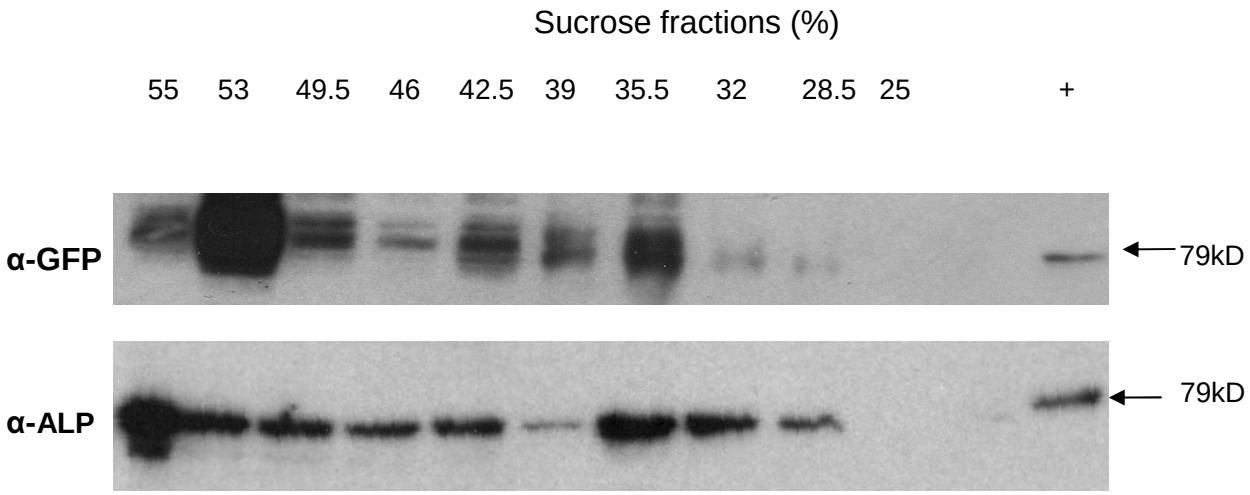

Fig. 3.4b: Subcellular localisation of GFP-tagged PfCHA. The *Δpmc1 Δvcx1 Δcnb1* yeast strain was transformed with the construct pVTGFPpfcha and grown in selective medium. Cells were harvested by centrifugation and converted to spheroplasts by zymolase treatment. Spheroplasts were lysed by resuspending in a solution of 12% sucrose, 10 mM TEA, 1 mM PMSF, 1 mM EDTA. Cell debris was pelleted and the supernatant containing the organelles was loaded on the top of a sucrose gradient (25-55%). After centrifugation, 10 fractions were collected. Proteins extracts from each fraction were separated by SDS-polyacrylamide gel electrophoresis and transferred to nitrocellulose. Proteins were immunodetected with antibodies for GFP and the vacuolar alkaline phosphatase α-ALP.

Being localized to the vacuole, we wanted to test if *pfcha* has calcium/hydrogen antiporter activity in yeast. For this purpose, a calcium tolerance assay was performed. The calcium tolerance assay investigates the yeast´s resistance to high Ca^{2+} concentration (200 mM) in moderately acidic conditions (pH 5.5) on agar plates (Hirschi *et al.*, 1996). In this calcium tolerance assay, *pfcha* as well as the chimera *vcxpfcha* were not able to complement the phenotype. As shown in Fig. 3.5, both constructs could not grow on yeast plates supplemented with 200 mM Ca^{2+} at pH 5.5. Even after one week incubation, the growth between PfCHA and the negative control (the triple mutant) were comparable. In contrast, VCX1 grew normally. Surprisingly the chimeric protein VCXPfCHA did not grow as well. The antiport activity function has probably been abrogated by the fusion.

Because there was no growth on agar plates, the calcium tolerance assays were repeated in liquid medium supplemented with 200 mM Ca^{2+} at pH 5.5, under vigorous shaking at 30℃. The growth of yeast was determ ined by measuring the OD_{600} of the medium at various time points. Under these conditions, *pfcha* was able to complement the calcium deficient to a certain extent. Indeed, the OD_{600} at day was 7 for PfCHA in comparison with VCX1 which was 17. The growth of PfCHA was significantly higher than the negative control (Fig. 3.6a).

Salt stress has previously been shown to stimulate calcium transport activities in yeast (Cheng *et al.*, 2002). Other reports have established that a P-type Ca^{2+} ATPase are induced by salt stress in plant (Perez-Prat, 1992,Wimmers, 1992). It is speculated that salt stress causes increases in cytosolic Ca^{2+} concentration. To investigate if the salt stress could stimulate the growth, PfCHA containing yeast cells were grown in the same selective liquid medium as described above and supplemented with various concentrations of NaCl. Growth was determined by measuring the OD_{600}. According to the results summarized in Fig. 3.6c, NaCl seems to have no influence at the used concentrations in the growth of PfCHA yeast.

Some calcium hydrogen antiporters are actually called cation hydrogen transporters due to their capacity to transport diverse divalent cations (Shigaki *et al.*, 2003). BLAST analysis has shown high similarities of *pfcha* with the yeast manganese resistance protein. To test if PfCHA could transport Mn^{2+}, a manganese tolerance experiment was performed. Yeast cells were grown in YPD medium

supplemented with 10mM Mn^{2+} and the growth was measured spectrophotometrically at day 4 (OD_{600}). There was almost no growth (OD_{600} was less than 1.0 at day 4) for all the constructs (Fig. 3.6d). That VCX1 containing cells did not grow is expectable as it does not transport Mn^{2+}. Although we did not have a positive control, it is likely that the absence of growth is due to the incapability of PfCHA to transport Mn^{2+}.

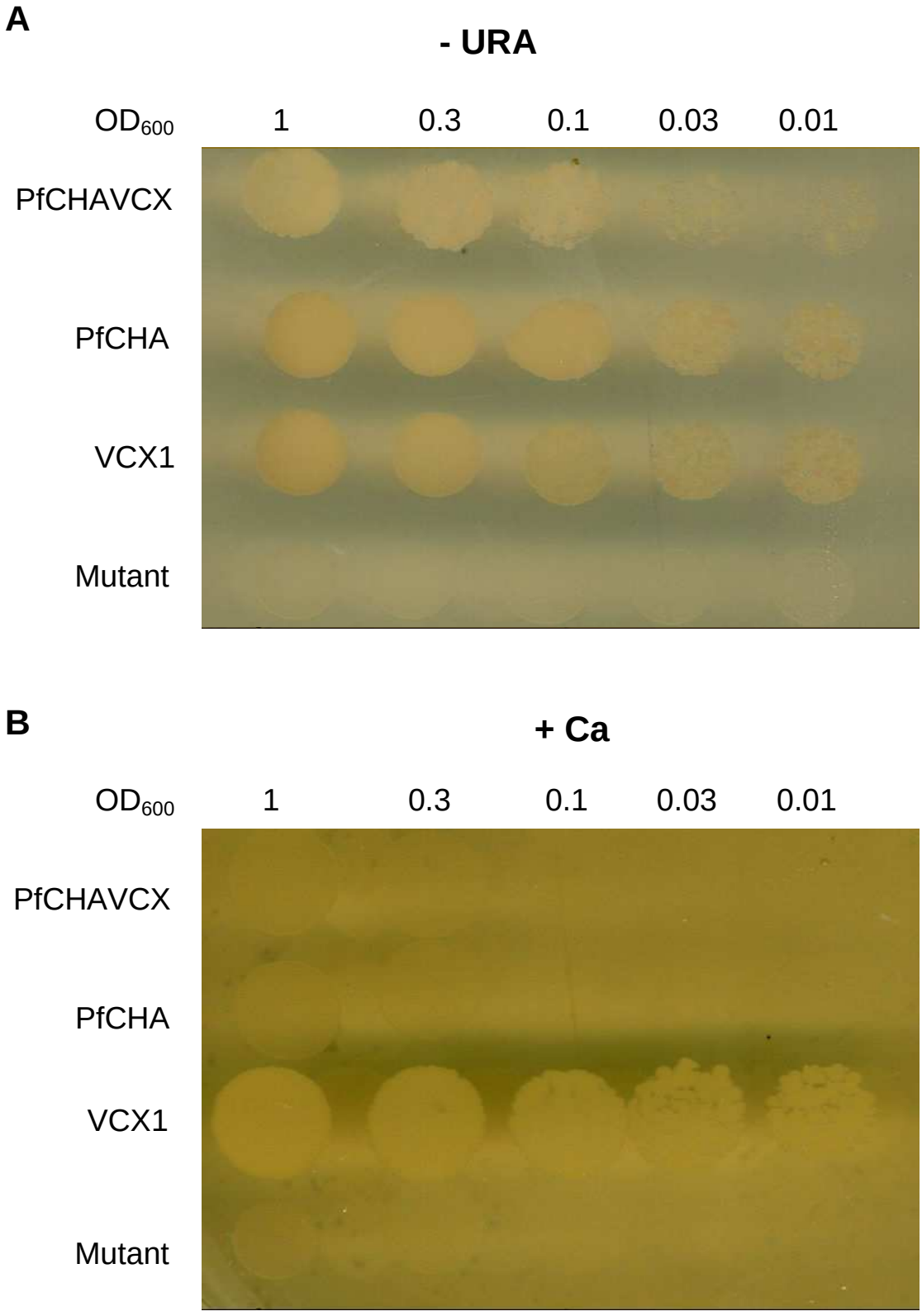

Fig. 3.5: Calcium tolerance assay. Overnight yeast cultures were diluted to OD_{600} 0.4 and further grown in a shaker at 30℃ to OD_{600} of 1.0 in YNB medium. The negative control (double mutant) was grown under the same conditions in YPD medium. Cells were diluted 4-fold and 10µl of each dilution was spotted on YNB plates without uracil (-URA) **(A)** and 10µl on YPD plates pH 5.5 supplemented with 200 mM $CaCl_2$ **(B)**. Plates were incubated for 3 days at 30℃

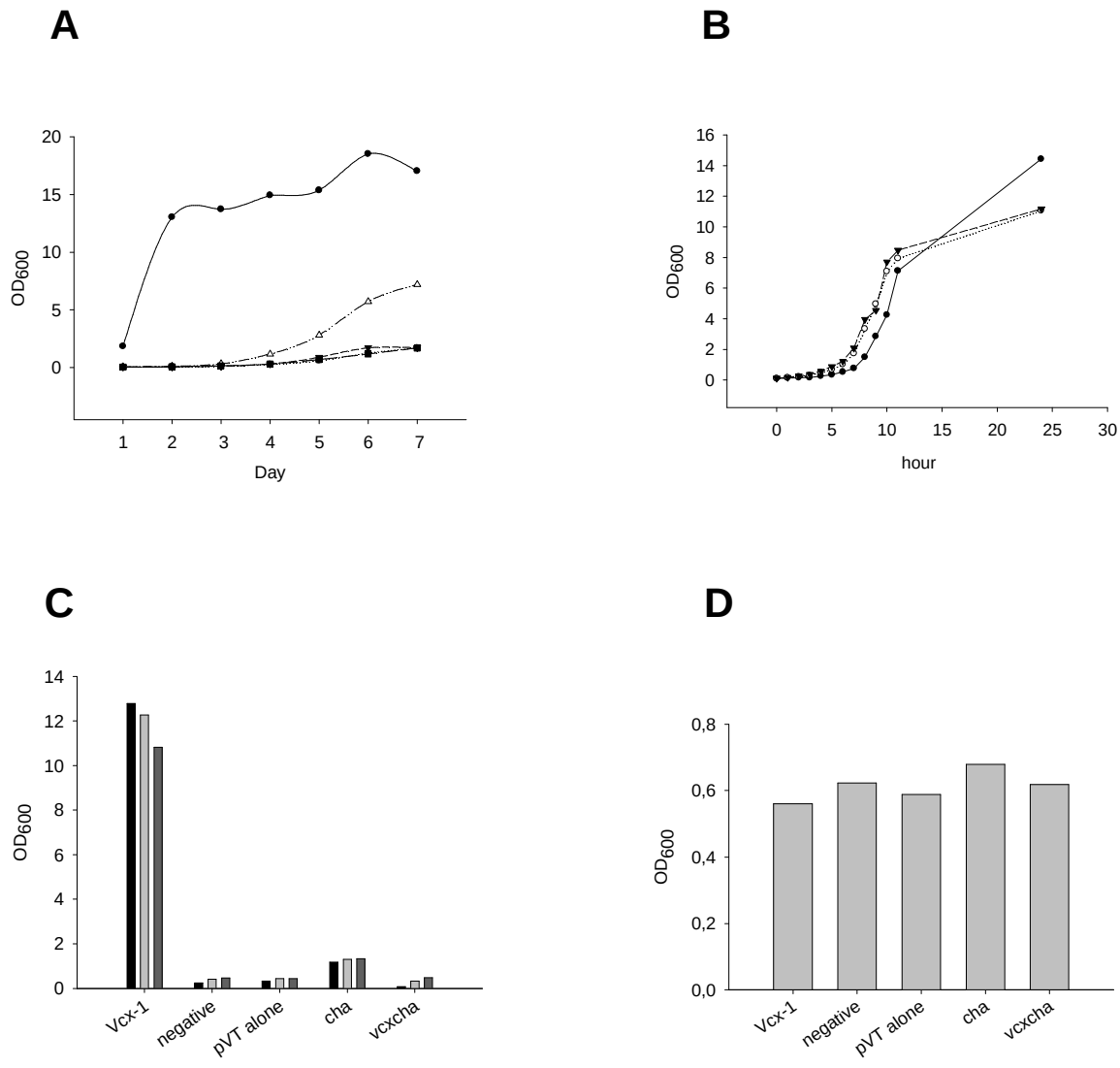

Fig. 3.6: Yeast complementation assays

(A) Yeast calcium tolerance assay in selective medium. Yeast cells were preincubated in YNB medium without uracil for 2 days. Then 10 µl was incubated in 10 ml of selective medium (pH 5.5, 200mM Ca^{2+}). OD_{600} was measured every day. Filled circle, vcx-1; open circle, vector alone; filled triangle, negative control; open triangle, *pfcha*, filled square, vcxcha. **(B)** Growth of yeast in normal YPD medium. Open circle, double mutant; filled circle, *vcxcha*; filled triangle, *pfcha*. **(C)** Yeast growth in selective medium with various concentrations of NaCl. Yeast was preincubated in YNB medium without uracil for 2 days. Then 10 µl was incubated in 10 ml of selective medium (pH 5.5, 200 mM Ca^{2+}) containing 0mM NaCl (black bars), 200 mM NaCl (light grey bars), and 400 mM (dark grey bars). OD_{600} was measured at day 4. **(D)** Yeast Mn^{2+} tolerance assay. The different yeast cells was preincubated in YNB medium without uracil for 2 days. 10µl was incubated in 10 ml of selective medium made of YPD supplemented with 10mM Mn^{2+}. The OD_{600} was measured at day 4.

3.3 Functional expression of putative *pfcha* in Xenopus oocytes

The Xenopus expression system is a valuable tool for studies of heterologuous pumps, channels and transporters (Weber, 1999). Malarial proteins have been already characterized by using this system (Carter *et al.*, 2000, Eckstein-Ludwig *et al.*, 2003; Nessler *et al.*, 2004). As a second approach, the *Xenopus laevis* oocyte expression system was chosen for a further and independent characterization of *pfcha*. For this purpose, the redesigned *pfcha* was cloned in the Xenopus oocyte vector pSP64T such that it was embedded in the sequence coding for the untranslated region of the ß-globin gene to enhance the expression. The *pfcha* fragment contained at its 3´end the hemagglutin epitope and contained at the 5' end just before the starting codon a Kozac sequence to enhance expression.

3.3.1 *pfcha* mediates Ca^{2+}/H^{+} exchange

To investigate the ability of PfCHA to exchange Ca^{2+} and protons, the uptake of $^{45}Ca^{2+}$ into oocytes incubated was measured at different pH values. At each pH, uptake in $cRNA_{pfcha}$ injected oocytes was compared to control oocytes. As shown in Fig. 3.7a, there is a pH-dependent uptake of $^{45}Ca^{2+}$ in *pfcha* expressing oocytes whereas in the control oocytes there is no pH-dependent uptake. The uptake increased with the pH: the highest $^{45}Ca^{2+}$ uptake in *pfcha* expressing oocytes occured when incubated in Ringer solution at pH 8.5. The uptake at pH 8.5 was at least four times higher than of the control oocytes. At pH of 6.5, there was almost no difference in $^{45}Ca^{2+}$ uptake between *pfcha* expressing oocytes and control oocytes. The rate of $^{45}Ca^{2+}$ uptake at pH 8.5 was linear over 60min (Fig. 3.7b).

If *pfcha* is a calcium proton exchanger, one would expect protons to leave the cell while Ca^{2+} is being taken up. To test this, an experiment was designed to estimate the external pH. To do so, oocytes were incubated in microvolumes of a weakly buffered Ringer solution dyed with the pH indicator Phenol-red. By doing so, even small variations in the external pH can be detected (Jaisser *et al.*, 1993). As expected the solution acidified for a pH of 8.1 to 7.3 when incubated with *pfcha*

expressing oocytes for 60 min. In contrast no pH shift was observed in the control oocytes where the pH remained the same i.e. pH 8.1 (Fig. 3.8).

To investigate if *pfcha* mediated protons extrusion changes intracellular pH homeostasis, the internal pH was measured by using double-barrelled electrodes which measured simultaneously the intracellular pH and the membrane potential. There was no significant difference in the internal pH measured between *pfcha* expressing oocytes and control oocytes when incubated in Ringer solution at pH 7.5. The internal pH measured for the *pfcha* expressing oocytes and the control oocytes was 7.45 ± 0.01 and 7.42 ± 0.02 respectively (Tab. 3.1). This is probably due to the high buffer capacity of the oocytes.

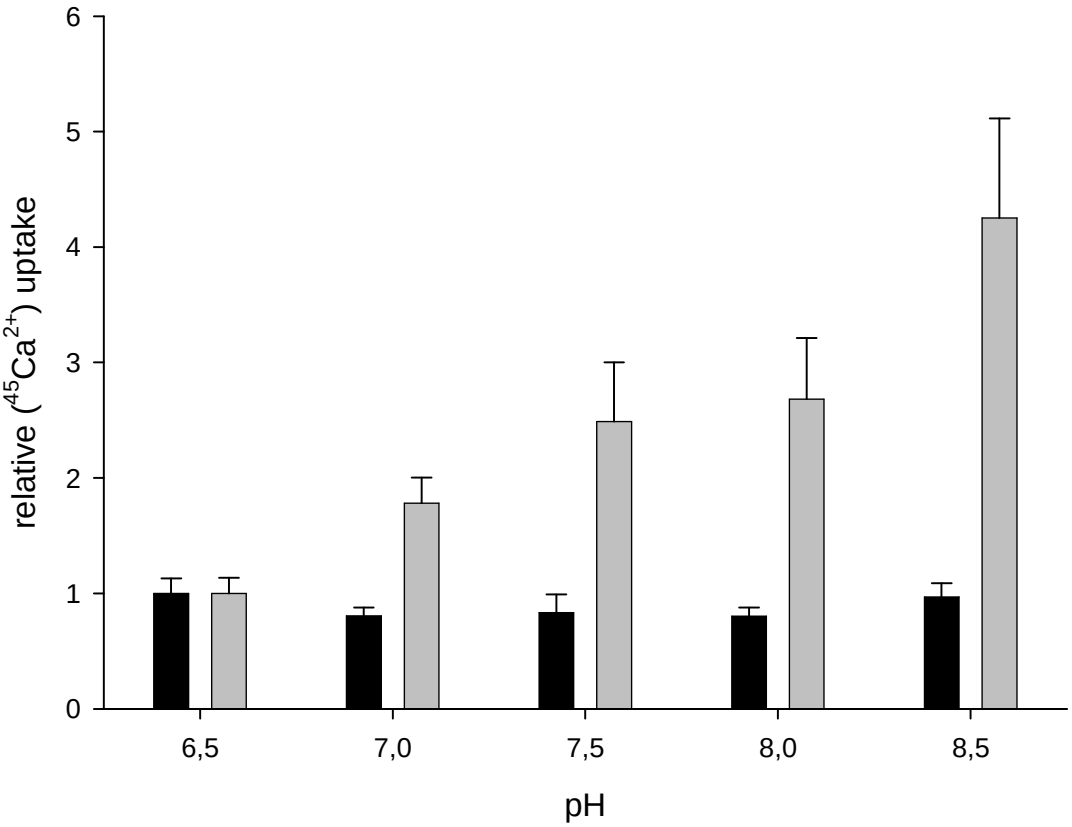

Fig 3.7a: pH-dependent $^{45}Ca^{2+}$ uptake of *pfcha* expressing oocytes (▒) and control oocytes (▉). Oocytes were investigated 3 days post RNA injection. For each pH, 10 water injected oocytes and 10 $cRNA_{pfcha}$ injected oocytes were separately incubated in 500 µl of Ringer solution containing 10 µCi/ml of $^{45}Ca^{2+}$ at the given pH for 1 h. After incubation the oocytes were thoroughly washed three times with a large volume of ice-cold Ringer medium. Each individual oocyte was subsequently lysed for 30 min with 200 µl of 5% SDS, before addition of 2.5 ml of scintillation fluid. The radioactivity of the solution was measured in a Beckman LS6000IC scintillation counter. $^{45}Ca^{2+}$ uptake was normalized to that obtained for control oocytes at pH 6.5

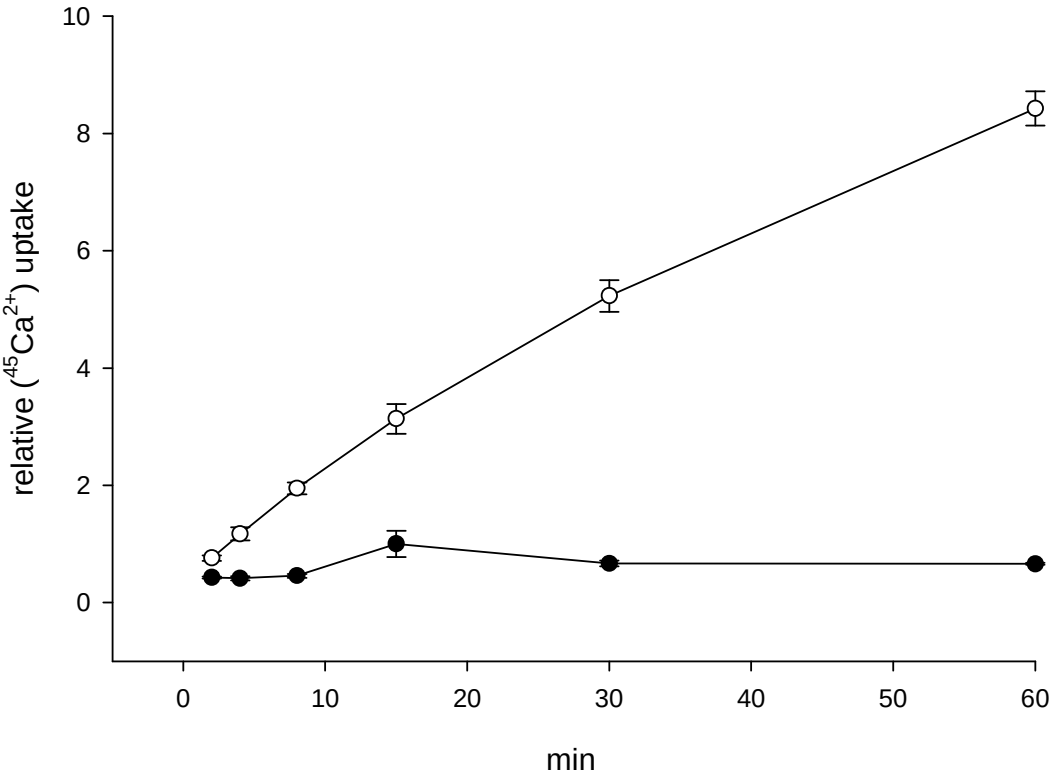

Fig 3.7b: Time course uptake of $^{45}Ca^{2+}$ uptake at pH 8.5 in *pfcha* expressing (o) oocytes and control oocytes (●). Experiment was performed 3 days after injection of $cRNA_{pfcha}$ and water. For each time point, 10 water injected oocytes and 10 $cRNA_{pfcha}$ injected oocytes were separately incubated in 500 µl of a Ringer solution at pH 8.5 containing 10 µCi/ml of $^{45}Ca^{2+}$. After incubation the oocytes were thoroughly washed three times with large volumes of ice-cold Ringer medium. Each individual oocyte was subsequently placed into a separate scintillation vial, dissolved for 30 min with 200 µl of 5% SDS, before addition of 2.5 ml scintillation fluid, and the solution radioactivity was counted in a Beckman LS6000IC scintillation counter. Black circles represent water injected oocytes, open circles $cRNA_{pfcha}$ injected oocytes. Results are the mean of three independent experiments. $^{45}Ca^{2+}$ uptake was normalized to that obtained for control oocytes at time point 2 min.

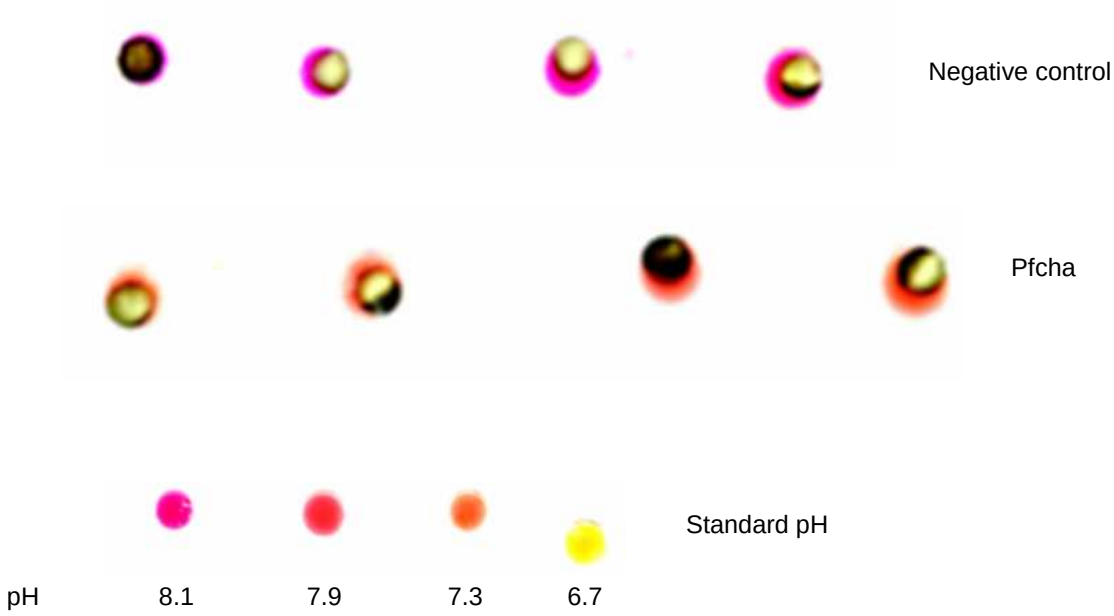

Fig. 3.8a: The expression of *pfcha* in the oocytes results in the acidification of the extracellular medium. Experiment was done 3 day after injection of $cRNA_{pfcha}$ and water. Oocytes injected with cRNA or RNAse free water (negative control) were placed under mineral oil in a 0.5-1.0µl droplet of Red phenol-dyed Ringer solution, pH 8.1. This picture was taken after 60 min. The pH of the surrounding solution of oocytes was approximately 7.3 for the $cRNA_{pfcha}$ injected oocytes and approximately pH 8.1 for the control oocytes when compared to pH standards.

To further characterize PfCHA and because it showed a calcium proton exchange activity, we wanted to know if this exchange is bidirectional. For this purpose, *pfcha* expressing oocytes and control oocytes were loaded with high amounts of radioactive calcium and the calcium efflux was measured at an external pH of 7.5. After 20min of incubation, the intracellular radioactive Ca^{2+} did not significantly change (Fig. 3.8b). This implies that PfCHA could not transport out Ca^{2+} out of the oocytes, under the experimental conditions. On the contrary, this experiment further supports the $^{45}Ca^{2+}$ uptake activity of PfCHA because the PfCHA containing oocytes were able to accumulate more $^{45}Ca^{2+}$ during preloading.

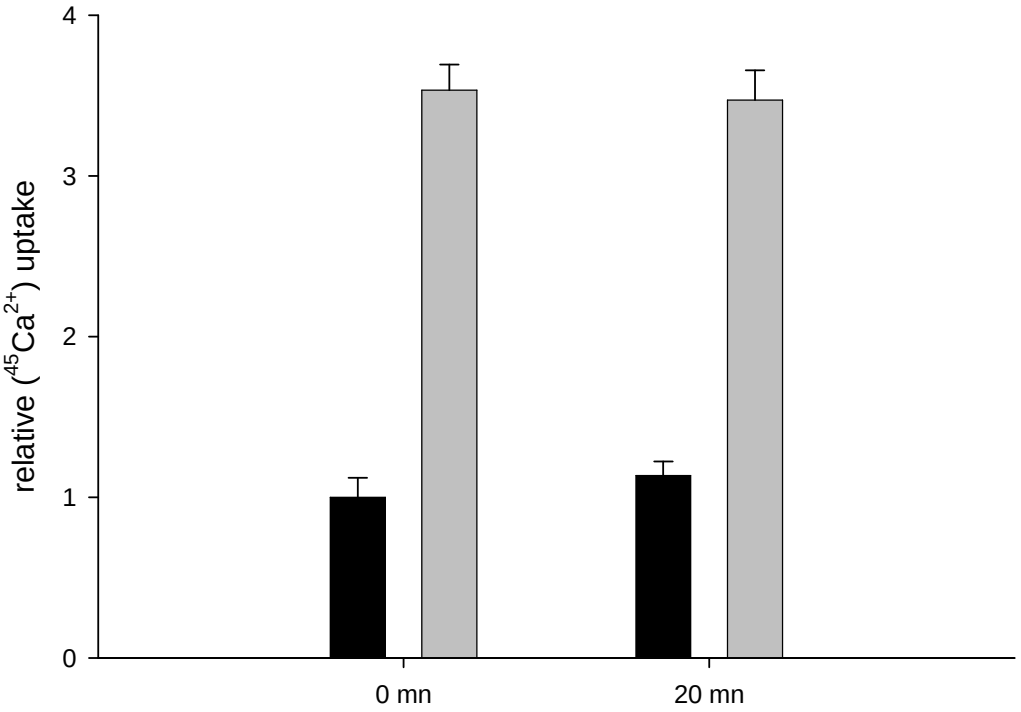

Fig. 3.8b: $^{45}Ca^{2+}$ efflux for *pfcha* expressing oocytes (▒) and control oocytes (■). 20 $cRNA_{pfcha}$ and 20 control oocytes were loaded with radioactive calcium. They were separately incubated in 1ml of Ringer solution containing 50 µl/ml of $^{45}Ca^{2+}$ for 3h. After incubation, the oocytes were thoroughly washed three times with a large volume of ice-cold Ringer medium. 10 oocytes from each batch were individually lysed with 200 µl of 5% SDS, before addition of 2.5 ml of scintillation fluid. The radioactivity of the solution was measured in a Beckman LS6000IC scintillation counter. The remaining oocytes were separately incubated in Ringer solution for 20min and then treated as the previous oocytes.

3.3.2 PfCHA is electrogenic

Exchangers can be electrogenic or electroneutral depending in the electrical balance of the charge species across the membrane. Few calcium antiporters have been so far studied but the existence of an electrogenic calcium antiporter has been already proposed (Zimniak and Barnes, 1980). To investigate the electrogenicity of PfCHA, the membrane potential were measured using double-barrelled electrodes. As shown in Tab. 3.1, *pfcha* expressing oocytes have a more positive membrane potential of –

30 ± 2 mVas compared to the control oocytes which have a membrane potential of -50 ± 3 mV.

Tab. 3.1: Internal pH (pHi) and membrane potential of *pfcha* expressing and control oocytes. Measurements were done 3 days after injection of oocytes incubated in Ringer solution at pH 7.5. Data are means ± SEM from n independent experiments. * no significant difference, P>0.05.

	pH_i	V_m
		mV
Control	7.42 ± 0,02 (3)*	-50 ± 3 (3)
pfcha	7.45 ± 0,01 (6)*	- 29 ± 2 (6)

3.3.3 The $^{45}Ca^{2+}$ uptake can be inhibited

Next we investigated if *pfcha* expressed in the oocytes was inhibitable. To do so, several compounds were tested: Lanthanum, La^{3+}, a known competitive inhibitor of Ca^{2+} transporter; two potent known Na^{2+}/Ca^{2+} exchanger inhibitors KB-R7983 and SEA-0400; and Verapamil, a L-type Ca^{2+} channel blocker. For the experiments, oocytes were incubated in Ringer solution supplemented with the compounds and the $^{45}Ca^{2+}$ uptake was measured as described in Material and Methods. 50µM verapamil and 1mM La^{3+} were able to almost completely inhibit $^{45}Ca^{2+}$ uptake with the amount of $^{45}Ca^{2+}$ uptake taken up being similar in *pfcha* expressing oocytes and control oocytes (Fig. 3.9). 4µM KB-R7943 was able to inhibit $^{45}Ca^{2+}$ uptake into *pfcha* expressing oocytes by 50% whereas 1µM SEA-0400 had no effect on the uptake.
Several antimalarials were tested in the same way to investigate if PfCHA is a drug target. Neither chloroquine nor artemisinin and quinine were able to inhibit the $^{45}Ca^{2+}$ uptake in the *pfcha* expressing oocytes under the conditions tested (Fig. 3.10).
Because KB-R7943 showed an inhibition activity on the $^{45}Ca^{2+}$ uptake in oocytes, its cytotoxic activity on the parasite was determined. An IC_{50}-value of 1.707µM and 1.85 µM was found for the chloroquine sensitive strain HB3 and the chloroquine resistant strain Dd2, respectively (Fig. 3.11).

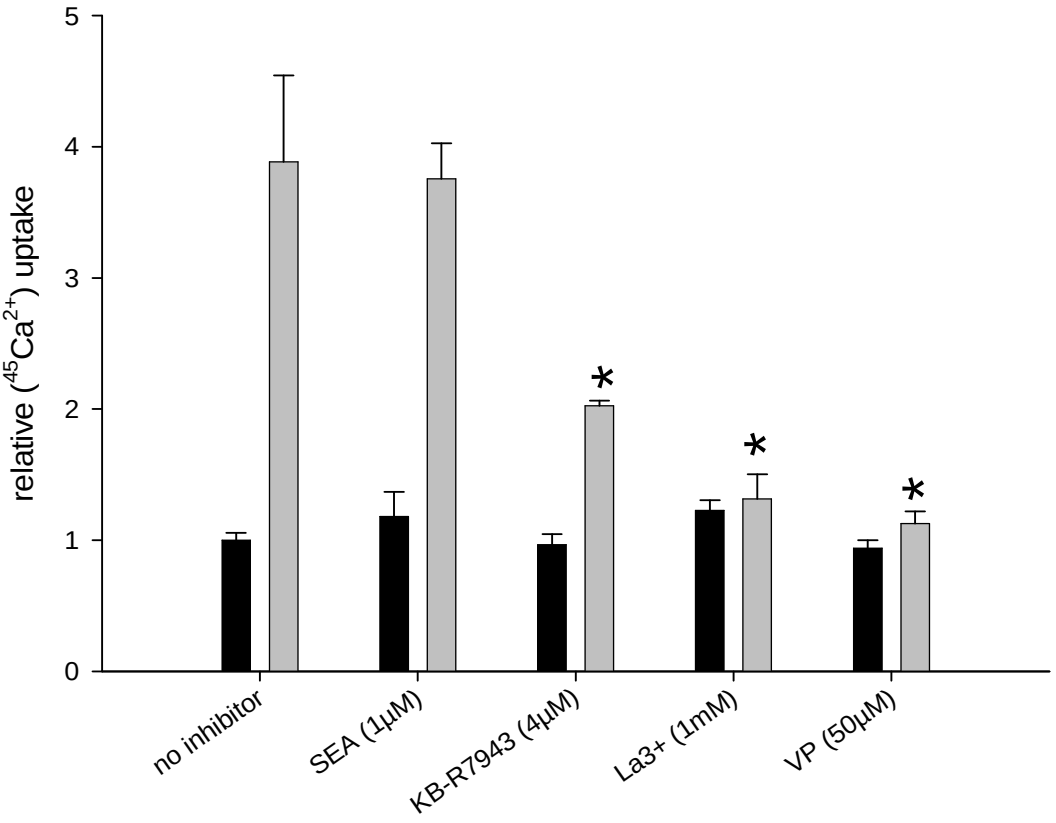

Fig 3.9: $^{45}Ca^{2+}$ uptake in *pfcha* expressing oocytes (▒) and control oocytes (▉) in presence of different inhibitors. For each inhibitor, 10 water injected oocytes and 10 $cRNA_{pfcha}$ injected oocytes were separately preincubated in Ringer solution (pH 7.5) containing the inhibitor for 15 min. They were then separately incubated in 500 µl of Ringer solution containing 10 µCi/ml of $^{45}Ca^{2+}$ and the inhibitor for 1 h. After incubation the oocytes were thoroughly washed three times with 100 ml of ice-cold Ringer medium. Each individual oocyte was subsequently dissolved for 30 min with 200 µl of 5% SDS, before addition of 2.5 ml of scintillation fluid, and the radioactivity of the solution was counted in a Beckman LS6000IC scintillation counter. * Significant difference in relative ($^{45}Ca^{2+}$) uptake (P-value < 0.01) between the $cRNA_{pfcha}$ injected oocytes in the absence of inhibitor and those in presence of inhibitors. The assay was normalized to control oocytes in the absence of any compound.

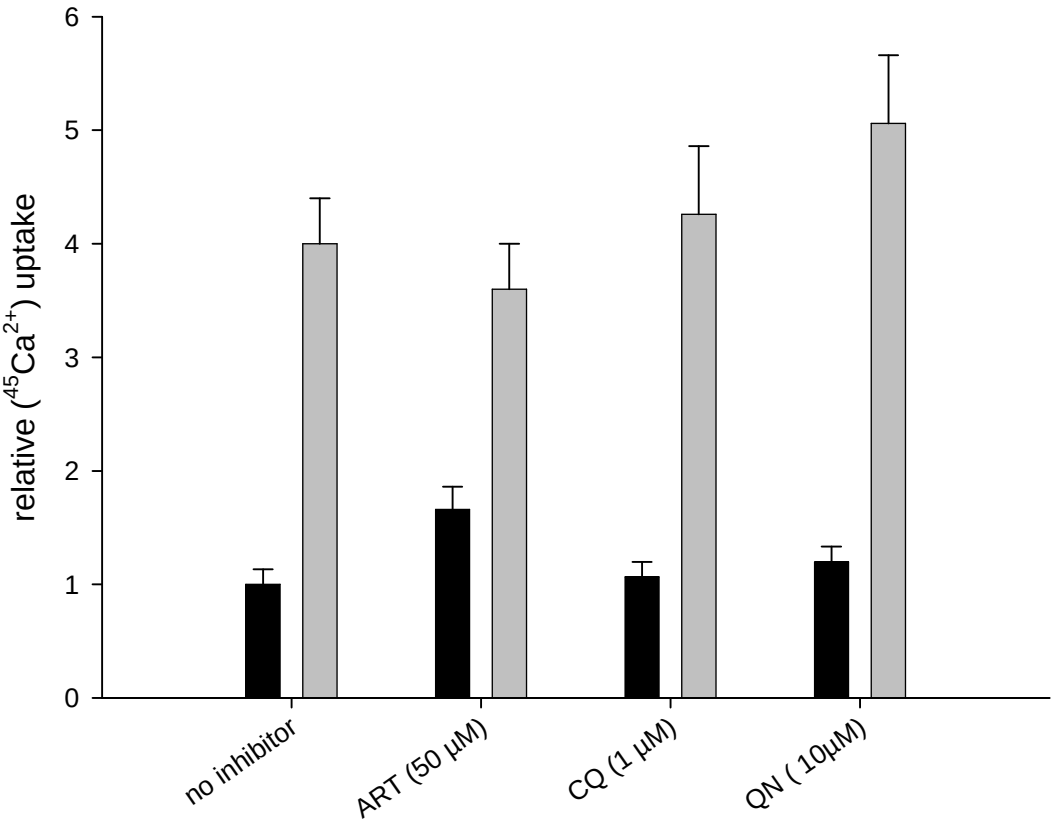

Fig. 3.10: $^{45}Ca^{2+}$ uptake in *pfcha* expressing oocytes (▒) and control oocytes (■) in presence of different antimalarial drugs. For each drug, 10 water injected oocytes and 10 $cRNA_{pfcha}$ injected oocytes were separately preincubated in Ringer solution (pH 7.5) containing the antimalarial during 15 min. They were then separately incubated in 500µl of a Ringer solution containing 10µCi/ml of $^{45}Ca^{2+}$ and the antimalarial for 1 h. After incubation the oocytes were thoroughly washed three times with 100 ml of the ice-cold Ringer medium. Each individual oocyte was lysed for 30 min with 200 µl of 5% SDS, before addition of 2.5 ml of scintillation fluid, and the radioactivity was counted in a Beckman LS6000IC scintillation counter. The values were normalized to control oocytes in the absence of compounds.

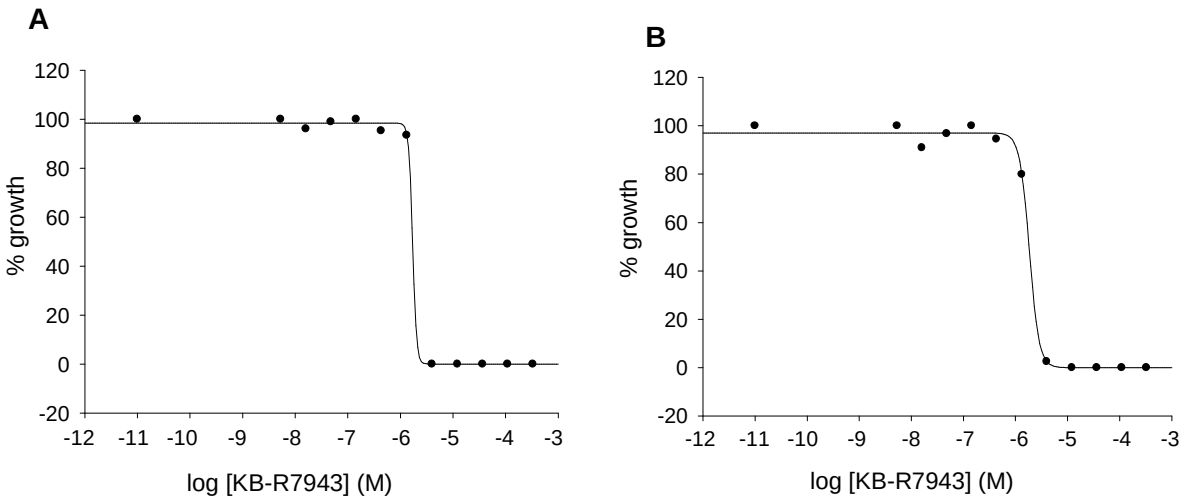

Fig. 3.11: Dose response curve of the CQS strain HB3 (**A**) and the CQR strain Dd2 (**B**) incubated with different concentrations of the Na^{+}/Ca^{2+} inhibitor KB-R7943. Percentage of growth inhibition is shown. IC_{50}-values are 1.7 10^{-6} M and 1.8 10^{-6} M for HB3 and Dd2 respectively.

4. DISCUSSION

With the underlying motivation of characterizing the putative *Plasmodium falciparum* calcium proton antiporter PfCHA, we have cloned, expressed *pfcha* in S. *cerevisiae* and in *Xenopus* oocytes. Our results indicate that PfCHA transports calcium against protons in *Xenopus* oocytes. In *S. cerevisiae*, this transport activity was found to be moderate in our study.

PfCHA shares a number of conserved residues with other Ca^{2+}/H^{+} exchangers and has an overall predicted membrane topology of 11 transmembrane domains consistent with other transporters within the calcium hydrogen exchanger family (Cunningham and Fink, 1996, Hirschi *et al.*, 1996, Ueoka-Nakanishi *et al.*, 1999). Regions determined to be of functional importance in previous studies are also found in *pfcha*. For example we have identified an acidic amino acid motif within a region between the transmembrane domain M6 and M7 that has been shown to be important for the binding of Ca^{2+} (Fig. 3.2) (Pittman *et al.*, 2002, Pittman *et al.*, 2002). This acidic motif is predicted to be located in the inside loop, though the predicted location varied depending on the hydropathy plot programme used. This predicted location is different to the other CAX proteins where this motif is in the outside loop. The presence of the motif in the outside loop is conceivable if we consider that the transport of calcium is directed into the vacuole. PfCHA possesses an extra acidic amino acid motif at its N-terminus. This could be a calcium binding domain, which may regulate PfCHA exchange activity as similar domains act to regulate exchange activity in the cardiac sarcolemmal Na^{+}/Ca^{2+} exchanger (Matsuoka and Hilgemann, 1992, Levitsky *et al.*, 1994).

In *Plasmodium falciparum*, *pfcha* is a single copy gene which is expressed throughout the asexual life cycle but its expression is significantly elevated during the trophozoite to the schizont stage (Fig. 4.1) (Bozdech *et al.*, 2003). Calcium levels in the parasite increase during its development and this correlation with the PfCHA expression suggests that PfCHA may be a key component in the calcium dependent processes during maturation of the parasite.

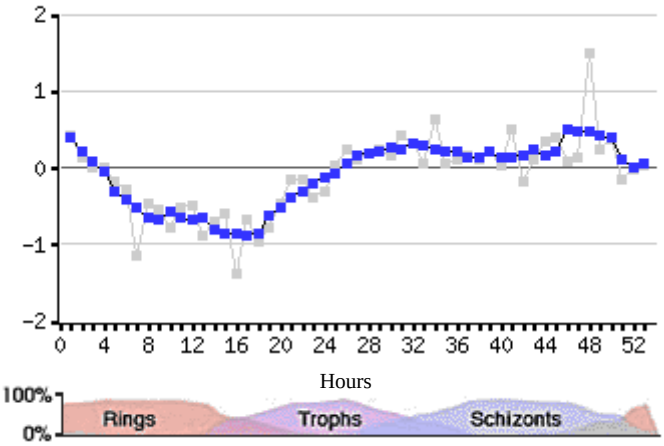

Fig. 4.1 Expression levels of PfCHA determined by glass slide microarray. Blue plot: averaged smoothed normalized log base (2) of Cy5/Cy3 for PfCHA grey plot: averaged normalized log base (2) of Cy5/Cy3 for PfCHA. Source: Derisi (Plasmodb.org)

Given the sequence features of PfCHA suggesting a calcium hydrogen antiporter, we were pleased that this putative function was further supported by our experiments performed in *Xenopus* oocytes. Although the *X. laevis* oocyte is endogenously equipped with a host of ion channels, transport systems and receptors, it has proven to be an excellent heterologuous expression system for the investigation and characterization of countless transport proteins and receptors. *Xenopus* oocytes are also suited to study developmental biology questions, intracellular signalling cascades and biochemical pathways. Fortunately, heterologuously expressed transporters can be distinguished from the endogenous ones (Weber, 1999). This makes the oocytes a suitable model to investigate transport process on a cellular level. The recent functional characterization of the malaria chloroquine resistance transporter PfCRT (Nessler *et al.*, 2004) and the previous characterization of two malaria Ca^{2+} transporters (Eckstein-Ludwig *et al.*, 2003; Krishna *et al.*, 2001) have confirmed that *X. laevis* oocytes are a valuable tool for heterologuous assay of malarial transport proteins. These calcium transporters were found to be calcium ATPases and so far, no calcium hydrogen antiporter has been identified.

We have used this *Xenopus* system to express PfCHA and measure $^{45}Ca^{2+}$ uptake in the oocytes. Having no antibody against PfCHA, we could only check the expression by using a HA-tag fused to the C terminus of PfCHA. The expression of PfCHA was unobservable using western analysis with an anti-HA antibody (data not

shown), although sequencing of the plasmid confirmed that the HA sequence was correct and in frame. The quality of the anti-HA antibody itself is undoubted as it could recognize another HA-tag protein, expressed in yeast, which we used as control. One reason for the failure to detect the HA-tag is that it may have been excised and degraded during the processing of PfCHA.

Nevertheless our functional characterization of PfCHA in *Xenopus* oocytes suggests that PfCHA is a calcium proton antiporter. This conclusion is supported by the $^{45}Ca^{2+}$ uptake experiments, the pH and the membrane potential measurements, as well as the inhibition studies on PfCHA. *Pfcha* expressing oocytes were able to transport ^{45}Ca against protons in a pH-dependent manner (Fig. 3.7a). Uptake is at least four times higher in *pfcha* expressing oocytes in comparison with the control oocytes. These data are consistent with other studies of labelled Ca^{2+} of calcium/cation exchangers (Ca^{2+}/Na^{+}) where the uptake was between 3 to 18 fold higher in expressing oocytes (Sigel *et al.*, 1988). The uptake of $^{45}Ca^{2+}$ was linear with time for *pfcha* expressing oocytes, feature which is similar to other transporters expressed in *Xenopus* oocytes (Carter *et al.*, 2000). Moreover, the $^{45}Ca^{2+}$ uptake of *pfcha* expressing oocytes is coupled to proton extrusions to the extracellular milieu. Although external solution pH measurement gives only a qualitative estimation and the protocol is technically challenging, one can clearly see a difference in pH between the external solution of the *pfcha* expressing oocytes and the control oocytes (Fig. 3.7b). However, this extrusion of protons is not supported by measurements of the cytoplasmic pH (Tab 3.1). There was no difference in the pH_i between the *pfcha* expressing oocytes and the control oocytes. One reason could be that the pH of the solution in which the oocytes were incubated (pH 7.5) was not high enough to drive a noticeable extrusion of protons in the extracellular milieu. Another reason could be that the buffer capacity of the oocyte was able to compensate for the extrusion of protons.

PfCHA can be inhibited. $LaCl_3$, a calcium competitor, was able to totally inhibit the $^{45}Ca^{2+}$ uptake by *pfcha* expressing oocytes as it has been reported elsewhere for heterologuous calcium transporters in *Xenopus* oocytes. KB-R7943, a specific inhibitor of Na^{+}/Ca^{2+} exchangers was also able to inhibit the $^{45}Ca^{2+}$ uptake by 50%. These evidences support the fact that the uptake of $^{45}Ca^{2+}$ in *pfcha* expressing oocytes is specific and related to PfCHA. The fact that KB-R7943 moderately inhibits the growth in vitro of *Plasmodium falciparum* is interesting. Although we can not

exclude an unspecific effect of KB-R7943, its IC_{50}-value in culture is comparable to the inhibiting value in the oocyte (Fig. 3.9, 3.11). This may imply that the target of KB-R7943 in the oocyte and in the parasite is the same. In other terms, PfCHA could be the target of KB-R7943 in the parasite.

PfCHA expressing oocytes revealed a change in a basic physiological parameter, the membrane potential (V_m). They exhibit a high resting V_m whereas the control oocytes have a resting membrane potential similar to values found in other studies (Nessler *et al.*, 2004). We cannot exclude the possibility that endogenous transporters, such as a not selective cationic conductance, were activated in *pfcha* expressing oocytes, as we found in other study (Nessler *et al.*, 2004), which explain the more positive V_m of *pfcha* expressing oocytes. Selectively, the influx of Ca^{2+} may account for the change in V_m.

In contrast to the calcium hydrogen antiport activity of PfCHA observed in *Xenopus* oocyte, the antiport activity was moderate in *S. cerevisiae*. We have found that PfCHA could only weakly complement the Ca^{2+} growth defect of yeast strains deficient in $Ca^{2+/}H^{+}$ antiporter (Fig. 3.5). This weak complementation has also been reported for other genes from the CAX family. Shigaki *et al.* found that AtHCX1, a *Arabidopsis* CAX-like gene was not able to complement yeast defects in vacuolar Ca^{2+} sequestration, and ZmHCX1 the monocot CAX-like gene could not strongly complement the Ca^{2+} growth defect (Shigaki and Hirschi, 2000). The inability of PfCHA to complement yeast mutants defective in vacuolar Ca^{2+} transport could be due to several reasons, including mislocalisation of PfCHA in yeast, post-translational modifications of PfCHA and inhibiting by an N-terminal autoinhibition.

In our results, confocal fluorescence microscopy and Western analysis (Fig. 3.4a,b) of subcellular fractions suggest a vacuolar localization of PfCHA. The localization of a green VCAX1 in vacuoles of transgenic tobacco has been published (Ueoka-Nakanishi *et al.*, 2000). However, the transport of integral membrane proteins to the yeast vacuole seems to occur by default (Nothwehr and Stevens, 1994). Conceivably, the high expression levels of PfCHA may result in it being targeted to the vacuole but in a non functional form. We do believe that at least some of the PfCHA is correctly localised to the vacuole in a functional form because we did observe a moderate calcium hydrogen antiporter activity (Fig. 3.5).

The second potential reason could be that PfCHA may require post-translational modifications or regulation to efficiently transport Ca^{2+} into the vacuole. Yeast may thus lack the necessary processing factors to activate a PfCHA-dependent vacuolar Ca^{2+} transport. Or, in the opposite, processing of PfCHA in yeast can result in an inactive form of it, e.g. an N-terminal glycosylation of PfCHA.
PfCHA calcium hydrogen antiport activity could be modulated by binding of suppressors or activators to a regulatory domain. For example in yeast, VCX1 appears to be negatively regulated at the post-translational level by the calcium/calmodulin-dependent phosphatase calcineurin (Cunningham and Fink, 1996).

The third potential reason for the moderate activity of *pfcha* expressing oocytes may be due to an autoinhibitory mechanism in PfCHA. Indeed a mechanism of N-terminal autoinhibition CAX1 has been reported in the Arabidopsis (Pittman *et al.*, 2002, Pittman *et al.*, 2002). Deletions of the first 10, 20, 30 amino acid at the N-terminus resulted in a protein that now could complement the Ca^{2+} sensitivity of the yeast strain K667, full length CAX1 failed to do so. We believe that this is the case with PfCHA because the N-terminus of PfCHA is more similar to AtCAX1 than it is to VCX1 (Fig. 3.1).

In summary, we have shown that PfCHA has a calcium hydrogen exchange activity in *Xenopus* oocytes and a moderate exchange activity in *S. cerevisiae*. The antiport activity in the oocytes was inhibitable by known Ca^{2+} inhibitors. We believe that PfCHA could be a potential drug target and further studies are needed to investigate this. Knock out experiments of *pfcha* and determination of the subcellular localisation of PfCHA in the parasite are important future steps. In the yeast system, the regulatory domains of the PfCHA could be evaluated by site directed mutagenesis and deletion/insertion experiments.

SUMMARY

Despite substantial efforts to control the spread of malaria, this infectious disease is still a major global health problem as chemotherapy of malaria parasites is limited by established drug resistance and lack of novel affordable treatment options. To combat malaria, identification and characterization of essential genes are needed. Although the calcium metabolism is very important in the life of *P. falciparum*, little is known about the genes which regulate the transport of calcium. With the release of the *P. falciparum* genome, a putative calcium hydrogen antiporter has been identified. To understand the role of this gene in the calcium metabolism of *P. falciparum* and to evaluate it as a drug target, we describe here the functional characterization by the heterologuous expression of this putative calcium hydrogen antiporter in *Xenopus* oocytes and in a *S. cerevisiae* strain which is deficient for the yeast vacuolar calcium hydrogen antiporter VCX1.

The putative 441-residue protein, which we designate PfCHA, is predicted to contain 11 membrane-spanning segments and is related to the calcium exchanger family. Expression of *pfcha* in *Xenopus* oocytes resulted in a higher and pH-dependent uptake of *pfcha* expressing oocytes, in comparison with control oocytes. External pH estimation showed that the calcium uptake was coupled to extrusion of protons out of the oocytes. In other experiments, we found that PfCHA has an antiport activity which is linear with time, unidirectional and electrogenic. Moreover PfCHA was inhibitable by La^{3+}, a calcium transporter competitor, and was moderately inhibited by a sodium calcium exchanger inhibitor KB-R7943. This inhibitor showed also a moderate inhibition on parasite growth in culture. In contrast to the *Xenopus* oocytes, expression of *pfcha* in yeasts mutants defective in the Ca^{2+} transport resulted in a weakly complementat ion of the calcium tolerance. Our subcellular experiments suggested that PfCHA was localized to the yeast vacuole. These results confirm that PfCHA is a calcium hydrogen antiporter and we speculate that PfCHA could be a potential drug target. Further studies are needed to localize it in the parasite and to evaluate it as a drug target.

ZUSAMMENFASSUNG

Trotz erheblicher Bemühungen die Verbreitung von Malaria einzuschränken, stellt diese infektiöse Krankheit immer noch ein globales Gesundheitsproblem dar, da die Chemotherapie der Malariaparasiten durch Medikamentenresistenz erschwert wird und es einen Mangel an neuen erschwinglichen Behandlungsmethoden gibt. Um Malaria bekämpfen zu können, ist die Identizifierung und die Charakterisierung von essentiellen Genen erforderlich. Gegenstand der vorliegenden Arbeit ist deshalb der Calciummetabolismus, welcher bedeutend für den Lebenszyklus von *P. falciparum* ist. Bislang ist allerdings wenig über die beteiligten Gene bekannt, die den Transport von Calcium regulieren. Nach der Vervollständigung des Genoms von *P. falciparum*, wurde ein mutmaßlicher Ca^{2+}/H^{+}-Austauscher identifiziert. Um die Rolle dieses Gens im Calciummetabolismus von *P. falciparum* verstehen zu können und um zu untersuchen, ob dieser Transporter als möglicher Angriffspunkt für ein Medikament dienen könnte, wurde der mutmaßliche Ca^{2+}/H^{+}-Austauscher zur funktionellen Charakterisierung in den Oozyten von X. laevis sowie in *S. cerevisiae* exprimiert. Der verwendete Stamm von *S. cerevisiae* weist einen defekten vakuolären Ca^{2+}/H^{+}-Austauscher (VCX1) auf.

Das 441 Aminosäuren umfassende Protein, welches als PfCHA bezeichnet wird, weist 11 vorhergesagte Transmembran-Domänen auf und gehört zur Familie der Ca^{2+}/H^{+}-Austauscher. Im Vergleich mit Kontroll-Oozyten, rief die Expression von *pfcha* in Oozyten von *X. laevis* einen höheren und pH-abhängigen Einstrom von $^{45}Ca^{2+}$ hervor. Externe pH Messungen zeigten, dass die Calcium-Aufnahme in Oozyten an eine Extrusion von Protonen gekoppelt ist. Weitere Experimente zeigten, dass PfCHA eine Antiportaktivität aufweist, die linear zur Zeit, elektrogen und unidirektional verläuft. Außerdem konnte PfCHA sowohl durch La^{3+}, ein Calciumtransporter-Inhibitor als auch durch den Na^{+}/Ca^{2+}-Austauscher-Inhibitor KB-R7943 gehemmt werden, wobei die Hemmung durch KB-R7943 schwächer war. KB-R7943 zeigte auch eine mittelstarke Inhibierung des Parasitenwachstums in der Kultur. Im Gegensatz zu *pfcha*-exprimierenden Oozyten von *X. laevis* ergab die Expression von *pfcha* in Hefemutanten, deren vakuolärer Ca^{2+}/H^{+}-Austauscher defekt ist, nur eine schwache Komplementierung der Calciumtoleranz. Weitere subzelluläre Experimente deuteten darauf hin, dass PfCHA in der Membran vom Hefevakuolen lokalisiert ist.

Die in der vorliegenden Arbeit gewonnenen Resultate bestätigen, dass PfCHA ein Ca^{2+}/H^{+}-Austauscher ist und es kann darüber spekuliert werden, dass PfCHA ein mögliches Angriffsziel für Medikamente sein könnte. Weitere Studien sind notwendig, um PfCHA im Parasiten zu lokalisieren und es als mögliches Medikamentenziel bewerten zu können.

REFERENCES

Adovelande, J., Bastide, B., Deleze, J. and Schrevel, J. (1993). Cytosolic free calcium in Plasmodium falciparum-infected erythrocytes and the effect of verapamil: a cytofluorimetric study. *Exp. Parasitol.*, **76**: 247-58.

Arav-Boger, R. and Shapiro, T.A. (2005). Molecular mechanisms of resistance in antimalarial chemotherapy: the unmet challenge. *Annu Rev Pharmacol Toxicol*, **45**: 565-85.

Arrizabalaga, G., Ruiz, F., Moreno, S. and Boothroyd, J.C. (2004). Ionophore-resistant mutant of Toxoplasma gondii reveals involvement of a sodium/hydrogen exchanger in calcium regulation. *J Cell Biol*, **165**: 653-62.

Baca, A.M. and Hol, W.G. (2000). Overcoming codon bias: a method for high-level overexpression of Plasmodium and other AT-rich parasite genes in Escherichia coli. *Int J Parasitol*, **30**: 113-8.

Biagini, G.A., Bray, P.G., Spiller, D.G., White, M.R. and Ward, S.A. (2003). The digestive food vacuole of the malaria parasite is a dynamic intracellular Ca^{2+} store. *J Biol Chem*, **278**: 27910-5.

Balasubramanyam, M., Kimura, M., Aviv, A. and Gardner, J.P. (1993). Kinetics of calcium transport across the lymphocyte plasma membrane. *Am J Physiol*, **265**: C321-7.

Barale, J.C., Blisnick, T., Fujioka, H., Alzari, P.M., Aikawa, M., Braun-Breton, C. and Langsley, G. (1999). Plasmodium falciparum subtilisin-like protease 2, a merozoite candidate for the merozoite surface protein 1-42 maturase. *Proc Natl Acad Sci U S A*, **96**: 6445-50.

Baron, S. (1996). Medical Microbiology. Galveston, The University of Texas Medical Branch.

Baruch, D.I., Ma, X.C., Singh, H.B., Bi, X., Pasloske, B.L. and Howard, R.J. (1997). Identification of a region of PfEMP1 that mediates adherence of Plasmodium falciparum infected erythrocytes to CD36: conserved function with variant sequence. *Blood*, **90**: 3766-75.

Beraldo, F.H., Almeida, F.M., da Silva, A.M. and Garcia, C.R. (2005). Cyclic AMP and calcium interplay as second messengers in melatonin-dependent regulation of Plasmodium falciparum cell cycle. *J Cell Biol*, **170**: 551-7.

Berridge, M.J., Bootman, M.D. and Roderick, H.L. (2003). Calcium signalling: dynamics, homeostasis and remodelling. *Nat Rev Mol Cell Biol*, **4**: 517-29.

Billker, O., Dechamps, S., Tewari, R., Wenig, G., Franke-Fayard, B. and Brinkmann, V. (2004). Calcium and a calcium-dependent protein kinase regulate gamete formation and mosquito transmission in a malaria parasite. *Cell*, **117**: 503-14.

Blackman, M.J., Chappel, J.A., Shai, S. and Holder, A.A. (1993). A conserved parasite serine protease processes the Plasmodium falciparum merozoite surface protein-1. *Mol Biochem Parasitol*, **62**: 103-14.

Blackman, M.J. (2002). Expression of recombinant Plasmodium falciparum subtilisin-like protease-1 in insect cells. Characterization, comparison with the parasite protease, and homology modeling. *J Biol Chem*, **277**: 29698-709.

Bozdech, Z., Llinas, M., Pulliam, B.L., Wong, E.D., Zhu, J. and DeRisi, J.L. (2003). The transcriptome of the intraerythrocytic developmental cycle of Plasmodium falciparum. *PLoS Biol*, **1**: E5.

Bradford, M.M. (1976). A rapid and sensitive method for the quantitation of microgram quantities of protein utilizing the principle of protein-dye binding. *Anal Biochem*, **72**: 248-54.

Bray, P.G., Mungthin, M., Ridley, R.G. and Ward, S.A. (1998). Access to hematin: the basis of chloroquine resistance. *Mol Pharmacol*, **54**: 170-9.

Bray, P.G., Janneh, O. and Ward, S.A. (1999). Chloroquine uptake and activity is determined by binding to ferriprotoporphyrin IX in Plasmodium falciparum. *Novartis Found Symp*, **226**: 252-60; discussion 260-4.

Carafoli, E. (1987). Intracellular calcium homeostasis. *Annu Rev Biochem*, **56**: 395-433.

Carter, N.S., Ben Mamoun, C., Liu, W., Silva, E.O., Landfear, S.M., Goldberg, D.E. and Ullman, B. (2000). Isolation and functional characterization of the PfNT1 nucleoside transporter gene from Plasmodium falciparum. *J. Biol. Chem.*, **275**: 10683-91.

Cheng, N.H., Pittman, J.K., Shigaki, T. and Hirschi, K.D. (2002). Characterization of CAX4, an Arabidopsis H(+)/cation antiporter. *Plant Physiol*, **128**: 1245-54.

Cheng, N.H. and Hirschi, K.D. (2003). Cloning and characterization of CXIP1, a novel PICOT domain-containing Arabidopsis protein that associates with CAX1. *J Biol Chem*, **278**: 6503-9.

Cheng, N.H., Pittman, J.K., Barkla, B.J., Shigaki, T. and Hirschi, K.D. (2003). The Arabidopsis cax1 mutant exhibits impaired ion homeostasis, development, and hormonal responses and reveals interplay among vacuolar transporters. *Plant Cell*, **15**: 347-64.

Christodoulou, J., Malmendal, A., Harper, J.F. and Chazin, W.J. (2004). Evidence for differing roles for each lobe of the calmodulin-like domain in a calcium-dependent protein kinase. *J Biol Chem*, **279**: 29092-100.

Clapham, D.E. (1995). Calcium signaling. *Cell*, **80**: 259-68.

Clapham, D.E. (1995). Intracellular calcium. Replenishing the stores. *Nature*, **375**: 634-5.

Cordeiro, J.M., Meireles, S.M., Vale, M.G., Oliveira, C.R. and Goncalves, P.P. (2000). Ca(2+) regulation of the carrier-mediated gamma-aminobutyric acid release from isolated synaptic plasma membrane vesicles. *Neurosci Res*, **38**: 385-95.

Cosloy, S.D. and Oishi, M. (1973). Genetic transformation in Escherichia coli K12. *Proc Natl Acad Sci U S A*, **70**: 84-7.

Cunningham, K.W. and Fink, G.R. (1994). Ca^{2+} transport in Saccharomyces cerevisiae. *J Exp Biol*, **196**: 157-66.

Cunningham, K.W. and Fink, G.R. (1996). Calcineurin inhibits VCX1-dependent H^{+}/Ca^{2+} exchange and induces Ca^{2+} ATPases in Saccharomyces cerevisiae. *Mol Cell Biol*, **16**: 2226-37.

Darbre, D.D. (1999). *Basic molecular biology*. John Wiley & Sons, Chichester.

Davis, T.M., Binh, T.Q., Thu le, T.A., Long, T.T., Johnston, W., Robertson, K. and Barrett, P.H. (2002). Glucose and lactate turnover in adults with falciparum malaria: effect of complications and antimalarial therapy. *Trans R Soc Trop Med Hyg*, **96**: 411-7.

Divo, A.A., Geary, T.G., Davis, N.L. and Jensen, J.B. (1985). Nutritional requirements of Plasmodium falciparum in culture. I. Exogenously supplied dialyzable components necessary for continuous growth. *J Protozool*, **32**: 59-64.

Doherty, J.P., Lindeman, R., Trent, R.J., Graham, M.W. and Woodcock, D.M. (1993). Escherichia coli host strains SURE and SRB fail to preserve a palindrome cloned in lambda phage: improved alternate host strains. *Gene*, **124**: 29-35.

Dzekunov, S.M., Ursos, L.M. and Roepe, P.D. (2000). Digestive vacuolar pH of intact intraerythrocytic P. falciparum either sensitive or resistant to chloroquine. *Mol Biochem Parasitol*, **110**: 107-24.

Eckstein-Ludwig, U., Webb, R.J., Van Goethem, I.D., East, J.M., Lee, A.G., Kimura, M., O'Neill, P.M., Bray, P.G., Ward, S.A. and Krishna, S. (2003). Artemisinins target the SERCA of Plasmodium falciparum. *Nature*, **424**: 957-61.

Elased, K.M. and Playfair, J.H. (1996). Reversal of hypoglycaemia in murine malaria by drugs that inhibit insulin secretion. *Parasitology*, **112 (Pt 6)**: 515-21.

Falcone, D. and Andrews, D.W. (1991). Both the 5' untranslated region and the sequences surrounding the start site contribute to efficient initiation of translation in vitro. *Mol Cell Biol*, **11**: 2656-64.

Fang, J. and McCutchan, T.F. (2002). Thermoregulation in a parasite's life cycle. *Nature*, **418**: 742.

Farias, S.L., Gazarini, M.L., Melo, R.L., Hirata, I.Y., Juliano, M.A., Juliano, L. and Garcia, C.R. (2005). Cysteine-protease activity elicited by Ca^{2+} stimulus in Plasmodium. *Mol Biochem Parasitol*, **141**: 71-9.

Farooq, U. and Mahajan, R.C. (2004). Drug resistance in malaria. *J Vector Borne Dis*, **41**: 45-53.

Fidock, D.A., Nomura, T., Talley, A.K., Cooper, R.A., Dzekunov, S.M., Ferdig, M.T., Ursos, L.M., Sidhu, A.B., Naude, B., Deitsch, K.W., Su, X.Z., Wootton, J.C., Roepe, P.D. and Wellems, T.E. (2000). Mutations in the P. falciparum digestive vacuole transmembrane protein PfCRT and evidence for their role in chloroquine resistance. *Mol Cell*, **6**: 861-71.

Gamain, B., Smith, J.D., Miller, L.H. and Baruch, D.I. (2001). Modifications in the CD36 binding domain of the Plasmodium falciparum variant antigen are responsible for the inability of chondroitin sulfate A adherent parasites to bind CD36. *Blood*, **97**: 3268-74.

Garcia, C.R., Dluzewski, A.R., Catalani, L.H., Burting, R., Hoyland, J. and Mason, W.T. (1996). Calcium homeostasis in intraerythrocytic malaria parasites. *Eur J Cell Biol*, **71**: 409-13.

Gazarini, M.L. and Garcia, C.R. (2004). The malaria parasite mitochondrion senses cytosolic Ca^{2+} fluctuations. *Biochem Biophys Res Commun*, **321**: 138-44.

Ginsburg, H. and Stein, W.D. (1991). Kinetic modelling of chloroquine uptake by malaria-infected erythrocytes. Assessment of the factors that may determine drug resistance. *Biochem Pharmacol*, **41**: 1463-70.

Ginsburg, H., Famin, O., Zhang, J. and Krugliak, M. (1998). Inhibition of glutathione-dependent degradation of heme by chloroquine and amodiaquine as a possible basis for their antimalarial mode of action. *Biochem Pharmacol*, **56**: 1305-13.

Goncalves, P.P., Meireles, S.M., Neves, P. and Vale, M.G. (2000). Distinction between Ca(2+) pump and Ca(2+)/H(+) antiport activities in synaptic vesicles of sheep brain cortex. *Neurochem Int*, **37**: 387-96.

Guillemin, J. (2002). Choosing scientific patrimony: Sir Ronald Ross, Alphonse Laveran, and the mosquito-vector hypothesis for malaria. *J Hist Med Allied Sci*, **57**: 385-409.

Hirschi, K.D., Zhen, R.G., Cunningham, K.W., Rea, P.A. and Fink, G.R. (1996). CAX1, an H^+/Ca^{2+} antiporter from Arabidopsis. *Proc. Nat.l Acad. Sci. U S A*, **93**: 8782-6.

Hyde, J.E. (2005). Exploring the folate pathway in Plasmodium falciparum. *Acta Trop*, **94**: 191-206.

Inoue, H., Nojima, H. and Okayama, H. (1990). High efficiency transformation of Escherichia coli with plasmids. *Gene*, **96**: 23-8.

Jaisser, F., Horisberger, J.D., Geering, K. and Rossier, B.C. (1993). Mechanisms of urinary K+ and H+ excretion: primary structure and functional expression of a novel H,K-ATPase. *J Cell Biol*, **123**: 1421-9.

Joet, T. and Krishna, S. (2004). The hexose transporter of Plasmodium falciparum is a worthy drug target. *Acta Trop*, **89**: 371-4.

Kasai, M. and Muto, S. (1990). Ca^{2+} pump and Ca^{2+}/H^{+} antiporter in plasma membrane vesicles isolated by aqueous two-phase partitioning from corn leaves. *J Membr Biol*, **114**: 133-42.

Kawamoto, F., Fujioka, H., Murakami, R., Syafruddin, Hagiwara, M., Ishikawa, T. and Hidaka, H. (1993). The roles of Ca^{2+}/calmodulin- and cGMP-dependent pathways in gametogenesis of a rodent malaria parasite, Plasmodium berghei. *Eur J Cell Biol*, **60**: 101-7.

Kirk, K. (2001). Membrane transport in the malaria-infected erythrocyte. *Physiol Rev*, **81**: 495-537.

Korkiamäki, T. (2002). Intercellular calcium-mediated cell signaling in keratinocytes cultured from patients with NF1 or psoriasis. Department of Anatomy and Cell Biology. OULU, University of Oulu.

Korsinczky, M., Chen, N., Kotecka, B., Saul, A., Rieckmann, K. and Cheng, Q. (2000). Mutations in Plasmodium falciparum cytochrome b that are associated with atovaquone resistance are located at a putative drug-binding site. *Antimicrob Agents Chemother*, **44**: 2100-8.

Kramer, R. and Ginsburg, H. (1991). Calcium transport and compartment analysis of free and exchangeable calcium in Plasmodium falciparum-infected red blood cells. *J. Protozool.*, **38**: 594-601.

Krishna, S., Woodrow, C., Webb, R., Penny, J., Takeyasu, K., Kimura, M. and East, J.M. (2001). Expression and functional characterization of a Plasmodium falciparum Ca^{2+}-ATPase (PfATP4) belonging to a subclass unique to apicomplexan organisms. *J Biol Chem*, **276**: 10782-7.

Krogstad, D.J., Gluzman, I.Y., Kyle, D.E., Oduola, A.M., Martin, S.K., Milhous, W.K. and Schlesinger, P.H. (1987). Efflux of chloroquine from Plasmodium falciparum: mechanism of chloroquine resistance. *Science*, **238**: 1283-5.

Krogstad, D.J., Gluzman, I.Y., Herwaldt, B.L., Schlesinger, P.H. and Wellems, T.E. (1992). Energy dependence of chloroquine accumulation and chloroquine efflux in Plasmodium falciparum. *Biochem Pharmacol*, **43**: 57-62.

Kwiatkowski, D., Cannon, J.G., Manogue, K.R., Cerami, A., Dinarello, C.A. and Greenwood, B.M. (1989). Tumour necrosis factor production in Falciparum malaria and its association with schizont rupture. *Clin Exp Immunol*, **77**: 361-6.

Kyes, S., Pinches, R. and Newbold, C. (2000). A simple RNA analysis method shows var and rif multigene family expression patterns in Plasmodium falciparum. *Mol Biochem Parasitol*, **105**: 311-5.

Lambros, C. and Vanderberg, J.P. (1979). Synchronization of Plasmodium falciparum erythrocytic stages in culture. *J Parasitol*, **65**: 418-20.

Lauer, S.A., Rathod, P.K., Ghori, N. and Haldar, K. (1997). A membrane network for nutrient import in red cells infected with the malaria parasite. *Science*, **276**: 1122-5.

Levitsky, D.O., Nicoll, D.A. and Philipson, K.D. (1994). Identification of the high affinity Ca^{2+} binding domain of the cardiac Na^{+}/Ca^{2+} exchanger. *J Biol Chem*, **269**: 22847-52.

Lew, V.L., Tsien, R.Y., Miner, C. and Bookchin, R.M. (1982). Physiological $[Ca^{2+}]i$ level and pump-leak turnover in intact red cells measured using an incorporated Ca chelator. *Nature*, **298**: 478-81.

Li, J.L., Baker, D.A. and Cox, L.S. (2000). Sexual stage-specific expression of a third calcium-dependent protein kinase from Plasmodium falciparum. *Biochim Biophys Acta*, **1491**: 341-9.

Lodish H, B.A., Zipursky SL, Matsudaira P, Baltimore D & Darnell JE (2000). *Molecular Cell Biology*. W.H. Freeman and Company, New York.

Loria, P., Miller, S., Foley, M. and Tilley, L. (1999). Inhibition of the peroxidative degradation of haem as the basis of action of chloroquine and other quinoline antimalarials. *Biochem J*, **339 (Pt 2)**: 363-70.

Luse, S.A. and Miller, L.H. (1971). Plasmodium falciparum malaria. Ultrastructure of parasitized erythrocytes in cardiac vessels. *Am J Trop Med Hyg*, **20**: 655-60.

Matsumoto, Y., Perry, G., Scheibel, L.W. and Aikawa, M. (1987). Role of calmodulin in Plasmodium falciparum: implications for erythrocyte invasion by the merozoite. *Eur J Cell Biol*, **45**: 36-43.

Matsuoka, S. and Hilgemann, D.W. (1992). Steady-state and dynamic properties of cardiac sodium-calcium exchange. Ion and voltage dependencies of the transport cycle. *J Gen Physiol*, **100**: 963-1001.

McDevitt, M.A., Xie, J., Gordeuk, V. and Bucala, R. (2004). The anemia of malaria infection: role of inflammatory cytokines. *Curr Hematol Rep*, **3**: 97-106.

Mercereau-Puijalon, O. and Fandeur, T. (2003). Antimalarial activity of artemisinins: identification of a novel target? *Lancet*, **362**: 2035-6.

Miller, L.H., Baruch, D.I., Marsh, K. and Doumbo, O.K. (2002). The pathogenic basis of malaria. *Nature*, **415**: 673-9.

Mons, B. (1990). Preferential invasion of malarial merozoites into young red blood cells. *Blood Cells*, **16**: 299-312.

Moreno, S.N. and Docampo, R. (2003). Calcium regulation in protozoan parasites. *Curr. Opin. Microbiol.*, **6**: 359-64.

Moskes, C., Burghaus, P.A., Wernli, B., Sauder, U., Durrenberger, M. and Kappes, B. (2004). Export of Plasmodium falciparum calcium-dependent protein kinase 1 to the

parasitophorous vacuole is dependent on three N-terminal membrane anchor motifs. *Mol Microbiol*, **54**: 676-91.

Naude, B., Brzostowski, J.A., Kimmel, A.R. and Wellems, T.E. (2005). Dictyostelium discoideum expresses a malaria chloroquine resistance mechanism upon transfection with mutant, but not wild-type, plasmodium falciparum transporter PfCRT. *J Biol Chem*,

Nessler, S., Friedrich, O., Bakouh, N., Fink, R.H., Sanchez, C.P., Planelles, G. and Lanzer, M. (2004). Evidence for activation of endogenous transporters in Xenopus laevis oocytes expressing the Plasmodium falciparum chloroquine resistance transporter, PfCRT. *J Biol Chem*, **279**: 39438-46.

Newbold, C.I., Craig, A.G., Kyes, S., Berendt, A.R., Snow, R.W., Peshu, N. and Marsh, K. (1997). PfEMP1, polymorphism and pathogenesis. *Ann Trop Med Parasitol*, **91**: 551-7.

Nothwehr, S.F. and Stevens, T.H. (1994). Sorting of membrane proteins in the yeast secretory pathway. *J Biol Chem*, **269**: 10185-8.

Pagola, S., Stephens, P.W., Bohle, D.S., Kosar, A.D. and Madsen, S.K. (2000). The structure of malaria pigment beta-haematin. *Nature*, **404**: 307-10.

Perez-Prat, E., Narasimhan, L., Binzel, M.L., Botella, M.A., Chen, Z., Valpuesta, V., Bressan, R.A., Hasegawa, P.M. (1992). Induction of a putative Ca^{2+}-ATPase mRNA in NaCl-adapted cells. *Plant. physiol.*, **100**: 1471-1478.

Peters, J.M., Chen, N., Gatton, M., Korsinczky, M., Fowler, E.V., Manzetti, S., Saul, A. and Cheng, Q. (2002). Mutations in cytochrome b resulting in atovaquone resistance are associated with loss of fitness in Plasmodium falciparum. *Antimicrob Agents Chemother*, **46**: 2435-41.

Peterson, D.S., Walliker, D. and Wellems, T.E. (1988). Evidence that a point mutation in dihydrofolate reductase-thymidylate synthase confers resistance to pyrimethamine in falciparum malaria. *Proc Natl Acad Sci U S A*, **85**: 9114-8.

Pittman, J.K. and Hirschi, K.D. (2001). Regulation of CAX1, an Arabidopsis Ca(2+)/H+ antiporter. Identification of an N-terminal autoinhibitory domain. *Plant Physiol*, **127**: 1020-9.

Pittman, J.K., Shigaki, T., Cheng, N.H. and Hirschi, K.D. (2002). Mechanism of N-terminal autoinhibition in the Arabidopsis Ca(2+)/H(+) antiporter CAX1. *J Biol Chem*, **277**: 26452-9.

Pittman, J.K., Sreevidya, C.S., Shigaki, T., Ueoka-Nakanishi, H. and Hirschi, K.D. (2002). Distinct N-terminal regulatory domains of Ca(2+)/H(+) antiporters. *Plant Physiol*, **130**: 1054-62.

Polson, H.E. and Blackman, M.J. (2005). A role for poly(dA)poly(dT) tracts in directing activity of the Plasmodium falciparum calmodulin gene promoter. *Mol Biochem Parasitol*, **141**: 179-89.

Pozos, T.C., Sekler, I. and Cyert, M.S. (1996). The product of HUM1, a novel yeast gene, is required for vacuolar Ca^{2+}/H^{+} exchange and is related to mammalian Na^{+}/Ca^{2+} exchangers. *Mol Cell Biol*, **16**: 3730-41.

Putney, J.W., Jr. (1990). Capacitative calcium entry revisited. *Cell Calcium*, **11**: 611-24.

Putney, J.W., Jr. (1999). TRP, inositol 1,4,5-trisphosphate receptors, and capacitative calcium entry. *Proc Natl Acad Sci U S A*, **96**: 14669-71.

Rasmussen, H. and Rasmussen, J.E. (1990). Calcium as intracellular messenger: from simplicity to complexity. *Curr Top Cell Regul*, **31**: 1-109.

Ream, W.F., K.G. (1999). *Molecular biology techniques*. Academic Press, London.

Ridley, R.G. (2002). Medical need, scientific opportunity and the drive for antimalarial drugs. *Nature*, **415**: 686-93.

Rohrbach, P., Friedrich, O., Hentschel, J., Plattner, H., Fink, R.H. and Lanzer, M. (2005). Quantitative calcium measurements in subcellular compartments of P. falciparum-infected erythrocytes. *J Biol Chem*,

Sachs, J. and Malaney, P. (2002). The economic and social burden of malaria. *Nature*, **415**: 680-5.

Sambrook, J., Fritsch, E. F., Maniatis, T. (1989). *Molecular Cloning. A Laboratory Manual.* Cold Spring Harbor Laboratory Press, NY.

Sanchez, C.P., McLean, J.E., Stein, W. and Lanzer, M. (2004). Evidence for a substrate specific and inhibitable drug efflux system in chloroquine resistant Plasmodium falciparum strains. *Biochemistry*, **43**: 16365-73.

Sanni, L.A., Jarra, W., Li, C. and Langhorne, J. (2004). Cerebral edema and cerebral hemorrhages in interleukin-10-deficient mice infected with Plasmodium chabaudi. *Infect Immun*, **72**: 3054-8.

Saris, N.E. and Carafoli, E. (2005). A historical review of cellular calcium handling, with emphasis on mitochondria. *Biochemistry (Mosc)*, **70**: 187-94.

Scheibel, L.W., Colombani, P.M., Hess, A.D., Aikawa, M., Atkinson, C.T. and Milhous, W.K. (1987). Calcium and calmodulin antagonists inhibit human malaria parasites (Plasmodium falciparum): implications for drug design. *Proc Natl Acad Sci U S A*, **84**: 7310-4.

Schlagenhauf, P. (2004). Malaria: from prehistory to present. *Infect Dis Clin North Am*, **18**: 189-205, table of contents.

Shigaki, T. and Hirschi, K. (2000). Characterization of CAX-like genes in plants: implications for functional diversity. *Gene*, **257**: 291-8.

Shigaki, T., Pittman, J.K. and Hirschi, K.D. (2003). Manganese specificity determinants in the Arabidopsis metal/H+ antiporter CAX2. *J Biol Chem*, **278**: 6610-7.

Sidhu, A.B., Valderramos, S.G. and Fidock, D.A. (2005). pfmdr1 Mutations contribute to quinine resistance and enhance mefloquine and artemisinin sensitivity in Plasmodium falciparum. *Mol Microbiol*, **57**: 913-26.

Sigel, E., Baur, R., Porzig, H. and Reuter, H. (1988). mRNA-induced expression of the cardiac Na^{+}-Ca^{2+} exchanger in Xenopus oocytes. *J Biol Chem*, **263**: 14614-6.

Smith, H., Crandall, I., Prudhomme, J. and Sherman, I.W. (1992). Optimization and inhibition of the adherent ability of Plasmodium falciparum-infected erythrocytes. *Mem. Inst. Oswaldo. Cruz.*, **87 Suppl 3**: 303-12.

Smith, J.D., Craig, A.G., Kriek, N., Hudson-Taylor, D., Kyes, S., Fagen, T., Pinches, R., Baruch, D.I., Newbold, C.I. and Miller, L.H. (2000). Identification of a Plasmodium falciparum intercellular adhesion molecule-1 binding domain: a parasite adhesion trait implicated in cerebral malaria. *Proc Natl Acad Sci U S A*, **97**: 1766-71.

Smith, J.D., Subramanian, G., Gamain, B., Baruch, D.I. and Miller, L.H. (2000). Classification of adhesive domains in the Plasmodium falciparum erythrocyte membrane protein 1 family. *Mol Biochem Parasitol*, **110**: 293-310.

Smith, J.D., Gamain, B., Baruch, D.I. and Kyes, S. (2001). Decoding the language of var genes and Plasmodium falciparum sequestration. *Trends Parasitol*, **17**: 538-45.

Snow, R.W., Trape, J.F. and Marsh, K. (2001). The past, present and future of childhood malaria mortality in Africa. *Trends Parasitol*, **17**: 593-7.

Snow, R.W., Guerra, C.A., Noor, A.M., Myint, H.Y. and Hay, S.I. (2005). The global distribution of clinical episodes of Plasmodium falciparum malaria. *Nature*, **434**: 214-7.

Srivastava, I.K., Rottenberg, H. and Vaidya, A.B. (1997). Atovaquone, a broad spectrum antiparasitic drug, collapses mitochondrial membrane potential in a malarial parasite. *J Biol Chem*, **272**: 3961-6.

Srivastava, I.K., Morrisey, J.M., Darrouzet, E., Daldal, F. and Vaidya, A.B. (1999). Resistance mutations reveal the atovaquone-binding domain of cytochrome b in malaria parasites. *Mol Microbiol*, **33**: 704-11.

Sullivan, D.J., Jr., Gluzman, I.Y., Russell, D.G. and Goldberg, D.E. (1996). On the molecular mechanism of chloroquine's antimalarial action. *Proc Natl Acad Sci U S A*, **93**: 11865-70.

Tanabe, K., Mikkelsen, R.B. and Wallach, D.F. (1982). Calcium transport of Plasmodium chabaudi-infected erythrocytes. *J. Cell. Biol.*, **93**: 680-4.

Tanabe, K., Mikkelsen, R.B. and Wallach, D.F. (1983). Transport of ions in erythrocytes infected by plasmodia. *Ciba Found Symp*, **94**: 64-73.

Trager, W. and Jensen, J.B. (1976). Human malaria parasites in continuous culture. *Science*, **193**: 673-5.

Triglia, T., Wang, P., Sims, P.F., Hyde, J.E. and Cowman, A.F. (1998). Allelic exchange at the endogenous genomic locus in Plasmodium falciparum proves the role of dihydropteroate synthase in sulfadoxine-resistant malaria. *Embo J*, **17**: 3807-15.

Trottein, F., Thompson, J. and Cowman, A.F. (1995). Cloning of a new cation ATPase from Plasmodium falciparum: conservation of critical amino acids involved in calcium binding in mammalian organellar Ca(2+)-ATPases. *Gene*, **158**: 133-7.

Troye-Blomberg, M., Worku, S., Tangteerawatana, P., Jamshaid, R., Soderstrom, K., Elghazali, G., Moretta, L., Hammarstrom, M. and Mincheva-Nilsson, L. (1999). Human gamma delta T cells that inhibit the in vitro growth of the asexual blood stages of the Plasmodium falciparum parasite express cytolytic and proinflammatory molecules. *Scand J Immunol*, **50**: 642-50.

Tsuchiya, T. and Rosen, B.P. (1976). Calcium transport driven by a proton gradient and inverted membrane vesicles of Escherichia coli. *J Biol Chem*, **251**: 962-7.

Ueoka-Nakanishi, H., Nakanishi, Y., Tanaka, Y. and Maeshima, M. (1999). Properties and molecular cloning of Ca^{2+}/H^{+} antiporter in the vacuolar membrane of mung bean. *Eur. J. Biochem.*, **262**: 417-25.

Ueoka-Nakanishi, H., Tsuchiya, T., Sasaki, M., Nakanishi, Y., Cunningham, K.W. and Maeshima, M. (2000). Functional expression of mung bean Ca^{2+}/H^{+} antiporter in yeast and its intracellular localization in the hypocotyl and tobacco cells. *Eur J Biochem*, **267**: 3090-8.

Uhlemann, A.-C., T.;Staalsoe,T.; Klinkert, M.; Hviid L (2000). Analysis of Plasmodium falciparum-infected red blood cells. *MACS&more*, **4**: 7-8.

Vennerstrom, J.L., Arbe-Barnes, S., Brun, R., Charman, S.A., Chiu, F.C., Chollet, J., Dong, Y., Dorn, A., Hunziker, D., Matile, H., McIntosh, K., Padmanilayam, M., Santo Tomas, J., Scheurer, C., Scorneaux, B., Tang, Y., Urwyler, H., Wittlin, S. and Charman, W.N. (2004). Identification of an antimalarial synthetic trioxolane drug development candidate. *Nature*, **430**: 900-4.

Vercesi, A.E., Grijalba, M.T. and Docampo, R. (1997). Inhibition of Ca^{2+} release from Trypanosoma brucei acidocalcisomes by 3,5-dibutyl-4-hydroxytoluene: role of the Na^{+}/H^{+} exchanger. *Biochem J*, **328 (Pt 2)**: 479-82.

Verdini, A.S., Chiappinelli, L. and Zanobi, A. (1991). Toward the elucidation of the mechanism of attachment and entry of malaria sporozoites into cells: synthetic polypeptides from the circumsporozoite protein of Plasmodium falciparum bind Ca^{2+} and interact with model phospholipid membranes. *Biopolymers.*, **31**: 587-94.

Villa, A., Garcia-Simon, M.I., Blanco, P., Sese, B., Bogonez, E. and Satrustegui, J. (1998). Affinity chromatography purification of mitochondrial inner membrane proteins with calcium transport activity. *Biochim Biophys Acta*, **1373**: 347-59.

Waditee, R., Hossain, G.S., Tanaka, Y., Nakamura, T., Shikata, M., Takano, J., Takabe, T. and Takabe, T. (2004). Isolation and functional characterization of Ca^{2+}/H^{+} antiporters from cyanobacteria. *J. Biol. Chem.*, **279**: 4330-8.

Wang, P., Read, M., Sims, P.F. and Hyde, J.E. (1997). Sulfadoxine resistance in the human malaria parasite Plasmodium falciparum is determined by mutations in dihydropteroate synthetase and an additional factor associated with folate utilization. *Mol Microbiol*, **23**: 979-86.

Wasserman, M., Alarcon, C. and Mendoza, P.M. (1982). Effects of Ca^{2+} depletion on the asexual cell cycle of Plasmodium falciparum. *Am J Trop Med Hyg*, **31**: 711-7.

Wasserman, M., Vernot, J.P. and Mendoza, P.M. (1990). Role of calcium and erythrocyte cytoskeleton phosphorylation in the invasion of Plasmodium falciparum. *Parasitol. Res.*, **76**: 681-8.

Weber, W. (1999). Ion currents of Xenopus laevis oocytes: state of the art. *Biochim Biophys Acta*, **1421**: 213-33.

Wimmers, L.E., Ewing, N.N, Bennett, A.B, (1992). Higher plant Ca^{2+}-ATPase: primary structure and regulation of mRNA abundance by salt. *Proc Natl Acad Sci U S A*, **89**: 9205-9209.

Withers-Martinez, C., Saldanha, J.W., Ely, B., Hackett, F., O'Connor, T. and

Zhang, J., Krugliak, M. and Ginsburg, H. (1999). The fate of ferriprotorphyrin IX in malaria infected erythrocytes in conjunction with the mode of action of antimalarial drugs. *Mol Biochem Parasitol*, **99**: 129-41.

Zimniak, P. and Barnes, E.M., Jr. (1980). Characterization of a calcium/proton antiporter and an electrogenic calcium transporter in membrane vesicles from Azotobacter vinelandii. *J Biol Chem*, **255**: 10140-3.